

Communication Strategies for Single User and Multi-user Slow Fading Channels

A Thesis
Presented to The Academic Faculty
by

Arumugam Kannan

In Partial Fulfillment of the Requirements for the Degree of
Doctor of Philosophy in Electrical Engineering



*School of Electrical and Computer Engineering
Georgia Institute of Technology*

December 2007

Communication Strategies for Single User and Multi-user Slow Fading Channels

Approved by:

Prof. John R. Barry (Advisor)
School of Electrical and Computer
Engineering
Georgia Institute of Technology

Prof. Gordon L. Stuber
School of Electrical and Computer
Engineering
Georgia Institute of Technology

Prof. Ye (Geoffrey) Li
School of Electrical and Computer
Engineering
Georgia Institute of Technology

Prof. James McClellan
School of Electrical and Computer
Engineering
Georgia Institute of Technology

Prof. Alfred Andrew
Department of Mathematics
Georgia Institute of Technology

Date of Approval : August 20, 2007

*To my parents, Chendamarai Kannan & Retna Kannan
and my brother, Sivaguru Kannan*

ACKNOWLEDGEMENTS

First of all, I would like to thank Dr. Barry for being an extremely supportive advisor, a patient teacher and a great person. I have been truly fortunate to have had the chance to work with him and learn from him through these five years. I wish I could someday emulate his simplicity of thought, clarity of expression, patience and attention to detail - I will certainly try. Apart from his unwavering support through my Ph.D, I would like to thank Dr. Barry for being a role model. I would like to thank Prof. Stuber, Prof. Li, Prof. McClellan and Prof. Andrew for being on my thesis committee. I would like to thank all my committee members for their valuable feedback on my thesis.

In all honesty, my years in Atlanta were my best ones and I have some great friends to thank for it. I would like to start with my GCATT-mates. Once in a while, you are fortunate enough to meet a person who leaves a lasting impression on your life. I met two, in a span of 15 seconds, on my first day in Atlanta and they are now the best of my friends. Well, I am not sure if Badri and Aravind realize this, but they are great influences in the lives of several other people - I am one of them, for sure. Thank you for everything, guys - you are inspirational in so many ways. Special thanks to Badri for our endless discussions on wireless communications which helped me gain valuable intuition into my research when I was starting out. (Nope, your greatest triumph in life has to wait a little longer !).

I would like to thank Souvik and Shayan for providing original entertainment of the highest quality at GCATT 562, the likes of which are unlikely to be ever seen again. I'm sure everyone else in the lab would like to thank Aravind and Badri for catalyzing the above mentioned entertainment and taking it to the next level. I would like to thank Pradnya for all her care, friendship and the free evening snacks ! I would like to thank Deric for being a very good friend, roommate and uhm... a pretty useful translator during my memorable stay in GT Lorraine. I would also like to thank Deric for patiently listening to all my crazy MIMO ideas, some of which found a place in my thesis, and others which should never have existed. Thanks to Yogesh for the cricket sessions and the good times we had in GTL - it was great fun.

Our move to Centergy was an exciting change and I would like to thank my Centergy-mates David Milliner, Matthieu Bloch, Demijan Kline and Arun Subramanian for making the new experience a fun and memorable one. Special thanks to David for all the chatter on football and stock markets alike. I hope our mutual information content grew richer ! I would like to thank Para, Nitin and Souvik for all our memorable lunch sessions and endless analysis of playoff basketball.

Since day one, I have been lucky enough to have great roommates. And of course, it has to start with Karthik; he was so much fun to be around and made life in general look easy - I heartily thank him for that. I would like to thank Sridhar for being a roommate but never being at home and Rajesh for not being a roommate and always being at our home. The times with you guys were a lot of fun and truly unforgettable. Special thanks to Sridhar for getting me into American football, I am now officially addicted. I would like to thank Srini on behalf of the entire Tam gang for the memorable TBS sessions and the mouthwatering *bajjis*. I would like to thank Srini, Rajesh, Sridhar and Karthik for driving me around for all the time that I didn't have a car, which was all five years !

I would like to specially thank Badri Vellambi for being a great friend and a responsible roommate of a rather less responsible yours truly. I enjoyed our marathon badminton sessions and even longer discussions on global issues of trivial importance. Wherever I move to, I should probably look out for a person named Badri - the name seems to work out pretty well for me. Thanks to Shyam for patiently listening to all my expert commentary on all sports. I am glad I actually had a listener - I never knew it.

I would like to thank my friends Lakshminarayanan, Preethi, Sai, Vijayaraghavan, Pradeep, Vijay, Sibi for being pillars of support during, before and hopefully long after my Ph.D. You guys make my life special by your mere presence. Laksh, looking back, you really inspired me to do a Ph.D and I would like to share this one with you. Thanks for always being there. Last but certainly not the least, I would like to thank my parents and my brother for their unconditional love, support and unwavering faith in me even when I might have questioned myself during this five year period. Dear Appa (Dad) and Amma (Mom) and Siva, thank you for everything you are giving me, I love you.

TABLE OF CONTENTS

DEDICATION	iii
ACKNOWLEDGEMENTS	iv
LIST OF FIGURES	xi
SUMMARY	xiv
1 Problem Introduction And Background	1
1.1 Multiple-Input, Multiple-Output (MIMO) Systems.....	3
1.2 Channel Model and System Assumptions	4
1.3 Organization of Part I of this work.....	9
 PART I: LAYERED SPACE-TIME ARCHITECTURES FOR MULTIPLE-INPUT, MULTIPLE-OUTPUT RAYLEIGH FADING CHANNELS	
2 A Survey of Layered Space-Time Architectures	12
2.1 The Simplest Layered Space-Time Transmitter.....	14
2.2 Linear detector	15
2.3 Successive Cancellation Decoder.....	17
2.3.1 Fixed ordered SC decoder	20
2.3.2 BLAST ordered SC decoder	21
2.4 Spatial Multiplexing with Rate Allocation.....	24
2.5 Optimum Outage Probability of Vertical Architectures.....	25
2.6 Numerical Results for Vertically Layered Architectures	26
2.7 Overview of the D-BLAST Architecture.....	28

2.8	Summary	33
3	Joint Transmitter-Receiver Optimization of V-BLAST	35
3.1	Receiver Optimization: Rate-Normalized Ordering	36
3.2	Transmitter Optimization	38
3.2.1	Transmitter Optimization with BLAST Ordering	39
3.2.2	Rate-Normalized Ordering	42
3.3	Numerical Results	44
3.4	Summary	47
4	Space-Time Active Rotation (STAR) Architecture	48
4.1	Basic Structure of the STAR Architecture	50
4.2	V-STAR: STAR with Vertical Layering	51
4.2.1	Transmitter	52
4.2.2	Receiver	52
4.2.3	Outage Probability and Diversity Order	54
4.2.4	Receiver Design: Ordering Algorithm	57
4.2.5	Simulation Results	60
4.3	G-STAR: STAR with Group Encoding and Decoding	65
4.3.1	Group Decoding	66
4.3.2	Simulation results for G-STAR	69
4.3.3	Performance-complexity tradeoff in G-STAR	70
4.4	D-STAR: STAR With Diagonal Layering	70
4.4.1	The D-STAR Transmitter	71
4.4.2	Decoding of D-STAR	72
4.4.3	Performance Results	73
4.5	Summary	74
5	Diversity-Multiplexing Tradeoff in Layered ST Architectures	76

5.1	Background and Definitions	77
5.2	Rate-Diversity Tradeoff in V-STAR	80
5.3	Diversity-Multiplexing Tradeoff in V-STAR	85
5.4	Diversity-Multiplexing tradeoff in G-STAR	88
5.5	Summary	89
6	Applications of STAR in multiple-access communications	90
6.1	Channel Model	91
6.2	The STAR Architecture	92
6.2.1	Transmitters	92
6.2.2	Receiver	93
6.3	Outage Probability	94
6.4	Diversity-Multiplexing Tradeoff	95
6.5	Simulation Results	96
6.6	Summary	97

**PART II: COOPERATIVE COMMUNICATIONS OVER FADING
MULTIPLE-ACCESS CHANNELS**

7	Problem Introduction and Background	101
7.1	Channel Model	103
7.1.1	Cooperation and Network Topology	104
7.1.2	Symmetric Network Assumption	107
7.2	Non-Cooperative Multiple-Access Schemes	109
7.3	Relay Techniques in a Cooperative Wireless Network	112
7.3.1	Amplify-and-forward (AF)	112
7.3.2	Amplify/decode-and-forward (ADF)	113

7.3.3	Selection-decode-and-forward (SDF)	114
7.4	State of the Art in Cooperation Protocols.	114
7.4.1	Laneman-Tse-Wornell (LTW) Protocol	114
7.4.2	NAF protocol.	119
7.5	Numerical Results	121
7.6	Summary.	122
8	Space-Division Relay: A high rate non-orthogonal cooperation protocol.	124
8.1	The Space-Division Relay Protocol	124
8.2	Outage Analysis	127
8.3	Numerical Results	131
8.4	Summary.	135
9	How Much Cooperation is Necessary in Cooperative Multiple Access Channels?	136
9.1	Partial Cooperation Framework	137
9.2	Example of Orthogonal Protocol with Partial Cooperation	138
9.2.1	Outage Analysis.	140
9.2.2	Numerical Results	144
9.3	Example of a Non-Orthogonal Protocol with Partial Cooperation	146
9.3.1	Outage Analysis.	148
9.3.2	Numerical Results	152
9.4	Summary.	154
10	Scalable High Rate Cooperation Protocols for Multiple-Access Channels.	155
10.1	Channel Model	156
10.2	Space-Division Relay (SDR) for N -users	158
10.3	Amplify-and-forward (AF)	160

10.3.1 Outage Analysis	162
10.4 Selection-Decode-and-Forward (SDF)	166
10.4.1 Selection	166
10.4.2 Forwarding	169
10.4.3 Outage Analysis	172
10.5 Numerical results	179
10.6 Summary	181
11 Conclusion	183
11.1 Main Contributions	183
11.2 Future Work	185
REFERENCES	186

LIST OF FIGURES

1. Illustration of the MIMO channel.	5
2. A 3-transmit antenna naive spatial multiplexer: Transmitter structure of V-BLAST. 14	14
3. Linear decoding for a t-transmit antenna naive spatial multiplexing system.	15
4. Successive cancellation decoding algorithm for a t-transmit antenna naive spatial multiplexer.	17
5. Naive spatial multiplexing vs. transmitter optimized spatial multiplexing with $t = 4$, $r = 4$	26
6. Performance-complexity tradeoff of spatial multiplexing techniques with $t = 4$, $r = 4$, $R = 8$ b/s/Hz.	27
7. The D-BLAST architecture, with $t = 3$	28
8. SNR gap of D-BLAST to MIMO channel outage probability as a function of fractional codelength in% with $t = 4$, $r = 4$ with $R = 8$ b/s/Hz.	32
9. Comparison of ordering algorithms for $\{R_i\} = \{0.00, 1.31, 2.99, 3.70\}$ for a 4-input, 4-output Rayleigh fading channel at $R = 8$ b/s/Hz.	45
10. Comparison of transmitter optimized SC decoders for a 4-input, 4-output Rayleigh fading channel at $R = 8$ b/s/Hz	45
11. Performance-complexity tradeoff of various spatial multiplexing techniques for $t = 4$, $r = 4$, $R = 8$ b/s/Hz.	46
12. The STAR transmitter with $t = 4$ transmit antennas.	50
13. The vertical space-time active rotation (V-STAR) transmitter with $t = 4$ transmit antennas.	51
14. The V-STAR successive cancellation decoder.	52
15. Comparison of outage probability of various spatial multiplexing systems with ZF-SC decoding over a 4×4 MIMO channel at $R = 8$ b/s/Hz.	61
16. V-STAR with ZF-SC decoding vs. optimum outage probability for spatial multiplexing systems over 3×3 , 4×4 and 8×8 MIMO channels at a data rate of 2 b/s/Hz per trans-	

mit antenna.	62
17. V-STAR with MMSE-SC decoding vs. optimum outage probability for spatial multiplexing systems over 3×3 , 4×4 and 8×8 MIMO channels at 2 b/s/Hz per transmit antenna.	62
18. Performance-complexity tradeoff of various spatial multiplexing techniques for $t = 4$, $r = 4$, $R = 8$ b/s/Hz.	63
19. Frame error rate performance of V-STAR with 16 QAM constellation and irregular LDPC codes.	65
20. G-STAR transmitter with $t = 8$ antennas divided into four groups of $q = 2$ antennas each.	66
21. G-STAR vs naive group encoding with SC and unconstrained decoding, $t = 8$, $r = 8$ and $q = 2$	69
22. Two possible configurations of D-STAR with $t = 3$	71
23. Outage probability of D-STAR vs. D-BLAST with different code lengths with $t = 4$, $r = 4$ and $R = 8$ b/s/Hz.	73
24. Diversity-multiplexing tradeoff for a vertically layered system over a 4×4 MIMO channel.	79
25. Lower bound on diversity order of V-STAR over square MIMO channels.	85
26. The timing of transmissions in a space-time active rotation (STAR) system with $K = 4$ users equipped with $t = 2$ antennas each.	92
27. Performance of STAR with SC and unconstrained decoding over a multiple-access channel with $K = 4$ users, $t = 2$, $r = 8$ and $R = 4$ bps/Hz per user.	97
28. A two-user cooperative multiple-access system: Possible communication links. . .	103
29. Two simple network topologies with two multiple-access users communicating with a common destination.	105
30. Two more simple network topologies with two multiple-access users communicating with a common destination.	106

31. i). TDMA with $N = 2$ users. ii). SDMA with $N = 2$ users	109
32. Illustration of the Laneman-Tse- Wornell (LTW) cooperation protocol.	115
33. Outage probabilities of various multiple access schemes for a 2-user system, with $R = 1$ bps/Hz.	121
34. Illustration of the space-division relay cooperation protocol.	125
35. Comparison of outage probabilities of various multiple access schemes for a 2-user system, with $R = 1$ bps/Hz.	132
36. Comparison of outage probabilities of non-orthogonal cooperation schemes for a 2-user system, with $R = 1$ bps/Hz.	133
37. Comparison of the SNR required for multiple-access schemes to achieve an outage probability of 10^{-3} as a function of the target data rate.	134
38. Partial cooperation with the LTW protocol for $N = 2$.	139
39. Outage performance of LTW with partial cooperation over a 2-user cooperative multiple access system, $R = 1$ b/s/Hz.	144
40. Outage performance of LTW with partial cooperation over a 2-user cooperative multiple access system, $R = 2$ b/s/Hz.	145
41. Partial cooperation with the SDR protocol for $N = 2$.	146
42. Outage performance of SDR with partial cooperation over a 2-user cooperative multiple access system, $R = 1$ b/s/Hz.	152
43. Outage performance of SDR with partial cooperation over a 2-user cooperative multiple access system, $R = 2$ b/s/Hz.	153
44. Example of an N -user cooperative multiple-access system with $N = 4$.	156
45. Extension of the SDR protocol to $N = 3$ users.	158
46. Comparison of outage probabilities of SDR and LTW protocols with AF and SDF relays for $N = 3$ with $R = 1$ b/s/Hz per user.	180
47. Comparison of outage probabilities of SDR and LTW protocols with AF and SDF relays for $N = 4$ with $R = 1$ b/s/Hz per user.	181

SUMMARY

Technological progress in the field of wireless communications over the past few years has only been matched by the increasing demand for sophisticated services at lower costs. A significant breakthrough was achieved in the design of efficient wireless communication systems with the advent of the diversity concept [1]-[3]. A communication system is said to have diversity if there are multiple paths, in time, frequency or space, between the transmitter and receiver. Diversity enables the system to mitigate the effects of multipath fading on signals transmitted through the wireless medium.

Spatial diversity exploits the availability of multiple spatial paths between the transmitter and receiver by placing antenna arrays at either end [3], [4]. In addition to improving the reliability of communication by creating redundant copies of the transmitted information at the receiver, wireless transceivers with multiple antennas exploit the spatial degrees of freedom to multiplex multiple streams of data and achieve significant gains in spectral efficiencies [1]-[4]. Spatial diversity is crucial to reliable communication over slow-fading wireless channels, where it is hard to achieve low error probabilities due to the lack of time diversity [4].

In this thesis, we design spatial diversity techniques for slow-fading wireless channels. There are two parts to this thesis: In Part I we propose spatial diversity techniques for point-to-point single-user wireless systems, while in Part II we propose multiuser cooperative diversity techniques for multiuser wireless communication systems.

In the first part, we propose a set of new wireless communication techniques for multiple-input, multiple-output (MIMO) channels over Rayleigh slow-fading wireless channels. In the last decade, several techniques have been proposed to achieve the multiplexing and diversity benefits and low error rates over MIMO systems [5]-[10]. However, achieving these objectives at an affordable computational complexity remains a challenging problem. We introduce MIMO transceivers that achieve high data rates and low error rates using a class of MIMO systems known as layered space-time (ST) architectures, which use low complexity, suboptimal decoders such as successive cancellation (SC) decoders.

We propose a set of improved layered space-time architectures and show that it is possible to achieve near-optimal error performance over MIMO channels while requiring just SC decoding at the receiver [28][56][58]. We show that these architectures achieve high rate and diversity gains while maintaining simple decoders with affordable computational complexity. We also show that some of the proposed layered space-time architectures could find applications in multiple-access communications as low-complexity solutions for achieving near-optimum performance [57].

In the second part of this thesis, we propose novel techniques for cooperative communication between terminals in multiuser wireless communication systems. Cooperative communication over wireless networks is a concept where neighboring terminals share their antennas and signal processing resources to create a “*virtual transmit array*” [61]-[65], [73]. In addition to transmitting their own information to the destination, users in a cooperative communication system listen to transmission from other users and relay this information to the destination, thus creating multiple paths between transmitter

and receiver. Cooperation amongst users creates a new form of diversity, known as cooperative diversity, which helps improve the reliability of all the users in a network collectively, compared to each user communicating independently with the destination.

Current cooperation protocols show that it is possible to improve the diversity gains significantly over multiple access channels, improving the outage performance at high SNR [63]-[68], [72]. The concept of cooperation necessitates that a user spend time, bandwidth, energy and signal processing resources to help the communication of other users in the network. This raises a fundamental question on the tradeoff between spending resources for one's own communication and helping other users [88]. Several state-of-the-art cooperation schemes, while effectively harnessing the diversity benefits of cooperation, incur a high penalty in transmission rate, thus affecting the outage performance. Specifically, the transmission rates of these protocols do not scale well as the number of users in the network increases [63][68][69][72][74].

We start with a simple three node multiple-access system where two users are communicating with a common destination [71]. We propose new high-rate cooperation strategies which achieve the full diversity gain offered by the cooperative channel for this simple system [89]. We propose a new framework to address the tradeoff between cooperation and independent transmission over a multiple access channel and determine the conditions under which each idea is better than the other. Finally, we propose a high rate cooperation protocol which achieves the maximum diversity over a multiple access system with an arbitrary number of users and achieves high rates which scale favorably as the number of users increases.

CHAPTER 1

PROBLEM INTRODUCTION AND BACKGROUND

Today's wireless devices have evolved into much more than just wireless telephones, with applications ranging from wireless internet, multimedia messaging and even high-definition television gaining entry into pocket-sized wireless devices. On the other hand, wireless local area networks (WLAN) are fast replacing wireline networks due to their flexibility and mobility. In order to meet the demands of these applications, wireless technologies must improve spectral efficiencies and reliability while maintaining affordable costs.

Signals transmitted over wireless channels are subjected to time-varying attenuation and phase-shifts — a phenomenon called *fading* — due to the constantly changing nature of the wireless medium. Multipath fading is often a major impediment to reliable communications over wireless channels. Specifically, the channel reliability is severely affected when the signals experience heavy attenuation — a phenomenon known as *deep fading*.

Recently, rapid progress have been made in wireless technology and much of this progress can be attributed to the concept of *diversity communications* [1][2]. Diversity refers to the availability of multiple independent channels between the transmitter and receiver. The idea of diversity communications is to mitigate multipath fading by exploiting these multiple paths to improve the reliability of communication, since the probability of several independent channels being in a deep fade simultaneously is small.

Diversity in fading channels can be in time, frequency or spatial domains [1][2]. *Time diversity* can be obtained by coding or interleaving information across different coherence intervals, so that different parts of the same codeword experiences independent fades and hence the performance is averaged over the “good” and “bad” fading realizations. Analogously, if the channel response is frequency selective over the bandwidth of the coded signal, then different parts of the same codeword experience independent fades in the frequency domain, creating *frequency diversity*. A third form of diversity, namely *spatial diversity*, can be created by placing multiple transmit and receive antennas to create multiple spatial paths between the transmitter and receiver [3][4]. If the antennas are spaced sufficiently far apart, then the channel between different antenna pairs fade independently.

Fading, in time, can be of two kinds: slow or fast fading [35]. Slow fading is the scenario where the coherence time of the channel is larger than the duration of the transmitted codeword, and fast fading is the scenario where the coherence time is shorter than the codeword. Achieving low error probabilities over fast fading channels is easier than in slow fading channels due to the time diversity created by time varying fading, provided the receiver has a proper estimate of the channel. The main challenge facing system design for fast fading channels is channel estimation, whereas in slow fading channels achieving low error probabilities is the key challenge, due to the lack of time diversity [35][36]. Most widespread practical applications such as cellular telephony and indoor wireless networks are narrowband communications systems, meaning they occupy

a small frequency band and hence sufficient frequency diversity may not always be available [2]. In such cases, spatial diversity becomes a crucial component in achieving reliable communication over wireless channels.

1.1 Multiple-Input, Multiple-Output (MIMO) Systems

Recently, communication systems with multiple transmit and receive antennas, also known as multiple-input, multiple-output (MIMO) systems have been effective in exploiting spatial diversity to achieve dramatic improvements in the reliability of communication over wireless channels [1]-[4]. In addition to spatial diversity, another important benefit of using MIMO systems is the *multiplexing*, which refers to the ability of MIMO systems to support more than one independent stream of data simultaneously [4][11][12]. While diversity improves *reliability*, multiplexing enables higher transmission *rates*.

An important practical obstacle in employing MIMO systems is the enormous decoding complexity incurred by the use of multiple antennas [33][34]. The complexity of the optimal joint maximum-likelihood (ML) decoder grows exponentially in the spectral efficiency and length of the codeword. Though several techniques have been proposed to achieve the full multiplexing [5] and diversity [7]-[10] benefits of MIMO systems, achieving these objectives at an affordable computational complexity still remains a challenging problem.

The problem of achieving a desirable tradeoff between performance and complexity in MIMO communication systems has been approached in two ways in literature: (1) consider systems with near-optimum error performance and find lower complexity

algorithms without affecting the performance significantly [50][51], or (2) consider suboptimal systems with low computational complexity and improve transmission and reception strategies to approach near-optimal performance while maintaining the virtue of low complexity [13]-[23], [55].

The former approach often translates into a receiver design problem, where the goal is to design lower complexity algorithms to approximate the optimal decoder. The latter often turns out to be transmitter optimization problem, where the goal is to design transmitters to suit low-complexity decoders. We take the latter approach to MIMO transceiver design, with the goal of designing transmission strategies, specifically layered ST architectures tailored to work well with suboptimal decoders.

We now describe the MIMO channel model and the basic system assumptions to be used in Part I of this work in Section 1.2. In Section 1.3, we outline the organization of the remainder of Part I.

1.2 Channel Model and System Assumptions

Over the last decade, there has been a significant body of work on the design of MIMO communication systems, with techniques ranging from space-time codes [7]-[10], [15] layered space-time architectures [14][16][17], beamforming and antenna selection strategies [13], [18]-[21] on the transmitter side to sphere decoding [50][51], decision feedback decoding [5][6] and lattice-reduction aided decoding at the receiver side [52][53]. The design of a good communication strategy is closely tied to the channel conditions, such as slow or fast fading, and system-level assumptions, such as the

presence or absence of feedback or presence or absence of an outer error correction code. In this section, we will describe the channel model used in this work and discuss some of these assumptions in detail.

In part I of this thesis, we consider a wireless communication system with t antennas at the transmitter and r antennas at the receiver, as shown in Fig. 1. The $r \times 1$ received vector at the k^{th} signaling interval is

$$\mathbf{y}_k = \mathbf{H}\mathbf{x}_k + \mathbf{n}_k. \quad (1)$$

where \mathbf{H} is the $r \times t$ channel matrix, \mathbf{x}_k is the $t \times 1$ vector of input symbols transmitted at the k^{th} signaling interval and \mathbf{n}_k is the $r \times 1$ vector of additive noise elements.

The elements of the $r \times 1$ noise vector \mathbf{n}_k are independent, circularly symmetric Gaussian random variables with zero mean and variance N_0 , so $E[\mathbf{n}_k \mathbf{n}_l^*] = \delta_{k-l} N_0 \mathbf{I}_r$, where \mathbf{A}^* denotes conjugate transpose of \mathbf{A} . The channel matrix \mathbf{H} is a random Rayleigh fading matrix, its entries being independent, circularly symmetric complex Gaussian random variables with zero mean and unit variance. Thus, $E[\mathbf{h}_k \mathbf{h}_l^*] = \delta_{k-l} \mathbf{I}_r$, where, \mathbf{h}_k denotes the k^{th} column of \mathbf{H} . The average transmitted energy per symbol period $E[|\mathbf{x}_k|^2] =$

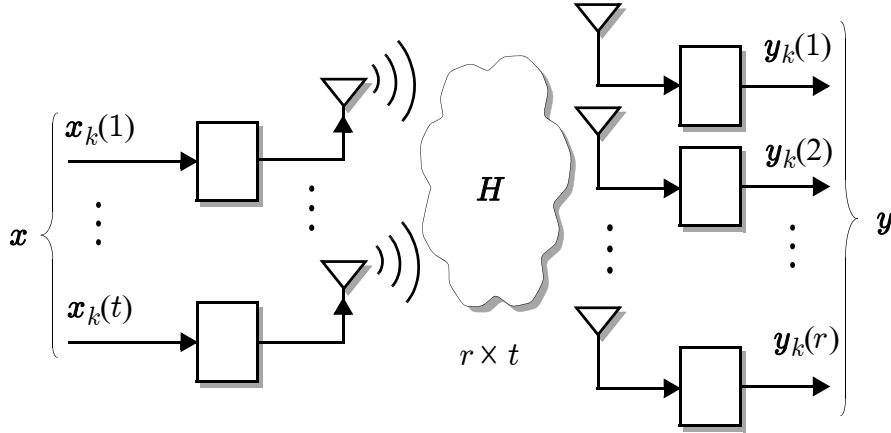


Fig. 1. Illustration of the MIMO channel.

E. Under these assumptions, the average signal-to-noise ratio (SNR) per receive antenna is $S = E / N_0$. The decoders considered in Part I of this thesis require that there be at least as many receive antennas as transmit. Hence, we work with the assumption that $r \geq t$.

We now state the assumptions on the channel model, performance metric and other system parameters to be used in this work.

- **Flat Fading:** We consider narrowband MIMO systems, where the frequency response of the channel is flat over the bandwidth of operation. Since this property is as much a function of the signal bandwidth as it is of the channel conditions, narrowband systems often experience flat fading [35][36]. Techniques designed for narrowband MIMO systems can be easily extended to broadband systems by using the transceiver in conjunction with the orthogonal frequency division multiplexing (OFDM) technique [33].
- **Quasistatic Fading:** The channel matrix \mathbf{H} is assumed to be quasistatic meaning that the channel response is assumed to be a constant over a frame of T symbol periods. The channel is assumed to take statistically independent values from one frame to another. This model is widely agreed to be a good representation of slow-fading channels, especially in systems which use frequency hopping from frame to frame [1]-[4], [11][12][33][34].
- **Open Loop System:** We assume that the receiver knows the channel \mathbf{H} perfectly. This is a valid assumption in most systems since channel estimation through pilot sequences is an integral part of most communication systems [33]. Moreover, we consider a scenario where there is no feedback path from the receiver to the trans-

mitter. This condition makes the system strictly ‘open-loop’ and precludes us from using techniques which depend on any kind of receiver feedback such as waterfilling, eigenbeamforming or antenna selection [19]-[21].

- **Outer Error Correcting Code:** The design of MIMO transceivers is strongly influenced by the presence or absence of outer error correcting codes [33]. In the former case, the MIMO transceiver works in conjunction with the outer code to harvest the diversity advantage of the MIMO channel [5][6], [13]-[23]. Stand-alone MIMO transceivers, on the other hand, cannot depend on the error correction capability of an outer code. For this reason, stand-alone MIMO transceivers such as space-time codes [7]-[10] are typically designed with the objective of maximizing diversity gain, so that the overall system achieves the desired reliability. In this work, we design MIMO transceivers in the presence of outer codes.
- **Performance Metric – Outage Probability:** The capacity of a quasistatic, Rayleigh fading channel is an unbounded nonnegative random variable, with a non-zero probability of being less than ϵ for any $\epsilon > 0$ [33]. Consequently, the *Shannon capacity* of a quasistatic fading channel is *zero* [4], since we cannot guarantee an arbitrarily small error probability for any nonzero data rate. Therefore, an important performance metric of communication systems operating over for quasistatic fading channels is the *outage probability* [4][11].

The event of *outage* is declared when the instantaneous capacity of the wireless channel is less than the transmitted data rate and *outage probability* is the probability of occurrence of this event [4].

While the *data rate* of a communication system is measured in bits per second, we are interested in the *spectral efficiency*, which is the data rate normalized with respect to the signal bandwidth. Throughout this thesis, we will use the term ‘data rate’ to denote the spectral efficiency, measured in b/s/Hz, since we consider systems operating over the same bandwidth. Consider a wireless communication system operating over a MIMO channel \mathbf{H} , with an average SNR of S and a target data rate of R b/s/Hz. Let the instantaneous capacity of this MIMO channel be $C(\mathbf{H}, S)$. Now, we define the following.

Definition 1. The *outage probability*, P_{out} , of a wireless communication channel is the probability that the instantaneous channel capacity is less than the transmitted data rate [3][4].

$$P_{out}(S, R) = \Pr(C(\mathbf{H}, S) < R) . \quad (2)$$

If an outage occurs during a frame, the error probability of that frame is bounded away from zero, while otherwise it is possible to decode the frame with arbitrarily small error probability, provided the outer error correcting code is sufficiently long. Therefore, the outage probability is a lower bound on the achievable frame error rate of the system [11]. The bound can be approached by using a powerful error control code such as an LDPC code [44], [45] or a turbo code [46] as the outer code. Another important indicator of system performance over a wireless channel is the diversity order, which is defined as follows.

Definition 2. The *diversity order*, d , of a wireless communication channel is defined by the asymptotic slope of the outage probability on a logarithmic scale with respect to $\log S$ [3]:

$$d = \lim_{S \rightarrow \infty} \frac{-\log P_{out}(S, R)}{\log S}. \quad (3)$$

Diversity order is a good indicator of system performance at high SNR. Higher the diversity order, the steeper is the fall of the error rate curve as a function of SNR.

1.3 Organization of Part I of This Work

The remainder of Part I is organized as follows.

- In chapter , we present a survey of the state of the art in layered space-time architectures including V-BLAST, optimized versions of V-BLAST, and D-BLAST. We also review the linear and successive cancellation decoders, the staple of decoders used with layered space-time architectures.
- In chapter , we propose a joint transmit-receive optimization strategy to enhance the performance of V-BLAST. A combination of rate-normalized ordering algorithm with the partially uniform rate and energy allocation improves the performance of V-BLAST at no extra cost.
- In chapter , we introduce the STAR family of layered space-time architectures. STAR is a new family of architectures designed specifically to suit linear and successive cancellation decoders. We propose three versions of STAR, namely V-STAR, G-STAR and D-STAR with vertical, group and diagonal coding, respectively. We show that each version of STAR outperforms existing layered space-time architectures with the corresponding layering scheme, while exploiting the layered transmitter structure to maintain low decoding complexity. We also show

that each variant of STAR achieves near-optimum outage performance with no feedback from the receiver to the transmitter.

- In chapter , we discuss the diversity-multiplexing tradeoff of V-STAR and G-STAR. We show that V-STAR achieves full diversity for vertically coded systems over a certain range of MIMO channel dimensions, while still maintaining a high rate and low computational complexity. G-STAR also shows near optimal diversity gains with a high rate.
- In chapter , we explore the applications of the STAR transmission strategy to multiple-access communications, based on its similarity to vertically layered space-time architectures. We present numerical results to compare STAR against conventional multiple-access strategies and show that STAR achieves significant performance improvement at low complexity, while requiring no feedback from the receiver to the transmitting users.

PART I

LAYERED SPACE-TIME ARCHITECTURES FOR MULTIPLE- INPUT, MULTIPLE-OUTPUT RAYLEIGH-FADING CHANNELS

In Part I of this work, we design MIMO transceivers that achieve high data rates and low error rates while maintaining a low decoding complexity. We use a class of MIMO systems known as layered space-time architectures [5][6] to achieve the stated objectives. Layered space-time architectures are a class of MIMO transceivers where the transmitter encodes information into independent *layers* using scalar channel codes and transmits the layers through multiple transmit antennas, while the receiver employs low complexity decoders which exploit the layered structure of the transmitter to keep the decoding complexity to a minimum [5].

Traditionally, layered space-time architectures have suffered from poor error performance due to the suboptimality of the decoders, leaving substantial room for improvement [14]-[18]. We design layered space-time architectures, specifically the transmitter, to suit low complexity decoders so that near-optimum error probabilities could be achieved while retaining the other merits of layered space-time architectures. We propose a set of new architectures and show that it is possible to achieve outage probabilities within a 1-2 dB of the optimal value while requiring just SC decoding at the receiver.

CHAPTER 2

A SURVEY OF LAYERED SPACE-TIME ARCHITECTURES

It has been more than a decade since Foschini and Gans [3] and Telatar [4] in their seminal papers showed the advantages of using multiple transmit and receive antennas to improve the capacity and reliability of wireless communications. Since then, several transmitter and receiver design approaches have been proposed to achieve the promised diversity and multiplexing benefits of MIMO channels [5]-[23].

In this thesis, we propose a set of new MIMO transceivers, specifically a class of MIMO communication systems called layered space-time architectures to harvest the benefits offered by multiple antennas. A layered space-time architecture is composed of a transmission strategy and a reception strategy. At the transmitter, a layered space-time architecture encodes information into *layers* using scalar channel codes and transmits the layers through the multiple transmit antennas. The receiver employs decoders which exploit the special layered structure of the transmitter to keep the decoding complexity to a minimum [5][6][59].

Layered space-time architectures can be classified into two categories: a) vertical and b) diagonal. *Vertically layered architectures* are those in which each layer is constrained to span only one antenna [5][6]. Since each codeword is transmitted independently through one antenna, this type of layering is also known as *independent coding*. In literature, vertical architectures are also referred to as *spatial multiplexing systems* [14], [19]-[21], since these structures resemble parallel independent layers multiplexed through the

transmit antennas. *Diagonally layered ST architectures* are those in which each layer spans multiple transmit antennas [39][54][55][59]. Since each codeword is allowed to jointly code across multiple antennas, this type of layering is also known as *joint coding*.

By not coding across transmit antennas, vertical architectures sacrifice the possibility of transmit diversity gain. Hence, the full diversity for vertical layered ST architectures is equal to the receive diversity, r [14]. The V-BLAST architecture is an example of a vertical architecture. By coding across transmit antennas, diagonal architectures provide transmit diversity as well as receive diversity. The D-BLAST architecture is an example of a diagonal architecture [59]. Despite its diversity advantages, D-BLAST has other disadvantages as we will discuss later in Section 2.7.

In this chapter, we will overview some of the currently available layered space-time architectures. This chapter is organized as follows: In Section 2.1, we introduce the simplest layered space-time transmitter, the vertically layered *naive spatial multiplexer*. In Section 2.2, we discuss the linear detector in conjunction with the naive spatial multiplexer and define its outage probability. In Section 2.3, we introduce two variants of the successive cancellation decoder, one of which is used along with the naive spatial multiplexer to form the V-BLAST architecture. In Section 2.4, we review another architecture which uses spatial multiplexing with rate allocation. In Section 2.5, we establish the best outage performance achievable by any vertically layered architecture as a benchmark. In Section 2.6, we present some numerical results for these layered space-time architectures. In Section 2.7, we review the diagonally layered D-BLAST architecture. In Section 2.8, we summarize the results of this chapter.

2.1 The Simplest Layered Space-Time Transmitter

The V-BLAST (vertical Bell Labs layered space-time) architecture was proposed by Wolniansky et al. of Bell Labs in 1997 [5] as a simple way of achieving high data rates over wireless channels, combining a simple transmitter with a low complexity decoder at the receiver.

The V-BLAST architecture uses a simple MIMO transmitter. This transmitter, which we will refer to as the *naive spatial multiplexer*, multiplexes t parallel independent data streams, each encoded using a scalar channel code, through the t transmit antennas, as shown in Fig. 2. Each of these t streams is known as a *layer*. Clearly, this is an example of a vertically layered architecture and hence the name vertical-BLAST. The i^{th} data stream carries an information rate of R_i b/s/Hz with an average energy of E_i . The total data rate is $R = \sum_{i=1}^t R_i$, and the average transmit energy is $E = \sum_{i=1}^t E_i$.

The layered structure of this transmitter enables sequential decoding of the layers, thereby allowing low complexity decoding. In the following we describe two candidate decoding algorithms, namely the linear detector and the successive cancellation decoder [5], before describing a specially optimized variant of the successive cancellation decoder used by V-BLAST.

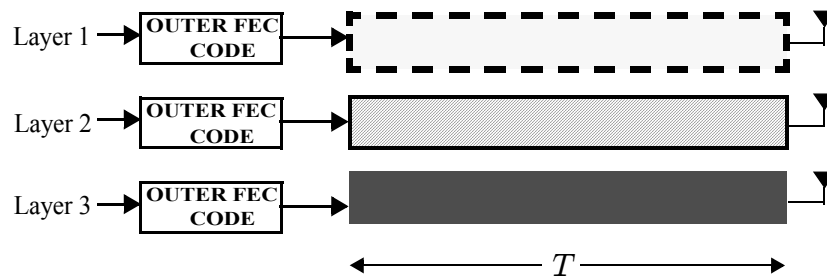


Fig. 2. A 3-transmit antenna naive spatial multiplexer: Transmitter structure of V-BLAST.

Since the channel is linear, flat-fading and quasistatic, the received vector at the k -th signaling interval is:

$$\mathbf{y}_k = \mathbf{H}\mathbf{x}_k + \mathbf{n}_k. \quad (4)$$

2.2 Linear detector

The linear detector is the simplest MIMO detector for layered space-time architectures [33]. The linear detector converts the problem of joint decoding of the layers into one of individual decoding of the layers, by applying a feed-forward filter on the received vector. The feed-forward filter could either be a *zero-forcing* (ZF) filter or an *minimum mean-square error* (MMSE) filter. The ZF filter decorrelates the layers, completely nulling out the interference between them, while the MMSE filter minimizes the squared error between the vector of transmitted symbols and its estimate [33].

A ZF linear detector multiplies the received vector with a feed-forward filter \mathbf{W} to get

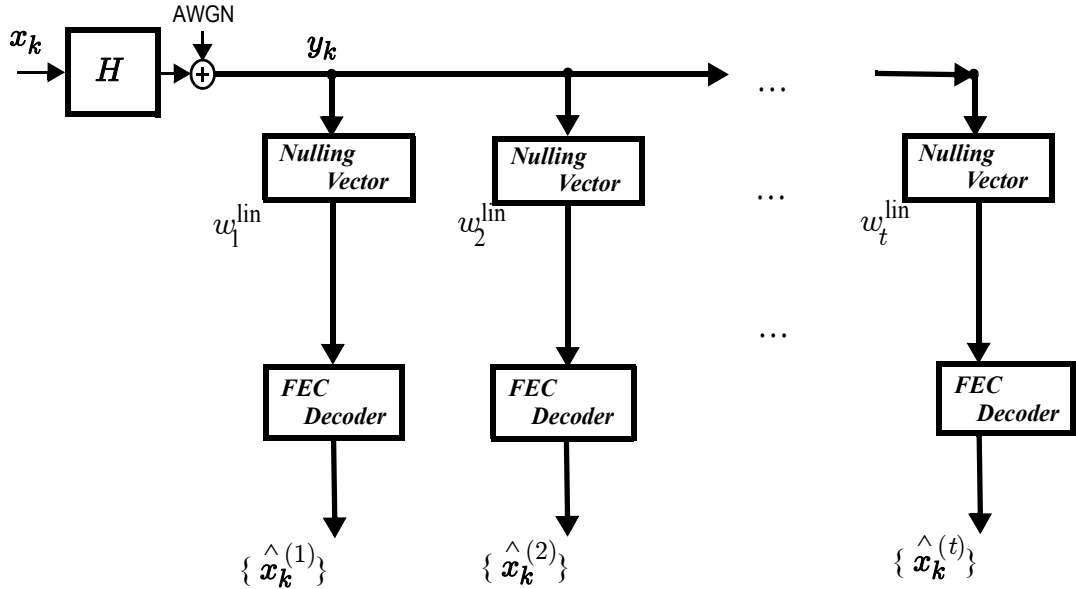


Fig. 3. Linear decoding for a t -transmit antenna naive spatial multiplexing system.

$$\mathbf{z}_k = \mathbf{W}\mathbf{y}_k = \mathbf{x}_k + \mathbf{W}\mathbf{n}_k, \quad (5)$$

where $\mathbf{W} = (\mathbf{H}^* \mathbf{H})^{-1} \mathbf{H}^*$ is the Moore-Penrose pseudo inverse of \mathbf{H} . Note that the components of effective noise $\mathbf{W}\mathbf{n}_k$ are no longer independent. Hence, the optimal way to decode the layers is to do so jointly. However, a linear decoder decodes the layers independently anyway to reduce complexity. The linear detector obtains the i^{th} decision stream, $\mathbf{z}_k^{(i)} = \mathbf{w}_i^{\text{lin}} \mathbf{y}_k$, where $\mathbf{w}_i^{\text{lin}}$ is the i^{th} row of \mathbf{W} . Thus the channel model reduces to

$$\mathbf{z}_k^{(i)} = \mathbf{x}_k^{(i)} + \mathbf{w}_i^{\text{lin}} \mathbf{n}_k. \quad (6)$$

The equivalent channel (6) is an AWGN channel with noise variance $N_0 \|\mathbf{w}_i^{\text{lin}}\|^2$. The estimates $\{\hat{\mathbf{x}}_k^{(i)}\}$ of the i^{th} layer are obtained from $\{\mathbf{z}_k^{(i)}\}$. The SNR of a layer for a given channel realization at the output of the linear detector is a function of $\gamma_i^{\text{lin}} = 1/\|\mathbf{w}_i^{\text{lin}}\|^2$.

Recall that the i^{th} data stream has an average energy E_i , hence the instantaneous SNR of the effective channel is $E_i \gamma_i^{\text{lin}} / N_0$, and the instantaneous capacity is $\log_2(1 + E_i \gamma_i^{\text{lin}} / N_0)$. Hence, an outage occurs if and only if

$$C_i(\mathbf{H}) \equiv \log_2(1 + E_i \gamma_i^{\text{lin}} / N_0) < R_i. \quad (7)$$

As shown in Fig. 3, the overall linear detector is a bank of parallel scalar decoders, one for each stream. If *all* data streams are outage-free, then the system is outage-free. However, if *any* of the streams is in outage, then the system is in outage. Thus, the outage probability of the coded system is

$$P_{\text{lin}}(S, R) = \Pr \left(\bigcup_{i=1}^t \{C_i(\mathbf{H}) < R_i\} \right). \quad (8)$$

2.3 Successive Cancellation Decoder

The successive cancellation (SC) decoder is a nonlinear decoder that can significantly outperform the linear detector [5][33]. SC decoders decode one layer at a time, subtracting out the estimated contribution of previously decoded layers from the received vector, before applying a feed-forward filter to detect a new layer.

In order to decode all the symbols $\{\hat{\mathbf{x}}_k^{(i)}\}$ in the i^{th} layer, the SC decoder cancels off the estimated contribution from the previously detected data streams to obtain

$$\mathbf{y}_k^{(i)} = \mathbf{y}_k - \sum_{l=1}^{i-1} \mathbf{h}_l \hat{\mathbf{x}}_k^{(l)}, \quad (9)$$

If previous decisions are correct, then $\{\mathbf{y}_k^{(i)}\}$ contains contributions only from the stream of interest i , and interference from the undecoded streams. To null out the interference, the zero-forcing SC decoder uses the *nulling vector* \mathbf{w}_i^{SC} , defined as the first row of the Moore-Penrose inverse of the matrix $[\mathbf{h}_i, \mathbf{h}_{i+1}, \dots, \mathbf{h}_t]$ [5]. Using the nulling vector, the

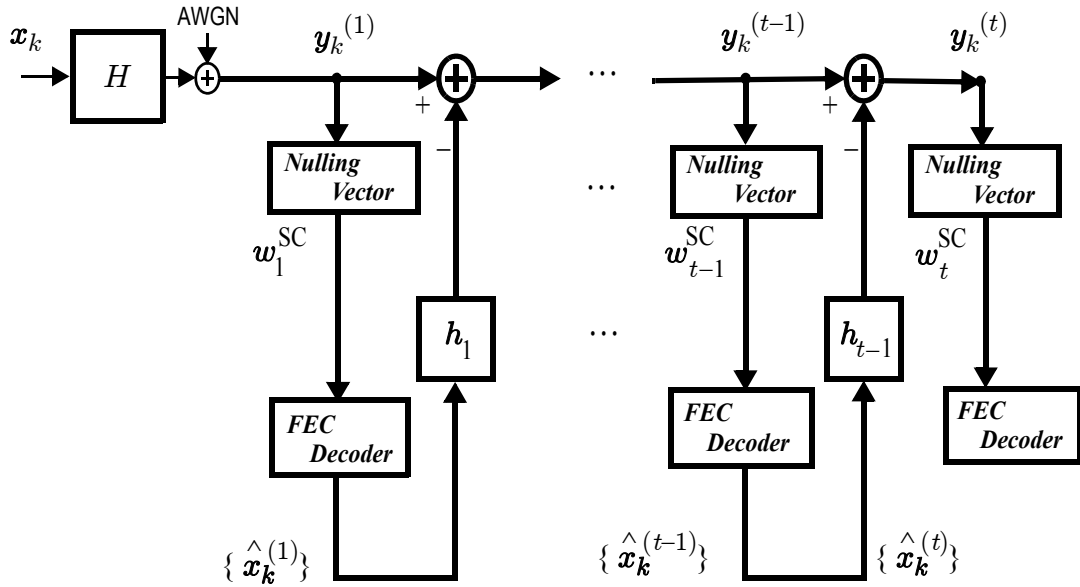


Fig. 4. Successive cancellation decoding algorithm for a t-transmit antenna naive spatial multiplexer.

SC decoder obtains the i^{th} decision stream, $\mathbf{z}_k^{(i)} = \mathbf{w}_i^{SC} \mathbf{y}_k^{(i)}$. Assuming perfect decision feedback, the channel model reduces to

$$\mathbf{z}_k^{(i)} = \mathbf{x}_k^{(i)} + \mathbf{w}_i^{SC} \mathbf{n}_k. \quad (10)$$

The equivalent channel (10) is an AWGN channel with noise variance $N_0 \|\mathbf{w}_i^{SC}\|^2$. The estimates $\{\hat{\mathbf{x}}_k^{(i)}\}$ of the i^{th} layer are obtained from $\{\mathbf{z}_k^{(i)}\}$. The SNR of a layer for a given channel realization at the output of the SC decoder is a function of $\gamma_i = 1/\|\mathbf{w}_i^{SC}\|^2$. The quantity $E_i \gamma_i / N_0$ is known as the post-detection SNR of the i^{th} layer and γ_i is known as the SNR scaling factor. We now quantify the outage probability of the SC decoder, as a function of $\{R_i\}$, $\{E_i\}$ and $\{\gamma_i\}$. The i^{th} layer has a post-detection SNR of $E_i \gamma_i / N_0$, and hence the instantaneous capacity is $\log_2(1 + E_i \gamma_i / N_0)$. If each data stream is coded using a capacity-achieving scalar error correcting code, a stream is incorrectly decoded if and only if an *outage* occurs, i.e., if and only if

$$C_i(\mathbf{H}) \equiv \log_2(1 + E_i \gamma_i / N_0) < R_i. \quad (11)$$

As shown in Fig. 4, the overall SC decoder is a bank of parallel scalar decoders, one for each stream. If *all* data streams are outage-free, the SC decoder is also outage-free. However, if *any* of the streams is in outage, the SC decoder is in outage, and hence has a nonzero probability of frame error. Consequently, the frame-error rate of the coded system is upper-bounded by the *outage probability*

$$P_{SC}(S, R) = \Pr \left(\bigcup_{i=1}^t \{C_i(\mathbf{H}) < R_i\} \right). \quad (12)$$

The performance of the SC decoder can be improved by changing the order of detection of the layers. The optimal order is channel dependent. The order can be described by the permutation $\pi(1, 2, \dots, t)$, where π_k is the index of the k^{th} detected layer. Let Π be the matrix whose k^{th} column is the π_k^{th} column of the identity matrix. Once the decoder computes the optimal order based on \mathbf{H} , it performs fixed ordered SC decoding on $\mathbf{H}\Pi$ instead of \mathbf{H} . Also, for convenience, we define the *inverse ordering vector* $\pi^{-1} = [\pi_1^{-1}, \pi_2^{-1}, \dots, \pi_t^{-1}]$ such that $q = \pi_{\pi_q}^{-1}$ for $q = 1, 2, \dots, t$.

For a given channel realization \mathbf{H} , the capacity of the k^{th} layer detected is given by

$$C_i(\mathbf{H}) = \log_2 \left(1 + \frac{E_i}{N_0} \|\mathbf{h}_i - \hat{\mathbf{h}}_i(\Omega)\|^2 \right), \quad (13)$$

where $\Omega = \{\pi_{k+1}, \dots, \pi_t\}$, and $\hat{\mathbf{h}}_i(\Omega)$ denotes the projection of \mathbf{h}_i on the subspace spanned by \mathbf{h}_l for all $l \in \Omega$, where we used the fact that [33]

$$\|\mathbf{w}_i\| = \frac{1}{\|\mathbf{h}_i - \hat{\mathbf{h}}_i(\Omega)\|}. \quad (14)$$

Alternatively, the SNR scaling factor can also be expressed in terms of the quadratic-residue (QR) decomposition of \mathbf{H} [22]. If the QR decomposition of \mathbf{H} is given by $\mathbf{H} = \mathbf{Q}\mathbf{R}$, the SNR scaling factor of the i^{th} layer is equal to the squared diagonal entries of \mathbf{R} ,

$$\gamma_i = \frac{1}{\|\mathbf{w}_i\|^2} = \|\mathbf{h}_i - \hat{\mathbf{h}}_i(\Omega)\|^2 = \mathbf{R}_{ii}^2. \quad (15)$$

In the following section, we will discuss two popular ordering algorithms for successive cancellation decoding of the naive spatial multiplexing transmitter.

2.3.1 Fixed ordered SC decoder

The simplest ordering algorithm is *fixed ordering*, where the streams are decoded simply in their natural order, i.e., $\pi = [1, 2, \dots, t]$, irrespective of \mathbf{H} . In this case, it is well known [26] that the SNR scaling factors of the different layers $\{\gamma_i\}$ are mutually independent random variables. Thus, the outage probability reduces to

$$P_{fixed}(S, R) = \Pr\left\{ \bigcup_{i=1}^t \left[\gamma_i < \frac{2^{R_i} - 1}{E_i/N_0} \right] \right\}. \quad (16)$$

Further, from [26], γ_i has a χ^2 -distribution with $2(r - t + i)$ degrees of freedom, hence

$$\Pr[\gamma_i < x] = 1 - \exp(-x) \sum_{l=0}^{r-t+i} \frac{1}{l!} \left(\frac{1}{x} \right)^l. \quad (17)$$

Substituting (17) in (16) gives a closed form expression for the outage probability with fixed ordered SC decoding. Also, (16) can be bounded using the union bound as:

$$P_{fixed}(S, R) \leq \sum_{i=1}^t \Pr\left\{ \gamma_i < \frac{2^{R_i} - 1}{E_i/N_0} \right\}. \quad (18)$$

It was shown in [11] that $\Pr[\gamma_i < \varepsilon]$ can be approximated as $\Pr[\gamma_i < \varepsilon] \rightarrow \varepsilon^n$ for $\varepsilon \rightarrow 0$, since γ_i is χ^2 -distributed with $2n$ degrees of freedom. For any layer with $E_i \neq 0$, we can write $E_i/N_0 = \lambda_i S$ for some $0 < \lambda_i \leq 1$. Therefore, $\frac{2^{R_i} - 1}{E_i/N_0} \rightarrow 0$ as $S \rightarrow \infty$, and consequently [22]

$$\Pr\left\{ \gamma_i < \frac{2^{R_i} - 1}{E_i/N_0} \right\} \rightarrow \left(\frac{2^{R_i} - 1}{\lambda_i} \right)^{(r-t+i)} \frac{1}{S^{(r-t+i)}} \quad (19)$$

as $S \rightarrow \infty$. From this result, we can infer that (18) is a summation of t probabilities each of which decays as different polynomial orders in S . The decay rate of the i^{th} layer outage probability is $r - t + i$, and consequently the diversity order of the i^{th} layer is $(r - t + i)$ [22]. Clearly, as S increases, the outage probability is limited by the probability with the slowest decay, which is the first layer. Hence, the diversity order, d_{fixed} , of fixed ordered SC decoding of the naive spatial multiplexer is [22]

$$d_{fixed} = r - t + 1. \quad (20)$$

Compare this with the optimal diversity order of spatial multiplexing systems, $d_{SM} = r$ [11]. The diversity order clearly indicates that fixed ordered SC decoding yields suboptimal outage performance.

2.3.2 *BLAST ordered SC decoder*

Another variant of the SC decoder uses a specially ordered SC decoder, known as the BLAST ordering algorithm [5]. The naive spatial multiplexer along with this decoder constitutes the popular V-BLAST architecture. This ordering algorithm can be summarized as follows.

Given \mathbf{H} , the first stream to be decoded, π_1 , is chosen as the one with the nulling vector of least magnitude, i.e., the maximum SNR scaling factor. The next stream, π_2 , is chosen to maximize γ_2 , among the remaining $t - 1$ choices, and so on. It was shown in [5] that this greedy ordering algorithm is also globally optimum, as stated below.

Remark 1. For stages $j = 1, 2, \dots, t$, the BLAST ordering algorithm chooses π_j so as to achieve the maximum value of γ_j among the $t - j + 1$ possibilities.

In the process, it also maximizes the minimum of the SNR scaling factors, namely $\min(\gamma_1, \gamma_2, \dots, \gamma_t)$ [5]. The optimal order is chosen as

$$\pi_k = \underset{i \notin \{\pi_1, \dots, \pi_{k-1}\}}{\operatorname{argmax}} \left\| \mathbf{h}_i - \hat{\mathbf{h}}_i(\Omega) \right\|^2, \quad (21)$$

where $\hat{\mathbf{h}}_i(\Omega)$ is the projection of \mathbf{h}_i on the subspace spanned by $\{\mathbf{h}_{\pi_{k+1}}, \mathbf{h}_{\pi_{k+2}}, \dots, \mathbf{h}_{\pi_t}\}$. The V-BLAST architecture is a combination of the naive spatial multiplexing transmitter with the BLAST-ordered SC decoder.

The SNR scaling factors $\{\gamma_1, \gamma_2, \dots, \gamma_t\}$ produced by BLAST ordering are not mutually independent and obtaining a closed form expression for the density function of $\{\gamma_i\}$ is still an open problem. For convenience, we define the SNR scaling vector $\Gamma = [\gamma_1, \gamma_2, \dots, \gamma_t]$. The BLAST ordering algorithm can be viewed as a function $\Psi(\mathbf{H})$ of the channel matrix \mathbf{H} , which outputs the pair (π, Γ) . The following properties hold for the ordering vector π and the SNR scaling vector Γ produced by the BLAST ordering algorithm.

Lemma 1. For a given channel matrix \mathbf{H} , suppose $\Psi(\mathbf{H}) = (\pi, \Gamma)$. Then, for all column permutation matrices \mathbf{P} ,

$$\Psi(\mathbf{H}\mathbf{P}) = (\mathbf{P}^T \pi, \Gamma). \quad (22)$$

Proof: Suppose the symbol x_q corresponding to $\pi(1) = q$ was decoded in the 1st stage with channel \mathbf{H} , the same symbol, re-labelled as $\pi'(1) = q'$, where $\pi' = \mathbf{P}^T \pi$ will be decoded in the 1st stage with the permuted channel $\mathbf{P}\mathbf{H}$. Clearly, the value of the maximum post detection SNR remains unchanged for that stage, since it corresponds

to the same symbol. Similarly, proceeding through the stages $k = \{2, 3, \dots, t\}$, the post detection SNRs remain invariant to permutation, and that multiplying \mathbf{H} by \mathbf{P} amounts to re-labelling the index of the symbols, as determined by \mathbf{P} .

It is well known that permuting the columns of Rayleigh fading matrices does not change their distribution. More precisely, the following result holds.

Lemma 2. Suppose \mathbf{H} is a Rayleigh fading matrix. Then, for all column permutation matrices \mathbf{P} , the random matrix $\mathbf{H}' = \mathbf{HP}$ is identical in distribution to \mathbf{H} .

From Lemma 2, \mathbf{HP} is identical in distribution to \mathbf{H} . Using Lemma 1, we arrive at the following corollary.

Corollary 1. $\Psi(\mathbf{HP}) = (\mathbf{P}^T \pi, \Gamma)$ is identical in distribution to $\Psi(\mathbf{H}) = (\pi, \Gamma)$.

Theorem 1. For a Rayleigh fading channel, the ordering vector π and the SNR scaling vector Γ produced by the BLAST ordering algorithm are independent. Further, π is uniformly distributed over the set of all permutations of $[1, 2, \dots, t]^T$.

Proof: From Corollary 1, since $\mathbf{P}^T \pi$ is identical in distribution to π , we conclude that π is uniformly distributed over all permutations of $[1, 2, \dots, t]^T$. Further, from Corollary 1, note that joint density function of (π, Γ) satisfies $p(\pi, \Gamma) = p(\mathbf{P}^T \pi, \Gamma)$. Now, using Bayes' rule and the fact π is uniformly distributed over $t!$ possibilities, we obtain the following expression for the joint density function, $p(\pi, \Gamma) = \frac{1}{t!} p(\Gamma | \pi)$. In particular, $p(\pi, \Gamma) = p(\mathbf{P}^T \pi, \Gamma) \Leftrightarrow p(\Gamma | \pi) = p(\Gamma | \mathbf{P}^T \pi)$ for all \mathbf{P} , implying that Γ and π are independent. This proves the second claim of Theorem 1.

2.4 Spatial Multiplexing with Rate Allocation

In this section, we review another layered space-time system which is obtained as a transmitter optimized version of spatial multiplexing proposed in [14], for successive cancellation decoders. Specifically, this scheme is obtained by allocating the available energy and data rate among the transmit antennas based on the statistical properties of the channel and the SC decoder.

The *transmitter optimization* problem can be stated as follows: Choose the $\{R_i\}$ and $\{E_i\}$ to minimize the outage probability of the spatial multiplexing system with fixed ordered SC decoding at a given SNR, under the constraints that $\sum_{i=1}^t R_i = R$ and $\sum_{i=1}^t E_i = E$.

The problem of optimum rate and energy allocations for a naive spatial multiplexing transmitter was solved in [14][22] by Prasad and Varanasi using constrained numerical optimization. Here, we provide a numerical example to illustrate this optimization procedure for a 4-input, 4-output MIMO system operating at a data rate of $R = 8$ b/s/Hz. At an SNR of $S = 15$ dB, numerical optimization yields the optimum data rate allocation to be $\{R_i\} = \{0, 1.31, 2.99, 3.70\}$ and the corresponding energy allocation to be $\{E_i\} = \{0, 0.25, 0.36, 0.39\}E$. At $S = 20$ dB with a fixed ordering, the optimal rates and energies are $\{0, 0, 3.63, 4.37\}$, and $\{0, 0, 0.49, 0.51\}E$, respectively, which leads to an outage probability of 0.002422. In comparison, a uniform rate allocation with fixed ordering gives an outage probability of 0.1201, about fifty times larger. Note that the streams detected later carry a higher data rate than streams detected early. This result is intuitively satisfying because a higher fraction of the bits are loaded into streams with higher diversity orders.

2.5 Optimum Outage Probability of Vertical Architectures

Thus far, we have discussed some suboptimal decoders which use the structure of layered architectures to enable low complexity decoding. We now define the optimum outage probability of any vertically layered architecture to serve as a benchmark for the performance of all vertical architectures.

The constraint of vertical layering makes a layered space-time architecture identical to a multiple-access system with t independent single-antenna transmitters and a receiver with r antennas. Hence, the minimum achievable outage probability of a vertically layered system is identical to that of a multiple access system and is given as [4][14]

$$P_{SM}(S, R) = \Pr\left(\bigcup_{\mathbf{v} \in \mathcal{N}} \left\{ \log_2 \det\left(\mathbf{I} + \frac{S}{t} \mathbf{H}_{\mathbf{v}} \mathbf{H}_{\mathbf{v}}^*\right) < \sum_{i \in \mathbf{v}} R_i \right\}\right), \quad (23)$$

where, \mathcal{N} is the set of all $2^t - 1$ nonempty subsets of $\{1, 2, \dots, t\}$, with \mathbf{v} denoting each element of \mathcal{N} . In (23), $\mathbf{H}_{\mathbf{v}}$ denotes the decimated channel matrix consisting of only those columns of \mathbf{H} specified by \mathbf{v} . For example, if $\mathbf{v} = [2, 3, 4]$, $\mathbf{H}_{\mathbf{v}} = \mathbf{H}_{[2, 3, 4]} = [\mathbf{h}_2, \mathbf{h}_3, \mathbf{h}_4]$, where \mathbf{h}_i denotes the i^{th} column of the channel matrix \mathbf{H} . The diversity order corresponding to this outage probability is $d_{SM} = r$.

The optimum outage probability is achievable by using a joint ML decoder at the receiver with the transmitter being a naive spatial multiplexer [33]. However the joint ML decoder is exponentially complex in the product of the number of transmit antennas and the length of the codeword. Although the naive spatial multiplexer is optimal in combination with the joint ML decoder, we will see in the next section that the same transmitter yields very poor outage performance with suboptimal decoders.

2.6 Numerical Results for Vertically Layered Architectures

In this section, we present numerical results for the outage probability of layered space-time architectures considered thus far. We consider a 4-transmit, 4-receive MIMO channel with a target data rate of $R = 8$ b/s/Hz.

Fig. 5 shows the outage probabilities of naive spatial multiplexing with linear decoding, fixed-ordered SC decoding, BLAST-ordered SC decoding, and spatial multiplexing with rate allocation with SC decoding, as a function of the average SNR per receive antenna. Also shown in the figure is the optimum outage probability of vertically layered architectures. From Fig. 5 we see that naive spatial multiplexing with linear decoding, fixed and ordered successive cancellation decoding suffer from lack of diversity, resulting in poor outage performance at high SNR. Transmitter optimized spatial

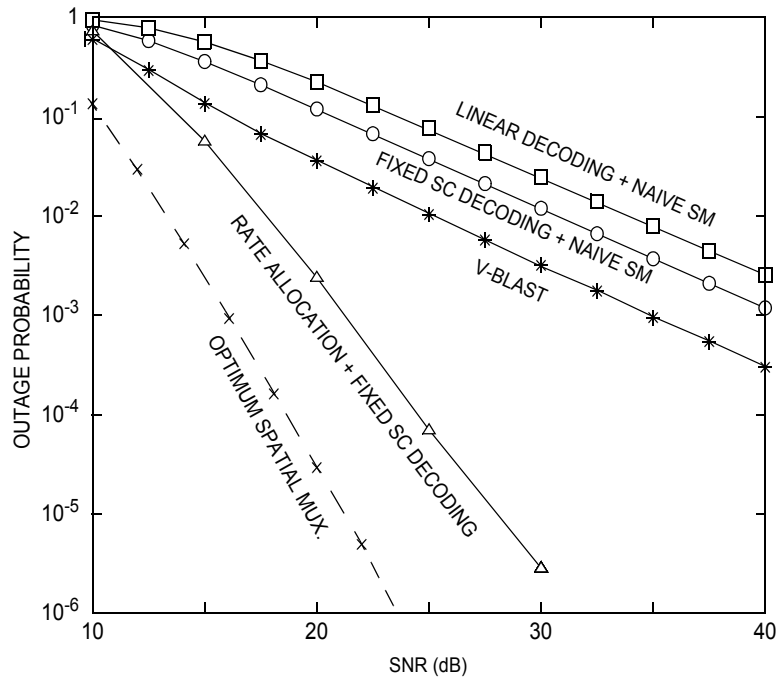


Fig. 5. Naive spatial multiplexing vs. transmitter optimized spatial multiplexing with $t = 4$, $r = 4$.

multiplexing significantly improves the outage performances over naive spatial multiplexing with SC decoding. At an outage probability of 10^{-3} , transmitter optimization with fixed ordering outperforms V-BLAST by 13.5 dB.

Fig. 6 summarizes the currently available spatial multiplexing techniques in terms of the tradeoff between outage performance and computational complexity. The x -axis represents an approximate estimate of the decoding complexity required by the scheme, while the y -axis represents the SNR required by the scheme to achieve an outage probability of 10^{-3} . We would like the ideal scheme to be placed as close to the bottom-left corner as possible. Naive spatial multiplexing with BLAST ordering is around 18.7 dB away from optimal. Transmitter optimization with fixed ordered SC decoding cuts the gap all the way down to 5.2 dB, but we see that there is scope for further improvement. As we discuss various new schemes, we will keep updating this tradeoff chart.

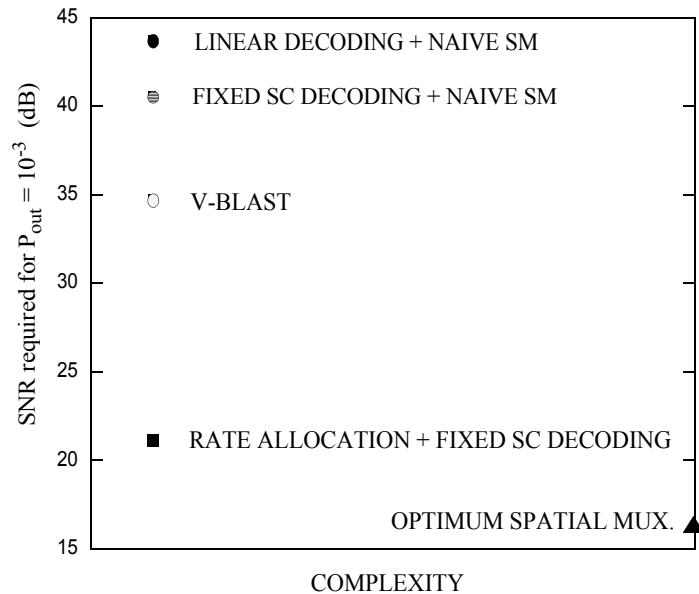


Fig. 6. Performance-complexity tradeoff of spatial multiplexing techniques for $t = 4$, $r = 4$, $R = 8$ b/s/Hz.

2.7 Overview of the D-BLAST Architecture

In this section, we briefly overview the *diagonal Bell Labs layered space-time architecture* (D-BLAST) proposed by Foschini in [59]. The D-BLAST architecture uses diagonal layering, where each layer spans multiple transmit antennas as opposed to just one in, say, V-BLAST.

The D-BLAST transmitter structure is shown in the Fig. 7. The transmitter encodes the information to be transmitted (message bits) into independent layers using powerful error correcting codes. The layers are then transmitted in a diagonal fashion as shown in Fig. 7. Each layer spans all the transmit antennas. At the transmitter, D-BLAST divides the static fading frame is divided into B_D blocks each of length T/B_D symbol periods, as represented by squares shaded with different patterns in Fig. 7. Each layer is tT/B_D symbol periods long and can be viewed as a concatenation of t segments containing T/B_D symbols each. The transmitter sends the i^{th} segment of the first layer through the i^{th} transmit antenna, during the i^{th} block. In general, the transmitter sends the i^{th} segment of the j^{th} layer through the i^{th} transmit antenna during the $(j - 1 + i)^{\text{th}}$ block. Hence, the first layer requires that there be minimum of t blocks, with each subsequent layer requiring one

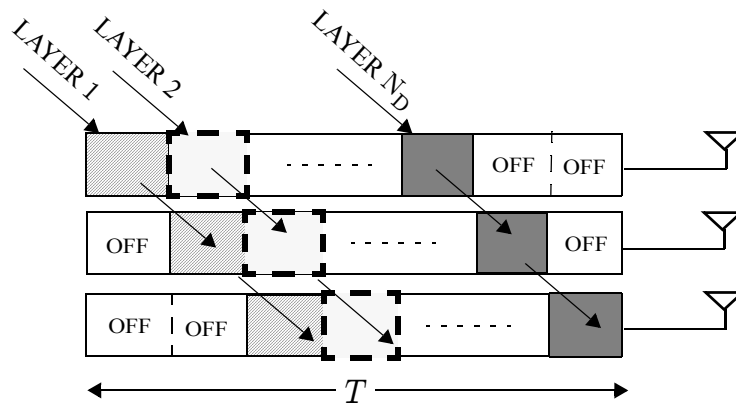


Fig. 7. The D-BLAST architecture, with $t = 3$.

additional block. Therefore, if the number of layers is N_D , then the corresponding number of blocks is $B_D = N_D + (t - 1)$. Each layer is transmitted with an energy of E/N_D with each block having an average energy E/tN_D , so that the total average SNR for the D-BLAST transmitter is $S = E/N_0$.

The receiver uses fixed ordered successive cancellation decoding to decode the layers, starting with the first layer. The decoding of the first layer proceeds as follows. Note that the first segment of the first layer has no interference from another layer, the second segment has one interfering layer, and so on. The decoder uses either ZF or MMSE nulling to obtain estimates of all t segments that compose the layer, and then decodes all t segments jointly. Subsequently, the contribution of this layer is cancelled out from the received symbols and the second layer is decoded in identical fashion. This sequential decoding process continues till all the layers are decoded. For this decoding procedure to work, D-BLAST requires the presence of inactive blocks at the beginning and end of a frame, as indicated by ‘OFF’ in Fig. 7.

Let the post-detection SNR of the j^{th} segment of the i^{th} layer be $S_i^{(j)}$. Then, the instantaneous capacity of the i^{th} layer in D-BLAST is [33]

$$C_i(\mathbf{H}) = \frac{1}{B_D} \sum_{j=1}^t \log(1 + S_i^{(j)}). \quad (24)$$

Note that $S_i^{(j)} = S_k^{(j)}$ and consequently $C_i(\mathbf{H}) = C_k(\mathbf{H})$ for any two layers i and k , since the all the layers are symmetric. Therefore, we substitute $S_i^{(j)} = S^{(j)}$ and $C_i(\mathbf{H}) = C(\mathbf{H})$. The outage probability, which is defined as the probability that any of the layers is in outage, is given by

$$\Pr(C(\mathbf{H}) < R) = \Pr\left(\frac{1}{B_D} \sum_{j=1}^t \log_2(1 + S^{(j)}) < \frac{R}{N_D}\right), \quad (25)$$

where, N_D is the total number of layers and R is the total target data rate. Further, substituting for B_D , (25) can be simplified as

$$\Pr(C(\mathbf{H}) < R) = \Pr\left(\sum_{j=1}^t \log_2(1 + S^{(j)}) < R\left(1 + \frac{t-1}{N_D}\right)\right). \quad (26)$$

It was shown in [59] that for D-BLAST with MMSE-SC decoding,

$$\sum_{j=1}^t \log_2(1 + S^{(j)}) = \log_2 \det\left(\mathbf{I} + \frac{(N_D + t - 1)S}{N_D t} \mathbf{H}^* \mathbf{H}\right). \quad (27)$$

Now, (26) and (27) can be combined to get

$$\Pr(C(\mathbf{H}) < R) = \Pr\left(\log_2 \det\left(\mathbf{I} + \left(1 + \frac{t-1}{N_D}\right) \frac{S}{t} \mathbf{H}^* \mathbf{H}\right) < R\left(1 + \frac{t-1}{N_D}\right)\right). \quad (28)$$

In the above equation, the term $\left(1 + \frac{t-1}{N_D}\right)$ on the right hand side represents a *rate penalty* because of the presence of the inactive blocks at the beginning and the end of a D-BLAST frame. Otherwise (28) is identical to the outage probability of a MIMO channel [4]. As the number of layers increases, i. e., as $N_D \rightarrow \infty$,

$$\lim_{N_D \rightarrow \infty} \Pr(C(\mathbf{H}) < R) = \Pr\left(\log_2 \det\left(\mathbf{I} + \frac{S}{t} \mathbf{H}^* \mathbf{H}\right) < R\right), \quad (29)$$

and this equation is identical to the outage probability of the MIMO channel. Consequently, it is claimed in [59] that D-BLAST approaches the MIMO capacity as the

number of layers increases, since the length of the OFF blocks keep getting shorter as the number of layers increase, and the corresponding penalty becomes progressively less significant. However, there is a problem with this argument.

As the number of layers is increased, the length of each layer is shortened and hence the length of the code used by a layer is shortened, eventually preventing the code from approaching layer capacity [33][39][54]. It is well known from Shannon's channel coding theorem that long codewords are required to approach capacity [25]. On the other hand, if longer codes are used, then N_D is not high anymore. Hence, there is a fundamental tradeoff between the codelength and the number of layers and consequently a tradeoff between the codelength and rate penalty incurred in a D-BLAST system [33].

We now evaluate the tradeoff between codelength and rate penalty in D-BLAST with the following simple computations. Each layer in D-BLAST occupies t segments, and the addition of one layer to the D-BLAST architecture occupies one more segment. Thus, the relationship between the number of layers and the length of each layer is

$$N_D + (t - 1) = Tt / L_D. \quad (30)$$

The maximum possible code length for a static fading frame of length T symbol periods is T . We define the *fractional code length* as the ratio of the actual code length to the maximum possible code length, T . This quantity is given by

$$L_D/T = t/(N_D + t - 1). \quad (31)$$

For example, when $t = 4$ and the number of layers is $N_D = 17$, then $L_D/T = 1/5$. This corresponds to a low *rate penalty* of $\left(1 + \frac{t-1}{N_D}\right) = 1.176$. However, this also corresponds to a codelength L only 20% of T . As the number of layers is increased further, the

codelength shrinks even further. In fact, the actual codelength in a D-BLAST transmitter is equal to the maximum possible codelength only if $N_D = 1$, i.e., with just one layer. However, the long codelength comes at a high *rate penalty* of $\left(1 + \frac{t-1}{N_D}\right) = t$. In order to approach the MIMO capacity, D-BLAST would require small rate penalties which corresponds to short codelengths [33][39]. On the other hand, long codes are required for practical codes to achieve capacity. Moreover, if the shortened codes fail to achieve capacity, error propagation effects can significantly harm system performance [33].

In Fig. 8, we present a simple plot to further illustrate the tradeoff between the codelength and number of layers and, consequently, the rate penalty. We consider the outage probability of a D-BLAST system given by (28) for a 4×4 MIMO channel with a target data rate of $R = 8$ b/s/Hz. Starting with $N_D = 1$, we evaluate the outage probability of D-BLAST as given by (28) for varying number of layers used in D-BLAST. For each case, we compute the SNR gap of the D-BLAST system to the optimum MIMO channel

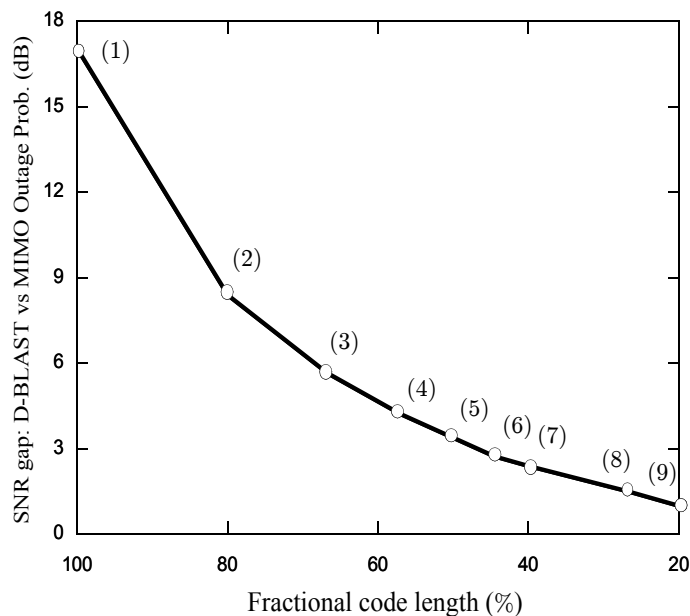


Fig. 8. SNR gap of D-BLAST to MIMO channel outage probability as a function of fractional code length with $t = 4$, $r = 4$ with $R = 8$ b/s/Hz at an outage probability of 10^{-3} . MIMO channel outage probability = 10^{-3} at $S = 11.01$ dB.

outage probability, given by (29), at an outage probability of 10^{-3} . For each of these cases, we also compute the corresponding fractional codelength, given by (31). Fig. 8 shows this SNR gap of D-BLAST to the MIMO channel outage probability as a function of the codelength, with the corresponding number of layers shown in brackets.

We observe that for long codelengths, D-BLAST suffers a high rate penalty and hence has a large gap to the MIMO channel outage probability. For example, for $N_D = 1$, D-BLAST is about 17 dB away from the optimum scheme. On the other hand, for $N_D = 9$, the gap is close as 1 dB. However, this allows for a codelength of only 20% of the maximum possible codelength, which may not approach the layer capacity, as discussed earlier.

As for the question of what code length is sufficient to ensure that each layer is decoded with sufficient reliability, it is a function of the actual channel code used along with the decoding scheme. A detailed characterization of this tradeoff is still an open problem. A promising approach would be to use the sphere packing bound and error exponents to quantify the performance of error control codes as a function of codelengths [4][60].

2.8 Summary

In this chapter, the concept of layered space-time architectures was briefly introduced along with the typical decoding schemes for these architectures. The state of the art in vertical and diagonal layered space-time architectures was reviewed, and their relative advantages and drawbacks were discussed. Currently, layered space-time architectures are viewed as high rate multiple-antenna transmission schemes which permit low decoding

complexity at the receiver due to their special structures. However, it was also observed that layered space-time architectures suffer from poor error performance due to a combination of suboptimal decoding and naive transmission schemes. From the observed results, the motivation to design better layered space-time architectures is clear. Ideally, we would like to have layered space-time architectures which improve the error performance compared to the state of the art, while not losing out on the previous advantages of high rate and low complexity.

CHAPTER 3

JOINT TRANSMITTER-RECEIVER OPTIMIZATION OF V-BLAST

In this chapter, we introduce a new vertically layered architecture obtained by optimizing the V-BLAST architecture. We propose two methods to reduce the outage probability when the receiver uses successive cancellation decoding, namely, the optimization of the receiver ordering algorithm, and the optimal allocation of rate and energy at the transmitter.

On the receiver side, we propose the *rate-normalized* ordering algorithm for SC decoding, which is shown to minimize the outage probability among all possible ordering algorithms for any given transmitter loading strategy. On the transmitter side, the rate and energy allocation is optimized numerically for the ordered SC decoder, as opposed to just fixed ordering. The combination of transmitter allocation with rate-normalized ordering is shown to jointly minimize the outage probability. Our main conclusion is that, for a wide range of data rates and SNR, the outage probability is minimized by a *partially uniform rate and energy (PURE)* allocation strategy, which distributes the available rate and energy *uniformly* over a fraction of the available transmit antennas.

This chapter is divided into four sections. In Section 3.1, we discuss our approach to receiver optimization using the rate-normalized ordering algorithm, which we show to be optimal in the sense of minimizing outage probability. In Section 3.2, we discuss the

problem of transmitter optimization for BLAST ordering and RN-BLAST ordering. In Section 3.3, we present simulation results comparing RN-BLAST to the current layered ST architectures. We summarize the contents of the chapter in Section 3.4.

3.1 Receiver Optimization: Rate-Normalized Ordering

In chapter , we defined the outage probability of the V-BLAST architecture with SC decoding. The instantaneous capacity of the i^{th} layer is $\log_2(1 + E_i\gamma_i/N_0)$. If each data stream has a capacity-achieving code, it is incorrectly decoded if and only if an *outage* occurs, i.e., if and only if

$$C_i(\mathbf{H}) \equiv \log_2(1 + E_i\gamma_i/N_0) < R_i, \quad (32)$$

or equivalently if and only if γ_i is less than $1/S_i^{\text{norm}}$, where S_i^{norm} is the *rate-normalized SNR* of the i^{th} data stream, as defined by Forney [24]:

$$S_i^{\text{norm}} = \frac{E_i/N_0}{2^{R_i} - 1}. \quad (33)$$

The rate-normalized SNR characterizes the error performance of the system better than just the SNR, since it captures the effect of the data rate and energy allocated to the layer as well. If *all* data streams are outage-free, the SC decoder is also error-free. However, if *any* of the streams is in outage, the SC decoder is in outage, and hence has a nonzero probability of frame error. Consequently, the frame-error rate of the coded system is upper-bounded by the *outage probability*

$$P_{\text{out}}(S, R) = \Pr \left[\bigcup_{i=1}^t \left\{ \gamma_i < \frac{1}{S_i^{\text{norm}}} \right\} \right]. \quad (34)$$

The expression for outage probability given by (34) can be re-written as

$$P_{\text{out}}(S, R) = \Pr \left(\bigcup_{i=1}^t \left\{ C_i(\mathbf{H}) < \frac{R}{t} \right\} \right) = \Pr(\min_i \{ C_i(\mathbf{H}) \} < R_i) \quad (35)$$

$$= \Pr \left(\min_i \left\{ \gamma_i S_i^{\text{norm}} \right\} < 1 \right). \quad (36)$$

Thus, to minimize the outage probability the order of detection must be chosen to maximize the minimum among layer capacities. We propose the *rate-normalized* (RN) ordering algorithm which minimizes the outage probability for any given transmitter rate allocation. Note from (36) that an outage occurs if and only if $\min\{\gamma_i S_i^{\text{norm}}\}$ across all the decoding stages is less than unity. From this observation, we state the following lemma.

Lemma 3. To minimize the outage probability (36), the ordering vector π should be chosen to ensure that $\min\{\gamma_i S_i^{\text{norm}}\}$ is maximized. For a given channel realization \mathbf{H} , the k^{th} layer detected is chosen according to

$$\begin{aligned} \pi_k &= \underset{i \notin \{\pi_1, \dots, \pi_{k-1}\}}{\operatorname{argmax}} \gamma_i S_i^{\text{norm}} \\ &= \underset{i \notin \{\pi_1, \dots, \pi_{k-1}\}}{\operatorname{argmax}} S_i^{\text{norm}} \|\mathbf{h}_i - \hat{\mathbf{h}}_i(\Omega)\|^2, \end{aligned} \quad (37)$$

where $\hat{\mathbf{h}}_i(\Omega)$ is the projection of \mathbf{h}_i on the subspace spanned by $\{\mathbf{h}_{\pi_{k+1}}, \mathbf{h}_{\pi_{k+2}}, \dots, \mathbf{h}_{\pi_t}\}$.

Theorem 2. At the i^{th} stage of decoding, the rate-normalized ordering algorithm chooses π_i so as to achieve the maximum value of $\gamma_i S_i^{\text{norm}}$ among the $t + i - 1$ possibilities. In the process, it maximizes the minimum of $\{\gamma_1 S_1^{\text{norm}}, \gamma_2 S_2^{\text{norm}}, \dots, \gamma_t S_t^{\text{norm}}\}$.

Proof: Define a scaled channel matrix by $\mathbf{H}' = \mathbf{H}\mathbf{D}$, where \mathbf{D} is a $t \times t$ diagonal matrix, whose i^{th} diagonal entry is $D_{ii} = \sqrt{S_i^{\text{norm}}}$. If the QR decomposition of \mathbf{H} is given by $\mathbf{H} = \mathbf{Q}\mathbf{R}$, then the scaled channel matrix can be written as $\mathbf{H}' = \mathbf{Q}\mathbf{R}\mathbf{D} = \mathbf{Q}\mathbf{R}'$. The post detection SNRs resulting from SC decoding of \mathbf{H} are equal to the squared diagonal entries of \mathbf{R} . Therefore, the i^{th} post detection SNR for the scaled channel \mathbf{H}' is $\gamma_i' = \mathbf{R}_{ii}^2 \mathbf{D}_{ii}^2 = \gamma_i S_i^{\text{norm}}$. Hence, the minimum of γ_i' is maximized by applying the conventional BLAST ordering algorithm of [5] on \mathbf{H}' instead of \mathbf{H} .

Combining Lemma 3 and Theorem 2, we conclude that the rate-normalized ordering algorithm minimizes the outage probability among all possible ordering algorithms.

3.2 Transmitter Optimization

In this section, we discuss the *transmitter optimization* problem, namely to choose the $\{R_i\}$ and $\{E_i\}$ to minimize the outage probability at a given SNR under the constraints that $\sum_{i=1}^t R_i = R$ and $\sum_{i=1}^t E_i = E$. The following remark about the optimum energy allocation holds for all ordering algorithms.

Remark 2. Suppose $\{R_i^*\}$ and $\{E_i^*\}$ are rate and energy allocations that minimize the outage probability for any of the layered space-time architectures

considered so far with SC decoding, the optimum energy and rate of the i^{th} data stream are related by

$$E_i^*/E = \frac{1 - 2^{-R_j^*}}{t \sum_{j=1} 1 - 2^{-R_j^*}}. \quad (38)$$

This is easily proved using Lagrange multipliers. The implication of Remark 2 is that the transmitter optimization is simplified to one of choosing only the data rates $\{R_j\}$, with the optimum energies E_i determined by (38). Thus, the number of variables to be optimized is reduced from $2t$ to t .

3.2.1 Transmitter Optimization with BLAST Ordering

As stated in Section 2.3, the SNR scaling factors produced by the BLAST ordering algorithm are statistically dependent, and no closed-form expression is known for their distribution. Consequently, the outage probability (34) cannot be evaluated. Instead, we suggest the *union bound* to get a tractable expression that can be used for transmitter optimization. From (34), it is clear that the outage probability is bounded by

$$P_{\text{UB}}(\{S_i^{\text{norm}}\}, \pi^{-1}) = \sum_{i=1}^t \Pr \left[\gamma_{\pi_i^{-1}} < \frac{1}{S_i^{\text{norm}}} \right]. \quad (39)$$

Each term in the summation can be further split into an average over the stage π_i^{-1} in which the i^{th} stream is decoded, giving

$$\begin{aligned}
\Pr\left[\gamma_{\pi_i^{-1}} < \frac{1}{S_i^{norm}}\right] &= \sum_{k=1}^t \Pr(\pi_i^{-1} = k) \\
&= \Pr[\gamma_k < \frac{1}{S_i^{norm}} \mid \pi_i^{-1} = k].
\end{aligned} \tag{40}$$

From Lemma 1, π_i^{-1} is uniformly distributed over $\{1, 2, \dots, t\}$, and hence $\Pr(\pi_i^{-1} = k) = 1/t$. Moreover from Lemma 1, γ_k is independent of the stage π_i^{-1} in which layer i is decoded. Thus conditioning on $\pi_i^{-1} = k$ does not change the distribution of γ_k . Substituting these facts in (40), we get

$$\Pr\left[\gamma_{\pi_i^{-1}} < \frac{1}{S_i^{norm}}\right] = \frac{1}{t} \sum_{k=1}^t F_k\left(\frac{1}{S_i^{norm}}\right), \tag{41}$$

where $F_k(x) = \Pr[\gamma_k < x]$ is the cdf for γ_k . Let $F(x) = \frac{1}{t} \sum_{k=1}^t F_k(x)$ denote the average of these distribution functions over the t symbols. From (41), $\Pr[\gamma_{\pi_i^{-1}} < 1/S_i^{norm}] = F(x)$.

Substituting in (39), we get the union bound on the outage probability of the BLAST ordering algorithm

$$\Pr_{\text{UB}}(\{S_i^{norm}\}, \pi^{-1}) = \sum_{i=1}^t F\left(\frac{1}{S_i^{norm}}\right). \tag{42}$$

The average distribution function $F(x)$ is not known in closed form, so even the simplified union bound (42) cannot be evaluated as is. However, we estimate the function $F(x)$ numerically as follows. We generate a large number of Rayleigh fading matrices, run

the BLAST algorithm for each one, and roundoff the resulting $\{\gamma_i\}$ to pre-selected bins. This gives a discrete approximation to the actual continuous distribution function for each γ_i . Averaging, we get a discrete approximation to $F(x)$.

The discrete approximation to $F(x)$ is used as the metric to optimize transmitter rate and power allocations at different SNR and data rates. Note that (42) is just the sum of the *same* function evaluated for each of the terms $\{1/S_i^{norm}\}$. Intuitively, this implies that unlike fixed ordering, BLAST ordering treats all the data streams identically. More precisely, if the data rates and energies of two streams i and i' are equal, then the two streams make the same contribution $F(1/S_i^{norm})$ to the union bound (42). From this observation, it is tempting to conclude that the optimum solution is to allocate identical data rates and energies, R/t and E/t respectively to all the streams. However, this conclusion is not valid because the function $F(x)$ is not *convex* in general.

For example, consider a 4-input, 4-output MIMO system operating at 8 b/s/Hz at an SNR of 20 dB. For this system, we numerically estimated $F(x)$ and performed a random search for the optimum data rate allocation. The uniform allocation yielded a union bound (42) equal to 3.4334×10^{-2} . However, the optimum allocation was the *partially* uniform allocation $\{4, 4, 0, 0\}$, which distributes the rates and energies uniformly over only *two* of the *four* available transmit antennas. This partially uniform allocation yielded a union bound of 1.1110×10^{-3} , which is significantly lower than that of the uniform allocation. Based on numerical optimization experiments, we state the following conjecture.

Conjecture 1. The union bound for the BLAST ordered SC decoder is minimized by a partially uniform rate allocation, with μ streams carrying a data rate of R/μ and

energy of E/μ , and the remaining $t - \mu$ data streams carrying zero data rate and zero energy.

Based on the above conjecture, numerical optimization reduces to finding the optimal number of active streams $\mu \in \{1, 2, \dots, t\}$. The optimum number of active inputs, μ , is typically less than t at high SNR and it decreases with increasing SNR.

3.2.2 Rate-Normalized Ordering

Now, we consider transmitter optimization for RN ordering. In Section 3.1, we derived the RN ordering algorithm which modifies BLAST ordering to account for different rates and energies on different data streams. For any given rate and energy allocation, the RN ordering algorithm minimizes the outage probability. We now attempt to find the optimum rate and energy allocation at the transmitter when the receiver employs RN ordering. Clearly, this combination would achieve the lowest possible outage probability among all SC decoders with a naive spatial multiplexing transmitter.

The actual expression for outage probability with RN ordering is intractable. Even the union bound on outage probability is intractable, because the distributions of Γ and j for the RN ordering algorithm depend on the rate allocations. Unlike the case of conventional BLAST, each term in the union bound expression (39) cannot be simplified further, rendering intractable the problem of optimizing rate and energy allocation for RN ordering.

However, based on heuristic observations, we state the following conjecture regarding the optimum data rate allocation.

Conjecture 2. The optimum data rate allocation for the rate-normalized ordering algorithm is either

- the optimum allocation for the case of fixed ordering, which is found by numerical optimization, or
- a partially uniform allocation, where μ inputs carry a data rate of R/μ each, and the rest carry zero data rate.

We state this conjecture based on the following key observations. When the transmitter uses a partially uniform allocation, then RN ordering simplifies to V-BLAST ordering, for which we concluded in Section 3.2.1 that the partially uniform allocation is optimum. Moreover, when the transmitter uses the optimum rate allocation corresponding to fixed ordering, then RN ordering achieves a strictly lower outage probability than fixed ordering according to Theorem 2. Though these observations do not guarantee that the outage probability is minimized by the above rate allocation schemes, our numerical experiment results for RN-BLAST support the results in Conjecture 2. An extensive random search in the space of valid data rate and energy allocations yields the lowest outage probability only with one of the two candidates proposed in Conjecture 2.

Based on Conjecture 2, one can restrict the search for the optimum data rate allocation to $t + 1$ possibilities. The first possibility is the optimum data rate allocation for fixed ordering. The other t are the partially uniform allocations with $\mu = 1, 2, \dots, t$ inputs. Given the data rate and SNR, one can simulate RN ordering for each of the $t + 1$ allocations with the energy allocations for each case chosen according to (38), and choose the allocation which has minimum outage probability.

Of particular interest in Conjecture 2 is the fact that a partially uniform allocation is often the optimum allocation for RN ordering. This claim can be explained by noting that with a partially uniform allocation, RN ordering amounts exactly to BLAST ordering, applied to the restricted set of μ active inputs. From Conjecture 1, a partially uniform allocation is optimum for BLAST ordering. Since RN ordering reduces to BLAST ordering with partially uniform allocation, the same allocation is expected to be a good solution for RN ordering.

When the allocation of rate and energy is partially uniform, the transmitter is identical to statistical antenna selection methods proposed in [17][18]. Hence, our work extends the antenna selection methods in two ways. First, it proves that the rate-normalized ordering algorithm is optimum. Secondly, Theorem 1 and the resultant union bound (42) give a justification for distributing the data rate *uniformly* over a *partial* set of channel inputs.

3.3 Numerical Results

In this section, we present numerical simulation results for SC decoding with fixed ordering, BLAST ordering and RN ordering with a naive spatial multiplexing transmitter operating over a 4×4 MIMO system operating at $R = 8$ b/s/Hz and $S = 20$ dB.

In Fig. 9 we compare the outage performance of the fixed ordering, conventional BLAST and rate-normalized ordering for a given rate and energy allocation scheme. The results are based on a rate allocation of $\{R_i\} = \{0.0 \ 1.31 \ 2.99 \ 3.70\}$, which minimizes the outage probability of the fixed ordered decoder at 15 dB. It is seen from Fig. 9 that the rate-normalized ordering outperforms optimized fixed ordered system by 1.5 dB and BLAST ordering by 2 dB at an outage probability of 10^{-3} .

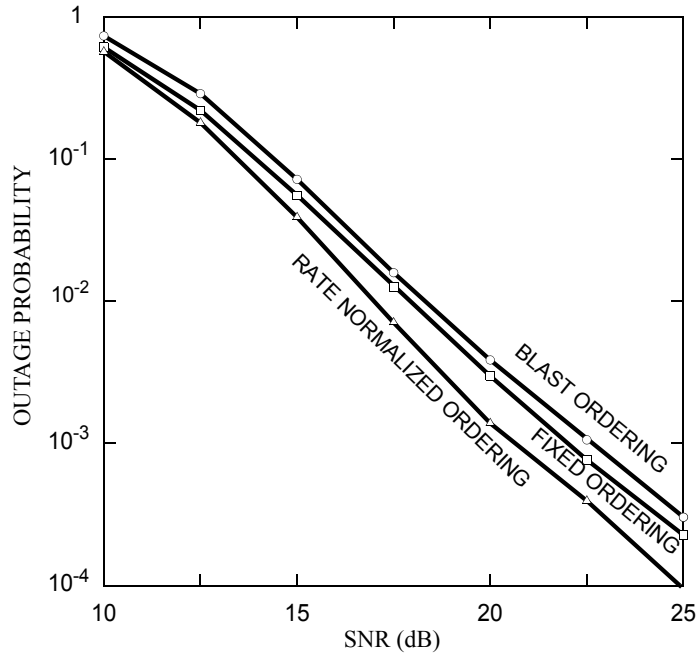


Fig. 9. Comparison of ordering algorithms for $\{R_i\} = \{0.00, 1.31, 2.99, 3.70\}$ for a 4-input, 4-output Rayleigh fading channel at $R = 8$ b/s/Hz.

Fig. 10 shows the optimum error performance achievable by fixed and optimal ordering, with transmitter optimization in comparison with the conventional BLAST

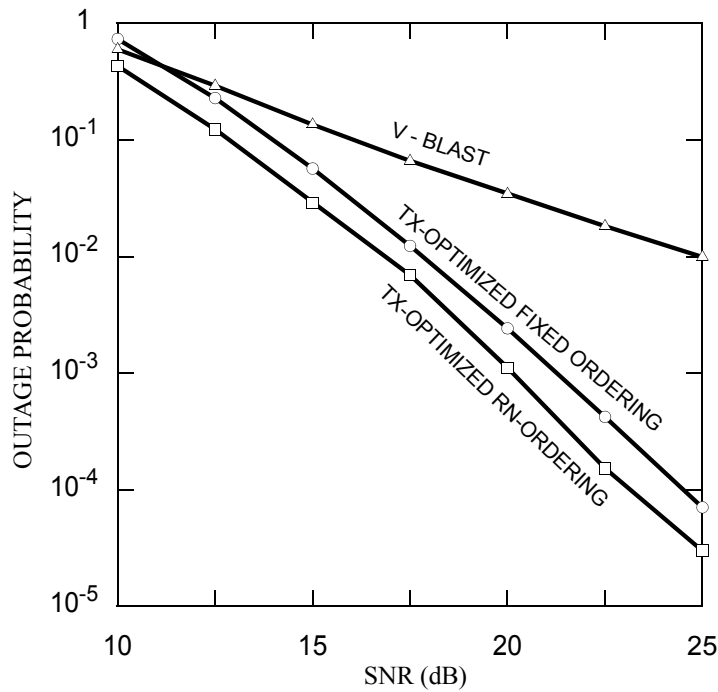


Fig. 10. Comparison of transmitter optimized SC decoders for a 4-input, 4-output Rayleigh fading channel at $R=8$ b/s/Hz

system. The jointly optimal system outperforms conventional BLAST by 15 dB at an outage probability of 10^{-3} . For the rate-normalized decoder, with $t = 4$ and $r = 4$, for a data rate of 8 b/s/Hz, transmitter optimization yields the following results. At $S = 15$ dB, the optimum solution is the partially uniform allocation $\{R_i\} = \{0, 2.67, 2.67, 2.67\}$. For $S = 20$ dB and 25 dB, the minimum outage probability is achieved by the partially uniform allocation with $K = 2$. From Fig. 10, we see that transmitter-optimized rate-normalized ordering outperforms transmitter-optimized fixed ordered receiver by 1.5 dB at an outage probability of 10^{-3} .

Finally, we summarize the updated performance complexity tradeoff picture in Fig. 11 with the inclusion of RN-BLAST. From Fig. 11, we observe that RN-BLAST significantly reduces the SNR required to achieve the target outage probability, while maintaining the

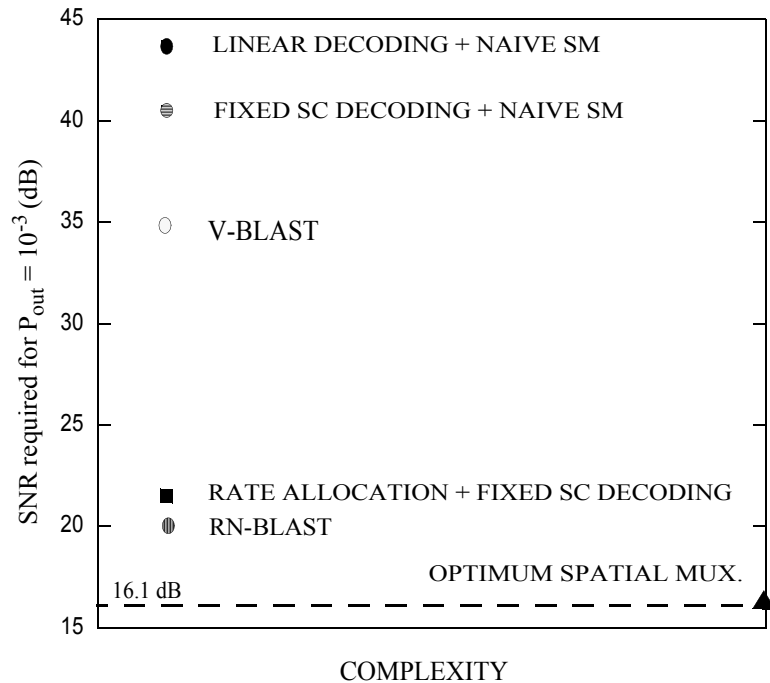


Fig. 11. Performance-complexity tradeoff of various spatial multiplexing techniques for $t = 4$, $r = 4$, $R = 8$ b/s/Hz.

low complexity of SC decoding. Specifically, RN-BLAST improves performance over transmitter optimized fixed ordering by 1.5 dB, while still falling 4.1 dB short of the optimum outage probability achievable by any vertically layered architecture.

3.4 Summary

We studied two ways of optimizing the V-BLAST system with the objective of minimizing the outage probability. We proposed the rate-normalized ordered detector and proved that it minimizes the outage probability among all possible ordering schemes. We investigated the optimal rate and power allocations to minimize the outage probability for the optimized successive cancellation decoder. We showed that the *partially-uniform* allocation is the minimizing solution for V-BLAST ordered detection over an i.i.d. Rayleigh fading channel. For the rate-normalized ordered decoder, we propose a rule for rate and power allocation to minimize the outage probability based on partial analytical results. Simulation results show that jointly optimizing the transmitter and receiver of the SC decoder improves the outage probability while incurring no extra cost in complexity.

CHAPTER 4

SPACE-TIME ACTIVE ROTATION (STAR) ARCHITECTURE

In the previous chapter, we proposed the RN-BLAST architecture and concluded that RN-BLAST is the best optimized version of the basic V-BLAST architecture [28]. However, we also observed that the performance of RN-BLAST still falls short of the optimal outage probability achievable using an unconstrained decoder. This indicates the need for developing new and improved layered space-time architectures, instead of merely optimizing V-BLAST, in order to bridge the gap to the optimal outage probability.

We answer this problem with a new family of layered space-time architectures for open-loop MIMO systems over quasistatic fading channels, called *space-time active rotation* (STAR). The basic idea of STAR is that the encoded layers of data are transmitted through a rotating set of active antennas.

In a STAR transmitter, the duration over which the channel response is constant is divided into t blocks. The first antenna is inactive during the first block, the second antenna is inactive during the second block, and so on. Thus, the set of active antennas rotates. The idea is that, in the absence of channel knowledge, active rotation isolates weaker and stronger antenna subsets and layered channel coding averages the system performance over these subsets, instead of being limited by the weakest antenna, as is the case in V-BLAST. We show that the combination of active rotation of antenna subsets with layered coding yields high diversity gain with just SC decoding.

We propose three layering schemes for the STAR architecture to obtain the following three variants.

- The vertically layered V-STAR, with independent outer codes for each antenna significantly outperforms V-BLAST, achieving near-optimal outage probability using a simple SC decoder.
- G-STAR is a vertically layered architecture operating over a group of antennas, instead of just one, that enables a flexible performance-complexity tradeoff with varying group sizes.
- The diagonally layered D-STAR employs coding across antennas, and hence improving the diversity gain, and is shown to alleviate practical issues relating to error propagation and length of the scalar channel codes.

This chapter is organized as follows. In Section 4.1, we describe the basic setup of the STAR architecture. In Section 4.2, we introduce the vertically layered V-STAR architecture, derive the decoding algorithm for V-STAR, compute its outage probability and show that it clearly outperforms V-BLAST and all its enhanced versions using numerical simulations. In Section 4.3, we present the G-STAR architecture, discuss the performance-complexity tradeoff that it enables and present numerical simulations to show that it achieves near-optimum outage probability with just successive cancellation decoding. In Section 4.4, we discuss the D-STAR architecture and compare it with D-BLAST. In Section 4.5, we summarize the STAR family of architectures and make some concluding remarks with directions to future work on this new architecture.

4.1 Basic Structure of the STAR Architecture

We now describe the basic transmit antenna set-up of the STAR architecture. The STAR transmitter has two primary components, the *antenna setup* and the *coding rule*.

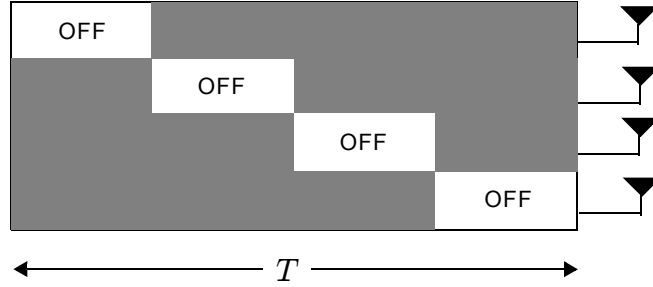


Fig. 12. The STAR transmitter with $t = 4$ transmit antennas.

First, we describe the basic antenna setup of STAR. The static fading frame is divided into t blocks. During the j^{th} block in the static fading frame, the j^{th} antenna is inactive. Thus, the effective channel matrix, $\mathbf{H}^{(j)}$, in the j^{th} block, is formed by removing the j^{th} column from the channel matrix \mathbf{H} . For $t = 4$, the frame is divided into four blocks as illustrated in Fig. 12.

The other component of the transmitter is the *coding rule*. A *layer* is defined as one codeword of the outer scalar error correcting code. The *coding rule* is the fashion in which the layers are transmitted through the transmit antennas. We propose three variants of the STAR architecture with three different coding schemes, namely *independent coding*, *group coding* and *joint coding* respectively.

The vertically layered V-STAR is restricted to employ independent coding, where each layer is encoded using an independent scalar channel code and transmitted through only one antenna. V-STAR is shown to achieve a high diversity order and outperform V-BLAST significantly while maintaining the simplicity of SC decoding.

G-STAR is the variant of STAR with group coding, where the t transmit antennas are divided into t/q groups of q antennas each, and a layer is constrained to span only one group. G-STAR enables a flexible performance-complexity trade-off with varying group sizes; larger the group size, lower the error rates, but higher the complexity.

The diagonally layered D-STAR employs joint coding where each layer spans across multiple transmit antennas. We show that D-STAR compares favorably with D-BLAST, its jointly coded counterpart, in several aspects. D-BLAST is known to be affected by a fundamental tradeoff between code length and the transmission rate as explained in Section 2.7. We show how D-STAR avoids this problem by allowing for sufficiently long code lengths, essential for practical codes to approach the system capacity.

Each variant of STAR employs SC decoding at the receiver, which maintains the low complexity of layer processing. We now describe each one of these architectures in detail.

4.2 V-STAR: STAR with Vertical Layering

In this section, we introduce the STAR architecture with independent coding. This system will hence be referred to as V-STAR (vertical STAR).

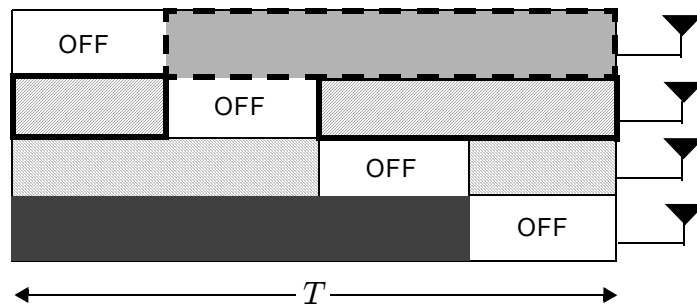


Fig. 13. The vertical space-time active rotation (V-STAR) transmitter with $t = 4$ transmit antennas.

4.2.1 Transmitter

In V-STAR, t independent streams of data are coded using t scalar SISO codes. The total number of layers is equal to t , the number of transmit antennas. In Fig. 13, the different layers are shaded by different patterns to show that they are encoded using independent error correcting codes. Contrast the V-STAR transmitter with that of V-BLAST, where all the antennas active at all times and parallel data streams are independently coded.

4.2.2 Receiver

As with V-BLAST, the layered nature of the V-STAR transmitter yields itself to simplified decoding using a successive cancellation (SC) decoder. SC decoders [5] decode one layer at a time, subtracting out the estimated contribution of previously decoded layers, and nulling out interference from undecoded layers. However, unlike V-BLAST, it will be seen that V-STAR with SC decoding achieves near-optimum outage probability of spatial multiplexing systems.

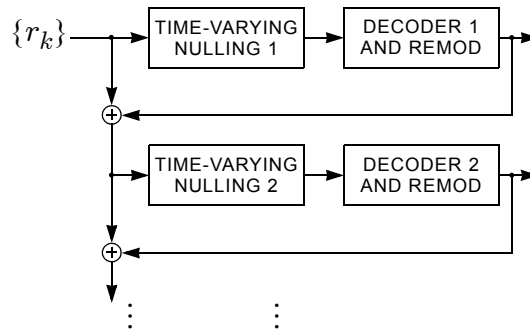


Fig. 14. The V-STAR successive cancellation decoder.

Define the i^{th} layer as the scalar coded data stream transmitted through the i^{th} antenna. The i^{th} layer is a concatenation of t blocks, with the i^{th} block being inactive. The SC decoding process outlined in Fig. 14 is a t -stage process, where each stage represents the detection and decoding of one layer. In the i^{th} stage, the SC decoder detects each active block $\{j = 1, 2, \dots, t, j \neq i\}$ in the i^{th} layer using the nulling procedure. The detected blocks are concatenated and decoded using the outer scalar decoder. Subsequently, the decoded layer is used to cancel out the interference before decoding the next layer.

To detect the j^{th} block in the i^{th} layer, the zero-forcing SC decoder nulls out the undecoded streams using the *nulling vector* $\mathbf{w}_i^{(j)}$, defined as the first row of Moore-Penrose inverse of matrix $[\mathbf{h}_i, \mathbf{h}_{i+1}, \dots, \mathbf{h}_{j-1}, \mathbf{h}_{j+1}, \dots, \mathbf{h}_t]$. Since the nulling vector $\mathbf{w}_i^{(j)}$ is different for different blocks within a layer, we refer to this procedure as time-varying nulling in Fig. 14. The $1 \times T/t$ decision vector in the j^{th} block of the i^{th} layer is obtained as $\mathbf{y}_i^{(j)} = \mathbf{w}_i^{(j)} \mathbf{r}^{(j)}$, where $\mathbf{r}^{(j)}$ is the $r \times T/t$ received vector during the j^{th} block. Thus, the channel model reduces to

$$\mathbf{y}_i^{(j)} = \mathbf{x}_i^{(j)} + \mathbf{w}_i^{(j)} \mathbf{n}^{(j)}. \quad (43)$$

The equivalent channel (43) is an AWGN channel with noise variance $N_0 \|\mathbf{w}_i^{(j)}\|^2$. The output of the SC detector forms the input to the outer scalar decoder. Also, since a layer is active for a fraction $(t - 1)/t$ of the frame, each layer transmits at energy $E/(t - 1)$ when active to satisfy the average energy constraint of E per symbol period. Thus, instantaneous signal to noise ratio of this block is $\rho_i^{(j)} = E/((t - 1)N_0 \|\mathbf{w}_i^{(j)}\|^2) = S/((t - 1)\|\mathbf{w}_i^{(j)}\|^2)$. The nulling process described thus far is called zero-forcing nulling. An alternative nulling method is minimum mean-squared error (MMSE) nulling, whose nulling vector

for the j^{th} block in the i^{th} layer is defined as the first row of $(\mathbf{H}_i^{(j)}\mathbf{H}_i^{(j)*} + N_0(t-1)\mathbf{I}/Et)^{-1}\mathbf{H}_i^{(j)*}$, where $\mathbf{H}_i^{(j)}$ is the matrix $[\mathbf{h}_i, \mathbf{h}_{i+1}, \dots, \mathbf{h}_{j-1}, \mathbf{h}_{j+1}, \dots, \mathbf{h}_t]$. The performance of the SC decoder can be improved by changing the order of detection of the layers. The optimal order is channel dependent. The order can be described by the permutation $\pi(1, 2, \dots, t)$, where π_k is the k^{th} detected layer. Let Π be the matrix whose k^{th} column is the π_k^{th} column of \mathbf{I} . Once the optimal order is computed based on \mathbf{H} , the receiver uses fixed ordered SC decoding on $\mathbf{H}\Pi$ instead of \mathbf{H} .

4.2.3 Outage Probability and Diversity Order

We now compute the instantaneous capacity and the outage probability of V-STAR with SC decoding. Note that capacity here refers to the information carrying capacity of the *equivalent channel* formed by the MIMO channel in conjunction with the soft output SC decoder. The capacity of the i^{th} layer, in bits/s/Hz, is:

$$C_i(\mathbf{H}) = \max_{p(x_1, x_2, \dots, x_t)} \frac{1}{T} I(\mathbf{X}_i, \mathbf{Y}_i | \mathbf{H}), \quad (44)$$

where, $\mathbf{X}_i = \{\mathbf{X}_i^{(1)}, \mathbf{X}_i^{(2)}, \dots, \mathbf{X}_i^{(t)}\}$ is the concatenation of transmitted blocks in the i^{th} layer and $\mathbf{Y}_i = \{\mathbf{Y}_i^{(1)}, \mathbf{Y}_i^{(2)}, \dots, \mathbf{Y}_i^{(t)}\}$ is the corresponding output of the soft output SC decoder. In (44), $p(x_1, x_2, \dots, x_t)$ denotes the joint probability density function of the transmitted symbols across all t layers. Since the noise is independent across time, the capacity of the i^{th} layer is

$$C_i(\mathbf{H}) = \max_{p(x_1, x_2, \dots, x_t)} \frac{1}{T} \sum_{j=1}^t I(\mathbf{X}_i^{(j)}, \mathbf{Y}_i^{(j)} | \mathbf{H}). \quad (45)$$

Each active block is of length T / t . After detection, each block is effectively an AWGN channel with instantaneous SNR equal to $\rho_i^{(j)}$. Hence, the mutual information is maximized by a Gaussian input which satisfies the power constraint that $E(\|\mathbf{X}\|^2)/T \leq E$ with equality, where $\mathbf{X}^T = \{\mathbf{X}_1^T, \mathbf{X}_2^T, \dots, \mathbf{X}_t^T\}$. The capacity of the j^{th} block of the i^{th} layer is $\log_2(1 + \rho_i^{(j)})$. The inactive blocks have zero capacity. Therefore, the capacity of the i^{th} layer is

$$C_i(\mathbf{H}) = \frac{1}{t} \sum_{j \neq i} \log_2(1 + \rho_i^{(j)}). \quad (46)$$

Thus, the layer capacity is the arithmetic mean of the capacities of the blocks. Since each data stream is assumed to have a capacity-achieving code, it is incorrectly decoded if and only if an *outage* occurs, i.e., if $C_i(\mathbf{H}) < R/t$. Note that, in V-STAR, the capacity of the i^{th} layer is averaged over t blocks in a static fading frame, as opposed to V-BLAST. The performance of V-BLAST might be degraded by one ‘*bad*’ antenna, whereas V-STAR guards against such an occurrence.

As defined in the previous chapters, if *all* data streams are outage-free, the SC decoder is also outage-free. However, if *any* of the streams is in outage, the SC decoder is in outage. Consequently, the *outage probability* is

$$P_{V\text{-}STAR}(S, R) = \Pr\left[\bigcup_{i=1}^t \left\{C_i(\mathbf{H}) < \frac{R}{t}\right\}\right]. \quad (47)$$

The outage probability is a lower bound on the achievable frame error rate of the system. The bound can be approached by using a powerful error control code such as an LDPC or a turbo code as the outer code.

The diversity order, d , of V-STAR is defined by the asymptotic slope of the outage probability

$$d = \lim_{S \rightarrow \infty} \frac{-\log P_{V-STAR}(S, R)}{\log S}, \quad (48)$$

and the diversity order, d_i , of the i^{th} layer in V-STAR is defined as

$$d_i = \lim_{S \rightarrow \infty} \frac{-\log \left(\Pr \left\{ C_i(\mathbf{H}) < \frac{R}{t} \right\} \right)}{\log S}. \quad (49)$$

We now prove the following results about the diversity order of the V-STAR system.

Lemma 4. The diversity order d of V-STAR with SC decoding is $d = \min\{d_1, d_2, \dots, d_t\}$, where d_i is the diversity order of the i^{th} layer.

Proof: The outage probability can be bounded as

$$\Pr \left\{ C_i(\mathbf{H}) < \frac{R}{t} \right\} < P_{V-STAR}(S, R) < \sum_{k=1}^t \Pr \left\{ C_k(\mathbf{H}) < \frac{R}{t} \right\}. \quad (50)$$

The lower bound in the above inequality is true for any i , whereas the upper bound is obtained using the union bound. We choose i such that $d_i = \min\{d_1, d_2, \dots, d_t\}$ so that the diversity order of the lower bound is $\min_i\{d_i\}$. As $S \rightarrow \infty$, the upper bound is dominated by the term with the lowest diversity order. Since the lower and upper bounds have the same diversity order, $d = \min_i\{d_i\}$.

Theorem 3. The diversity order d of V-STAR with SC decoding is bounded as

$$\min_i \{ \max_j \{ d_i^{(j)} \} \} \leq d \leq r, \quad (51)$$

where $d_i^{(j)}$ is the diversity order of the j^{th} block in the i^{th} layer.

Proof: The capacity of the i^{th} layer can be upper bounded for any block j in layer i as

$$C_i(\mathbf{H}) > \frac{1}{t} \log_2(1 + \rho_i^{(j)}). \quad (52)$$

Choose block j^* in the i^{th} layer such that $d_i^{(j^*)} = \max_j \{ d_i^{(j)} \}$. Then, using (52) the following holds true,

$$\Pr\left(C_i(\mathbf{H}) < \frac{R}{t}\right) < \alpha \cdot S^{-\max_j \{ d_i^{(j)} \}}, \quad (53)$$

for some constant α . Combining (53) with Lemma 4, we get $d \geq \min_i \{ \max_j \{ d_i^{(j)} \} \}$.

The second part can be proved using the fact that $P_{\text{V-STAR}}(S, R) \geq P_{\text{SM}}(S, R)$. It is well known [12] that the diversity order of $P_{\text{SM}}(S, R)$ is r .

The above result is useful in determining the diversity order of V-STAR with SC decoding when the diversity order of any one of the blocks is known, as we will see in chapter .

4.2.4 Receiver Design: Ordering Algorithm

The performance of the SC decoder depends on the order in which the layers are detected. For every instance of \mathbf{H} , the receiver determines the optimal order of detection, π , which minimizes the outage probability. The expression for outage probability given by (34) can be rewritten as

$$\Pr\left(\bigcup_{i=1}^t \left\{C_i(\mathbf{H}) < \frac{R}{t}\right\}\right) = \Pr\left(\min_i \{C_i(\mathbf{H})\} < \frac{R}{t}\right). \quad (54)$$

Thus, the order of detection must be chosen to maximize the minimum among layer capacities, to minimize the outage probability. We propose a simple, greedy ordering algorithm along the lines of [5] and we prove that it minimizes the outage probability.

We propose the following ordering algorithm which greedily maximizes the layer capacity at every stage of detection. For a given channel realization \mathbf{H} , π_k , the k^{th} layer detected is chosen as

$$\pi_k = \underset{i \notin \{\pi_1, \dots, \pi_{k-1}\}}{\operatorname{argmax}} \frac{1}{t} \sum_{j \neq i} \log_2 \left(1 + \frac{S}{t-1} \|\mathbf{h}_i - \hat{\mathbf{h}}_i(\bar{\Omega})\|^2\right), \quad (55)$$

where

$$\Omega = \{i, j, \pi_1, \dots, \pi_{k-1}\} \text{ and } \bar{\Omega} = \{1, 2, \dots, t\} - \Omega \quad (56)$$

and $\hat{\mathbf{h}}_i(\bar{\Omega})$ is the projection of \mathbf{h}_i on the subspace spanned by the r -dimensional column vectors \mathbf{h}_ω for all $\omega \in \bar{\Omega}$. Contrast this to the ordering rule in V-BLAST

$$\pi_k = \underset{i \notin \{\pi_1, \dots, \pi_{k-1}\}}{\operatorname{argmax}} \log_2 \left(1 + \frac{S}{t} \|\mathbf{h}_i - \hat{\mathbf{h}}_i(\bar{\Omega})\|^2\right), \quad (57)$$

where $\Omega = \{i, \pi_1, \dots, \pi_{k-1}\}$.

We now prove that the proposed ordering algorithm is optimal in terms of minimizing the outage probability.

Theorem 4. The minimum among all layer capacities is maximized, if, at each stage of decoding $i = \{1, 2, \dots, t\}$, the layer detected is chosen such that it has the maximum capacity among the $t - i + 1$ undetected layers at that stage.

Proof: We prove this result along the same lines as the proof of optimal ordering in [5]. The capacity of the i^{th} layer given by

$$C_i = \frac{1}{t} \sum_{j \neq i} \log_2 \left(1 + \frac{S}{t-1} \left\| \mathbf{h}_i - \hat{\mathbf{h}}_i(\bar{\Omega}) \right\|^2 \right). \quad (58)$$

Given an order of detection π , define the constraint set of π_i as the set of undetected layers given by $\{\pi_{i+1}, \pi_{i+2}, \dots, \pi_t\}$, with the constraint set being the null set if $i = t$. For the given ordering, let the capacity of the i^{th} detected layer be C_{π_i} . In order to prove this result, we revisit the following results from [5].

Lemma 5. For two given orderings A and B , if $A_i = B_i$ and the constraint sets of A_i and B_i are identical, irrespective of their order, then $C_{A_i} = C_{B_i}$.

Lemma 6. For two given orderings A and B , if $A_i = B_i$ and the constraint set of A_i is a subset of the constraint set of B_i , then $C_{A_i} \geq C_{B_i}$.

Consider another ordering, apart from π , say $\xi = \{\xi_1, \dots, \xi_t\}$. Without loss of generality, let $\{\pi_1, \dots, \pi_{x-1}\} = \{\xi_1, \dots, \xi_{x-1}\}$ for some x . Let $\xi_y = \pi_x$, where $y > x$. Now, consider a modified order $\xi^* = \{\xi_1, \dots, \xi_{x-1}, \xi_y, \xi_{x+1}, \dots, \xi_t\}$, with ξ_y displaced from its original position. Comparing the layer capacities of ξ and ξ^* , we get $C_{\xi_1} = C_{\xi_1^*}, \dots, C_{\xi_{x-1}} = C_{\xi_{x-1}^*}$ using Lemma 5. From Lemma 6, we get $C_{\xi_{x+1}^*} \geq$

$C_{\xi_{x+1}}, \dots, C_{\xi_t} \geq C_{\xi_t}^*$. Since we use a local maximization procedure, it is also clear that $C_{\xi_x}^* \geq C_{\xi_x}$. (Note that $C_{\xi_x}^* = C_{\xi_y} = C_{\pi_x}$). Thus,

$$\min_i C_{\xi_i}^* \geq \min_i C_{\xi_i}. \quad (59)$$

Hence, ξ^* is a better ordering compared to ξ . An inductive extension of this perturbation procedure leads us to the conclusion that

$$\min_i C_{\pi_i} \geq \min_i C_{\xi_i}, \quad (60)$$

for any ξ . Hence, π is the globally optimum order which maximizes the minimum capacity among all layers.

4.2.5 Simulation Results

In this section, we present simulation results for V-STAR with ZF-SC and MMSE-SC decoding. We consider a 4×4 MIMO system operating at a data rate $R = 8$ b/s/Hz, distributed equally among the transmit antennas.

In Fig. 15, we compare the outage probabilities of the vertically layered architectures thus far. As discussed in Section 2.6, V-BLAST suffers from poor outage performance at high SNR, due to low diversity gain. Fig. 15 shows that spatial multiplexing and RN-BLAST improve the diversity gain by transmitter and receiver optimization of the naive spatial multiplexing transmitter as discussed in chapter and chapter . From Fig. 15, we see that the V-STAR architecture with SC decoding achieves the best outage probability among all currently known vertical architectures. Also shown in the figure is the optimum

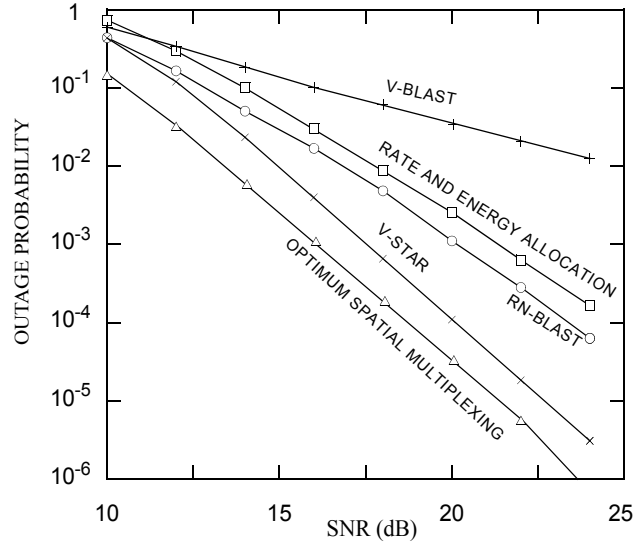


Fig. 15. Comparison of outage probability of various spatial multiplexing systems with ZF-SC decoding over a 4×4 MIMO channel at $R = 8$ b/s/Hz.

outage probability achievable by any vertically layered architecture. Recall that this performance is achieved using a significantly more complex maximum likelihood decoder.

Fig. 15 shows that the outage probability of V-STAR with ZF-SC is 1.7 dB away from the minimum possible outage probability of the 4×4 spatial multiplexing systems. Numerical results also shown that V-STAR outperforms the unoptimized V-BLAST system by 17.4 dB. V-STAR outperforms the transmitter optimization methods for V-BLAST namely optimal rate and energy allocation in [14] by 3.9 dB and RN-BLAST [28] by 2.4 dB at an outage probability of 10^{-3} .

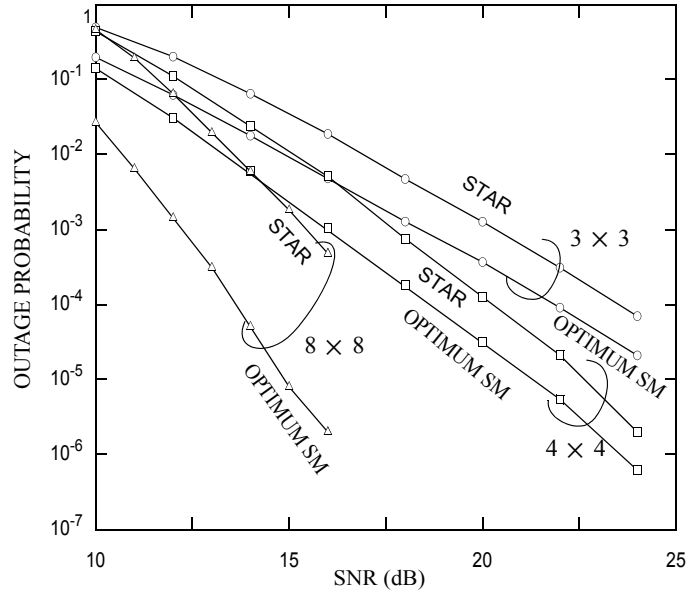


Fig. 16. V-STAR with ZF-SC decoding vs. optimum outage probability for spatial multiplexing systems over 3×3 , 4×4 and 8×8 MIMO channels at 2 b/s/Hz per transmit antenna.

Fig. 16 shows the performance of V-STAR with ZF-SC decoding in comparison to the optimum outage probability for $t = 3, 4$ and 8 transmit antennas, with a data rate of 2 b/s/Hz per transmit antenna. At an outage probability of 10^{-3} , the gap to optimum for the

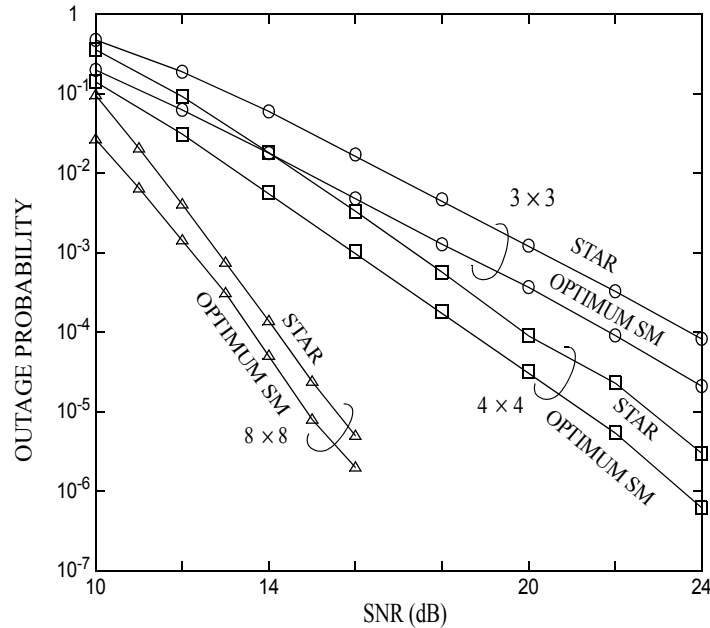


Fig. 17. V-STAR with MMSE-SC decoding vs. optimum outage probability for spatial multiplexing systems over 3×3 , 4×4 and 8×8 MIMO channels at 2 b/s/Hz per transmit antenna.

three systems are 2.0 dB, 1.7 dB, and 3.2 dB respectively. In Fig. 17 we make a similar comparison for V-STAR with MMSE-SC decoding. At an outage probability of 10^{-3} , the gap to optimum for $t = 3, 4$ and 8 transmit antennas are 2.0 dB, 1.4 dB, and 0.6 dB respectively at a data rate of 2 b/s/Hz per transmit antenna.

Fig. 18 summarizes the performance-complexity tradeoff of the following spatial multiplexing techniques: naive spatial multiplexing with linear decoding, fixed ordered as well as BLAST ordered SC decoding and optimal decoding; V-STAR with linear decoding, optimally ordered SC decoding and optimal decoding; and finally spatial multiplexing with rate and energy allocation with SC decoding. We see that the V-STAR lies in the ideal region on the bottom-left corner. Another critical observation here is that V-STAR with SC decoding and V-STAR with unconstrained decoding achieve almost the same outage probability. This observation shows that using a suboptimal SC decoder with

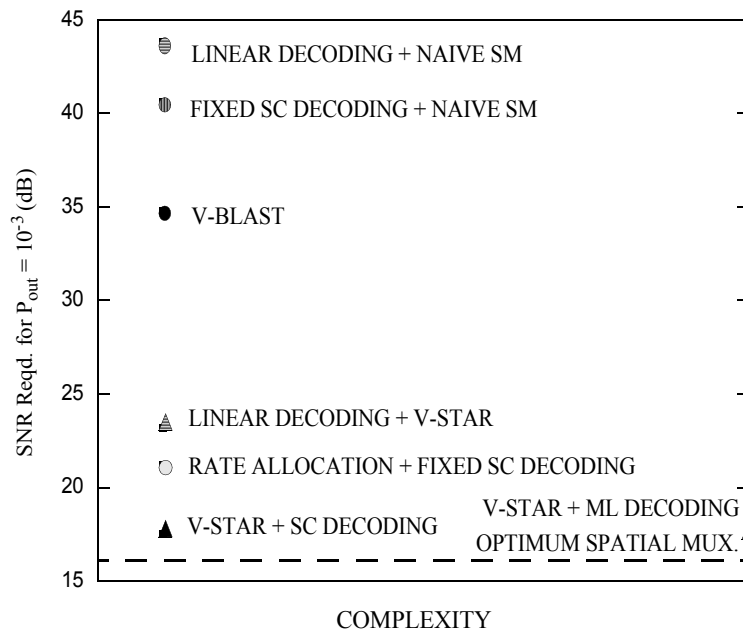


Fig. 18. Performance-complexity tradeoff of various spatial multiplexing techniques for $t = 4, r = 4, R = 8$ b/s/Hz.

V-STAR does not cost much in performance compared to the optimal decoder. This property further validates our approach of designing layered space-time architectures tailored to suboptimal decoding algorithms.

So far, we have analyzed the performance of V-STAR with SC decoding with outage probability as the performance metric. Now, we evaluate the performance of V-STAR in combination with a practical error correction code. We consider a flat, Rayleigh fading channel for this simulation study. We assume that the channel is quasi-static, and remains constant for the length of one codeword, before changing to an independent value. The symbols transmitted from each antenna are drawn from a 16-QAM alphabet with Gray mapping.

In this study, we assume that V-STAR uses MMSE-SC decoding to obtain the equivalent scalar channel for each layer. Then, the LLR of each bit in a layer is computed using the maximum a posteriori probability of that bit. Subsequently, the bits are decoded using a message passing decoder, which is set to have a maximum of 50 iterations. The decoded layer is then remodulated, multiplied by the corresponding channel and cancelled out of the received symbols, before moving on to the next layer. The decoding is complete when the last layer is decoded, with no turbo processing between the MIMO detector and LDPC decoder.

In Fig. 19, we compare the frame error rates for V-STAR over 3×3 and 4×4 MIMO channels against the corresponding outage probabilities. For V-STAR over a 4×4 MIMO channel, the information bits are encoded using a rate- $2/3$ irregular LDPC code of length 3000 bits. This amounts to a data rate of 8 b/s/Hz. We observe that the frame error rates approach to within 4.2 dB of the outage probability for a 4×4 MIMO channel.

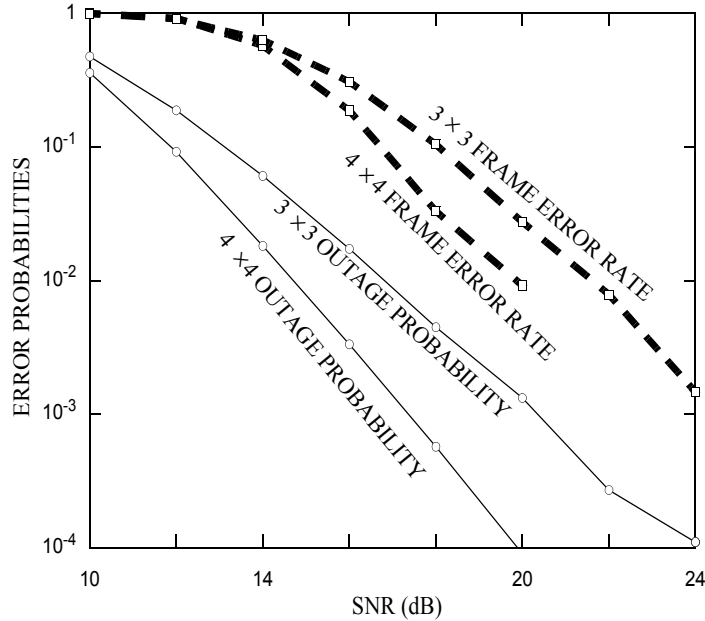


Fig. 19. Frame error rate performance of V-STAR with 16 QAM constellation and irregular LDPC codes.

For a 3×3 MIMO channel, we use a rate- $3/4$ irregular LDPC code of length 2000 bits, which amounts to a data rate of $R = 6$ b/s/Hz. In this case, we see that the frame error rate performs to within 4 dB of the outage probability. This result shows the significant improvement in diversity that V-STAR achieves even with a codes of length less than 3000 bits. With more powerful error correcting codes, the frame error rates of V-STAR is expected to approach the outage probability even more closely.

4.3 G-STAR: STAR with Group Encoding and Decoding

Thus far, we have considered V-STAR, the variant of STAR with independent coding, where each codeword spans just one antenna. We now propose the G-STAR scheme, which combines the STAR architecture with group encoding. Group encoding is a scheme where the t antennas are divided into t/q groups of q antennas each. The q antennas in each group are coded jointly with one channel code [14]. The receiver employs group

detection, a popular MIMO detection technique [14][32], where joint ML decoding is performed on each group followed by interference cancellation to facilitate the decoding of the next group. Group decoding has been previously used in conjunction with V-BLAST, where each layer would consist of q antennas, as opposed to just one in V-BLAST. We will refer to this coding scheme as *naive group encoding*.

In G-STAR, the static fading frame is divided into t/q blocks and one group of antennas is turned *off* over each block. For example, if $t = 8$ and $q = 2$, we have four groups of 2 antennas each, say $\{g_1, g_2, g_3, g_4\} = \{(1, 2), (3, 4), (5, 6), (7, 8)\}$. As illustrated in Fig. 20, the frame is divided into four blocks and the group $\{g_l\}$ with $l = q$ is turned off during the q^{th} block. Thus, in the first block, g_1 is inactive; during the next block, g_2 is inactive and so on. The channel faced by the l^{th} group is denoted by $\mathbf{H}_l = [\mathbf{h}_{q(l-1)+1}, \dots, \mathbf{h}_{ql}]$. Hence, the t/q antenna groups are encoded using t/q independent SISO channel codes. Hence, the rate of the G-STAR transmitter is $t - q$.

4.3.1 Group Decoding

In G-STAR, the i^{th} group is a concatenation of t/q blocks, with the i^{th} block being inactive. The SC decoding process is a t/q -stage process. In the i^{th} stage, the SC decoder detects each active block $\{j = 1, 2, \dots, t/q, j \neq i\}$ in the i^{th} group, by nulling out the

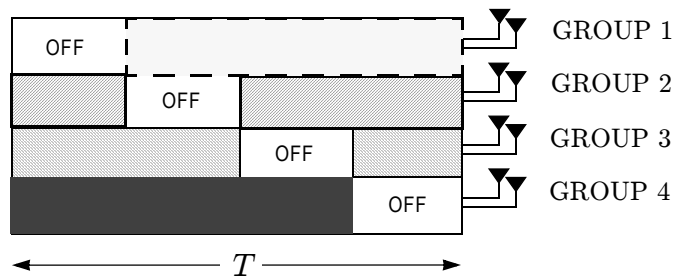


Fig. 20. G-STAR transmitter with $t = 8$ antennas divided into 4 groups of $q = 2$ antennas each.

undetected groups. Subsequently, the bits in the i^{th} group are decoded using a joint ML decoder. The decoded group is used to cancel out the interference before decoding the next group.

To decode the j^{th} block in the i^{th} group, the zero forcing SC decoder nulls out the undecoded groups using the *nulling matrix* $\mathbf{W}_i^{(j)}$, defined as the first q rows of the Moore-Penrose inverse of the matrix $[\mathbf{H}_i, \mathbf{H}_{i+1}, \dots, \mathbf{H}_{j-1}, \mathbf{H}_{j+1}, \dots, \mathbf{H}_{t/q}]$. The estimate of the j^{th} block in the i^{th} group is obtained as $y_i^{(j)}(1, 2, \dots, q) = \mathbf{W}_i^{(j)}\mathbf{r}^{(j)}$. Thus, the channel model reduces to

$$y_i^{(j)}(1, 2, \dots, q) = x_i^{(j)}(1, 2, \dots, q) + \mathbf{W}_i^{(j)}n_i^{(j)}. \quad (61)$$

The equivalent channel (61) is a set of q dependent AWGN channels with the $q \times q$ noise covariance matrix $N_0\mathbf{W}_i^{(j)}\mathbf{W}_i^{(j)\dagger}$. In order to decode this group, the log-likelihood ratios (LLR) of the corresponding bits are obtained using a joint MAP detector and input to the outer code decoder. Now, we compute the instantaneous capacity of the *equivalent channel* formed by the MIMO channel and the group SC decoder. Since the noise covariance matrix of the equivalent AWGN channels is $N_0\mathbf{W}_i^{(j)}\mathbf{W}_i^{(j)\dagger}$, the capacity of the i^{th} group is

$$C_i(\mathbf{H}) = \frac{1}{(t/q)} \sum_{j \neq i} \log_2 \det \left(I + \frac{S}{t-q} (\mathbf{W}_i^{(j)}\mathbf{W}_i^{(j)\dagger})^{-1} \right). \quad (62)$$

The i^{th} group is in outage if $C_i(\mathbf{H}) < Rq/t$. If *any* of the streams is in outage, the decoder is in outage. Hence, the outage probability is

$$P_{G-STAR}(S, R) = \Pr\left[\bigcup_{i=1}^{t/q} \left\{C_i(\mathbf{H}) < \frac{Rq}{t}\right\}\right]. \quad (63)$$

The performance of the group decoder depends on the order of detection of the groups. The order can be described by the permutation $\pi(1, 2, \dots, t)$, where π_k is the k^{th} detected group. We extend the ordering algorithm used in V-STAR to this case. The following ordering algorithm greedily maximizes the group capacity at every stage of detection. For a given channel realization \mathbf{H} , π_k , the k^{th} layer detected is chosen as

$$\pi_k = \underset{i \notin \{\pi_1, \dots, \pi_{k-1}\}}{\operatorname{argmax}} \frac{1}{(t/q)} \sum_{j \neq i} \log_2 \det\left(I + \frac{S}{t-q} \mathbf{Q}_i^{(j)}\right), \quad (64)$$

where,

$$\mathbf{Q}_i^{(j)} = (\mathbf{W}_i^{(j)} \mathbf{W}_i^{(j)\dagger})^{-1}, \quad (65)$$

$$\tilde{\mathbf{W}}_i^{(j)} = (\mathbf{H}_{\Omega(i,j)}^\dagger \mathbf{H}_{\Omega(i,j)})^{-1} \mathbf{H}_{\Omega(i,j)}^\dagger, \quad (66)$$

and $\mathbf{W}_i^{(j)}$ is the matrix formed by the first q rows of $\tilde{\mathbf{W}}_i^{(j)}$, as given by

$$\mathbf{W}_i^{(j)} = \tilde{\mathbf{W}}_i^{(j)}(\{1, 2, \dots, q\}, :), \quad (67)$$

and

$$\Omega(i, j) = [i, 1, \dots, i-1, i+1, \dots, t] - [j, \pi_1, \dots, \pi_{k-1}]. \quad (68)$$

This ordering algorithm can be proved to be optimal in terms of minimizing the outage probability, along the lines of Theorem 4.

4.3.2 Simulation results for G-STAR

We now present the simulation results for G-STAR. We consider an 8×8 MIMO system where the transmitter is divided into 4 groups of two antennas each. The total data rate of $R = 16$ b/s/Hz is distributed equally among the 4 transmit groups. Fig. 21 compares the outage probability of G-STAR to the naive group encoding strategy, both with unconstrained decoding and SC decoding. Note that the transmitter of naive group encoding is identical to the group-constrained channel itself and hence, with unconstrained decoding, naive group encoding achieves the outage probability of the group-constrained channel. Thus, the left-most curve was calculated using (5) of [14]. Fig. 21 shows that the outage probability of G-STAR with SC decoding is only 1.6 dB short of the outage probability of the group-constrained channel. Moreover, when restricted to SC decoding, G-STAR outperforms naive group encoding by 8.2 dB. G-

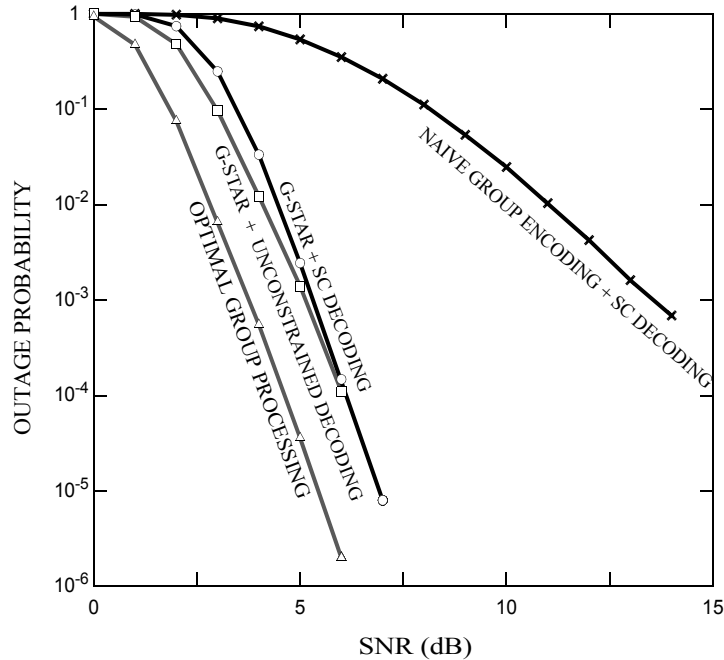


Fig. 21. G-STAR vs naive group encoding with SC and unconstrained decoding, $t = 8$, $r = 8$ and $q = 2$.

STAR with SC decoding is only 0.2 dB away from G-STAR with unconstrained decoding. However, the naive group encoding strategy with SC decoding loses 9.8 dB to the corresponding unconstrained decoder at an outage probability of 10^{-3} . Thus, we see that G-STAR is much better suited to SC decoding than is the naive group encoding strategy.

4.3.3 Performance-complexity tradeoff in G-STAR

The structure of G-STAR allows for flexible performance-complexity tradeoff as the group size is varied. The minimum group size is 1 and this set-up is identical to V-STAR, whereas the maximum group size is t , which yields a MIMO system coded jointly over t antennas. The minimum group size corresponds to the case where the complexity is minimum, whereas the outage probability is also the highest. The complexity of decoding is exponential in the group size, but only polynomial ($\mathcal{O}(n^3)$) in the number of groups. Clearly, the exponential part dominates the total decoding complexity. For a MIMO system with 8 transmit antennas, the possible group sizes are $q = 1, 2, 4$ and 8. The decoding complexity is proportional to q^M where M is the size of the constellation used for transmission. Depending on the available computational resources, one can choose the appropriate version of G-STAR.

4.4 D-STAR: STAR With Diagonal Layering

In this section, we introduce the STAR architecture with diagonal coding, D-STAR.

4.4.1 The D-STAR Transmitter

In D-STAR, $t - 1$ independent streams of data are each coded using scalar SISO codes, constituting $t - 1$ layers, and each layer is transmitted such that it spans multiple transmit antennas. In Fig. 22 we show two possible diagonal coding schemes for a simple 3-transmit antenna system to obtain two variants of the D-STAR architecture, D-STAR 1 and D-STAR 2.

In both layering schemes, $t - 1$ independent streams of data are coded using scalar SISO codes to produce $t - 1$ layers. The general coding rule for these two schemes, which can be extended to an arbitrary number of antennas, is defined as follows:

D-STAR 1: The $t - 1$ layers are transmitted such that the i^{th} layer is transmitted through the i^{th} active antenna. Contrast this with the i^{th} antenna in V-STAR. For example, from Fig. 22, the active antennas during the first block are $\{2, 3\}$. Hence, the first active antenna is 2 and the second active antenna is 3. Hence, in the first block, the first layer is transmitted from the 2nd antenna and the second layer is transmitted from the 3rd antenna.

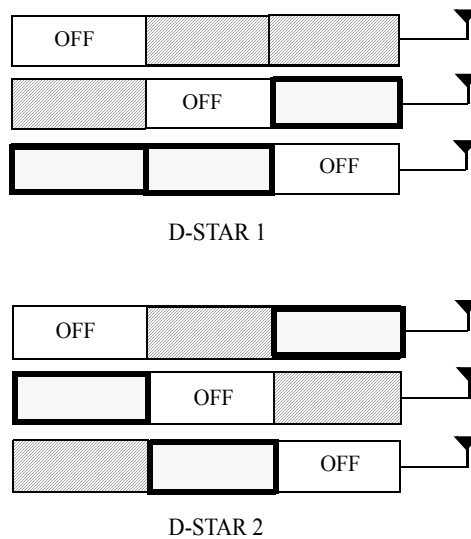


Fig. 22. Two possible configurations of D-STAR with $t = 3$.

We define a *segment* of a layer as that part of layer which is transmitted during one block. Clearly, a segment is T/t symbol periods long.

D-STAR 2: The $t - 1$ layers are transmitted such that

- No two segments of any layer are transmitted from the same antenna.
- No two segments of any layer are transmitted during the same block.

For example, in Fig. 22, we see that the 1st layer is transmitted through the 2nd antenna in the first block, 3rd antenna in the second block and 1st antenna in the third block. Similarly, the 2nd layer is transmitted through the 3rd antenna in the first block, 1st antenna in the second block and 2nd antenna in the third block. Note that as opposed to D-BLAST, the length of each layer in D-STAR is equal to the maximum possible code length T . This will enable the frame error rates of D-STAR to approach the outage probability closely, since the codewords are sufficiently long.

4.4.2 *Decoding of D-STAR*

The optimal way to decode D-STAR is to jointly decode all the layers using an ML decoder. However, this is too complex. Hence, we use ordered SC decoding to decode the layers of D-STAR. The decoding proceeds in the same fashion as V-STAR and D-STAR, namely all blocks in one layer are decoded and their contribution is cancelled out before the next layer is decoded. The order of decoding is chosen so as to maximize the minimum among layer capacity. This is done using the same greedy algorithm as in V-STAR.

4.4.3 Performance Results

In this section, we present numerical results for the outage probability of D-STAR over a 4×4 MIMO channel with $R = 8$ b/s/Hz. Fig. 23 compares the outage probabilities of D-STAR with D-BLAST with the outage probability of the MIMO channel.

Firstly, we note that the performance of D-STAR 1 and D-STAR 2 are almost identical. Hence, for the rest of our discussions, we will use D-STAR 1 as the representative of the outage performance of the D-STAR architecture. At an outage probability of 10^{-3} , D-STAR is about 3.5 dB away from the channel outage probability, while just requiring SC decoding. Compare this to the joint encoding and joint ML decoding required to achieve the channel outage probability. The outage probability of D-BLAST, as discussed before, depends on the code length versus rate tradeoff.

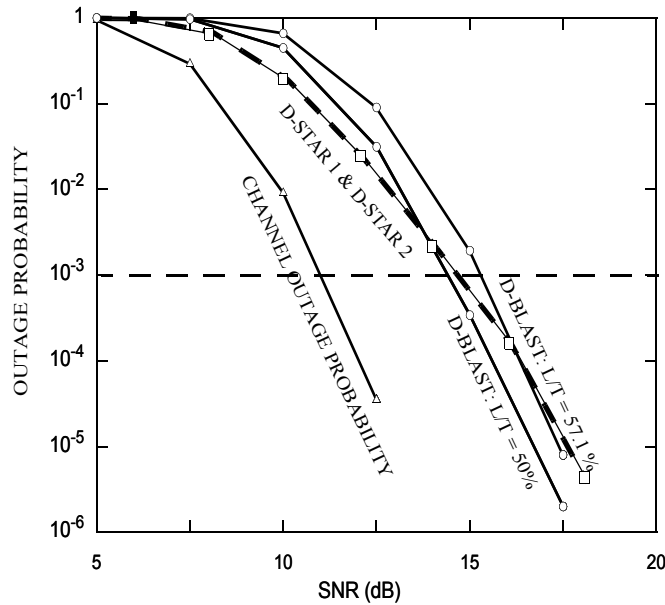


Fig. 23. Outage probability of D-STAR vs. D-BLAST with different code lengths with $t = 4$, $r = 4$ and $R = 8$ b/s/Hz.

Fig. 23 shows two curves corresponding to D-BLAST with code lengths of 50% and 57.1% of the full code length, which corresponds to $N_D = 5$ and $N_D = 4$ respectively. At an outage probability of 10^{-3} , D-STAR lies between these two curves. The inference from this plot is that, *if each layer of D-BLAST were to achieve capacity with code lengths shorter than 50% of T , then D-BLAST is better than D-STAR. On the other hand, if D-BLAST requires codelengths longer than or equal to 57.1%, D-STAR outperforms D-BLAST.*

The question of what codelength is sufficient for D-BLAST is an open research problem. Answering this question numerically for a specific family of error control codes might not be easy, however a tool which characterizes the performance of error control codes as a function of code lengths [60], such as the error exponent [27] of the equivalent channel created by D-BLAST, may be a promising way to approach the problem.

4.5 Summary

We introduced the space-time active rotation (STAR) family of layered space-time architectures. We consider STAR with vertical, group and diagonal layering at the transmitter with successive cancellation decoding at the receiver. We considered the vertically layered V-STAR architecture decoding and show that it achieves near optimum outage performance, for example, to within 1.4 dB of the optimum outage probability over a 4×4 spatial multiplexing system, with just an SC decoder. Then, we introduced the G-STAR architecture, which uses group processing to enable a flexible performance-complexity tradeoff. We showed that G-STAR achieves an outage probability within 1.6 dB of the optimum outage probability of group-encoded systems over an 8×8 MIMO

system with a group size of 2. Finally, we introduced the diagonally layered D-STAR architecture and showed that it gets to within 3.5 dB of the outage probability of a 4×4 MIMO channel with an SC decoder. We also show D-STAR overcomes the drawback of code-length vs. rate tradeoff that is inherent to D-BLAST. In summary, we have proposed the STAR family of layered space-time architectures that achieve near-optimum outage performance just SC decoding at the receiver, while requiring no form of receiver feedback.

CHAPTER 5

DIVERSITY-MULTIPLEXING TRADEOFF IN LAYERED ST ARCHITECTURES

The tradeoff between multiplexing and diversity benefits offered by MIMO systems has been a topic of significant interest. For long, questions on the existence and the nature of a tradeoff between diversity, rate and multiplexing generated a lot of interest in the research community [29][30]. The seminal work of Zheng and Tse [11][12] on diversity-multiplexing tradeoff (DMT) answered several questions on this topic.

Since then, DMT has been a valuable tool in evaluating any scheme proposed for any wireless communication system over quasistatic fading channels. In this chapter, we evaluate the STAR architecture using the DMT framework. The key to understanding and quantifying the tradeoff between the rate, multiplexing and diversity benefits of a MIMO system is a set of appropriate definitions of each of these quantities. Therefore, we define a few terms before proceeding further.

This chapter is organized as follows: In Section 5.1, we define the problem and provide some background on the framework being considered. In Section 5.2, we discuss the rate-diversity tradeoff in V-STAR and propose the generalized V-STAR structure. In Section 5.3, we analyze the V-STAR protocol under the DMT framework. In Section 5.4, we analyze the G-STAR framework under the DMT framework and summarize our conclusions in Section 5.5.

5.1 Background and Definitions

Conventionally, the *rate* of a transmission scheme is defined as the number of independent symbols transmitted by the system per channel use. Contrast the symbol rate with the data rate, R , of a system which is measured in b/s/Hz. The maximum rate for a transmitter with t antennas is t .

However, there are instances when a linear combination of symbols is transmitted as a new symbol, for example, two independent symbols z_1 and z_2 could be combined linearly to get $z = a_1 z_1 + a_2 z_2$ and be transmitted through one antenna. In such cases, we would like the definition of the rate to regard z as simply one symbol from a bigger constellation and not two independent symbols z_1 and z_2 , since the latter could lead to a case where, technically, the rate of a system could be infinite. In order to avoid this quandary, we present the following formulation.

We consider *linear space-time codes* operating over t transmit antennas and N_{ST} symbols periods. In one block of encoding, the space-time code takes a vector $\mathbf{u} \in \mathbb{C}^{N_u \times 1}$ of complex input symbols and produces $Z \in \mathbb{C}^{t \times N_{\text{ST}}}$ such that each element of Z is a linear combination of the input symbols. Specifically, the encoder applies a linear transformation $L \in \mathbb{C}^{t N_{\text{ST}} \times N_u}$ on \mathbf{u} to obtain a vector $\mathbf{z} = L\mathbf{u}$, where $\mathbf{z} \in \mathbb{C}^{t N_{\text{ST}} \times 1}$. The vector \mathbf{z} with $t N_{\text{ST}}$ elements is rearranged into a space-time codeword $Z \in \mathbb{C}^{t \times N_{\text{ST}}}$. For any space-time code which can be expressed in this form, we define the symbol rate as follows.

Definition 3. The *symbol rate*, μ , of the linear space-time transmission scheme above is equal to $\text{rank}(L) / N_{\text{ST}}$.

We now summarize the diversity multiplexing tradeoff framework, which was formulated by Zheng and Tse [11][12]. Here, we recall some of the definitions used in this framework.

Definition 4. In the diversity-multiplexing tradeoff framework, a *coding scheme* for any transceiver is defined as a family of codes $\{\Omega(S)\}$, one for each SNR S . The DMT framework allows the data rate R to scale with the SNR as quantified by the *multiplexing gain*, which is defined as

$$\rho = \lim_{S \rightarrow \infty} \frac{R}{\log S}. \quad (69)$$

Remark 3. For a fixed data rate system, the limit of the ratio of data rate to $\log S$ is zero, and hence the multiplexing gain is zero.

Definition 5. The outage probability of the transceiver decays as $S^{-d(\rho)}$ for large S , where $d(\rho)$ is the *diversity order*, defined as:

$$d(\rho) = \lim_{S \rightarrow \infty} \frac{-\log P_{\text{out}}(S, R)}{\log S}. \quad (70)$$

Zheng and Tse showed in [11] that there is the following fundamental tradeoff between $d(\rho)$ and ρ for an unconstrained transmission scheme over a MIMO Rayleigh fading channel.

$$d(\rho) = (t - \rho)(r - \rho), \quad \rho = 0, 1, \dots, \min(t, r). \quad (71)$$

Remark 4. The maximum achievable diversity order is tr , and the maximum achievable multiplexing gain is $\min(t, r)$.

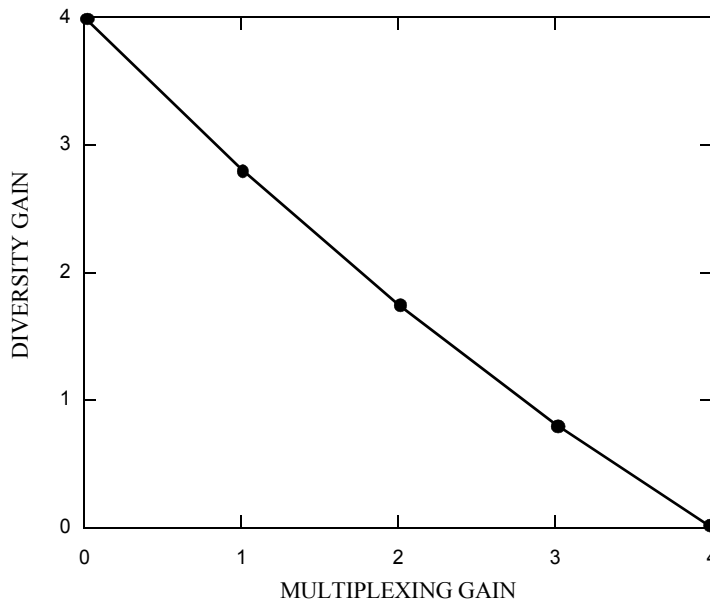


Fig. 24. Diversity-multiplexing tradeoff for a vertically layered system over a 4×4 MIMO channel.

Remark 5. The result in (71) implies that any constant (that does not scale with S) data rate R corresponds to a multiplexing gain of 0. Hence, one can achieve the full diversity tr for any fixed data rate. Thus, *full rate* ($\mu = t$) and full diversity ($d = tr$) are simultaneously achievable. However, the full multiplexing gain $\min(t, r)$ and full diversity (tr) are not simultaneously achievable.

Hence, while there is a *fundamental tradeoff* between *diversity and multiplexing gain* over MIMO channels, there is *no fundamental rate-diversity tradeoff* over Rayleigh fading MIMO channels. The above statement is true only when there are *no constraints* on the system. The tradeoff characteristic can change when a constraint of any kind is imposed on the system. For instance, when a system is restricted to SC decoding, the full diversity and full rate may not be simultaneously achievable. Therefore, when a constraint such as a *complexity constraint* is imposed on the system, there could be a nontrivial rate-diversity

tradeoff and hence the need to determine the *optimal rate-diversity tradeoff* which yields the minimum outage probability (error rate). In such cases, rate and diversity are tools which help us design good transceivers.

As an example, when the constraint of vertical layering is placed on a system, the best diversity-multiplexing tradeoff achievable is given by [12]

$$d_{SM}^*(\rho) = \begin{cases} \left(1 - \frac{\rho}{t}\right)\left(r - \frac{\rho}{t}\right), & \rho \leq t \min\left(1, \frac{r}{t+1}\right) \\ (t - \rho)(r - \rho), & \rho \geq t \min\left(1, \frac{r}{t+1}\right) \end{cases}. \quad (72)$$

5.2 Rate-Diversity Tradeoff in V-STAR

The V-STAR architecture, in comparison to V-BLAST, can be viewed as a technique which sacrifices rate to gain in diversity. So far, we have considered V-STAR with antenna subsets of size $t - 1$, so that the *rate* of the system is $t - 1$. In this section, we generalize V-STAR to enable all possible rates, $\mu = 1, 2, \dots, t$.

In the generalized V-STAR system, if the rate is chosen to be μ , the static fading frame would be divided into $N = \binom{t}{\mu}$ blocks, with one distinct antenna subset of size μ being active over one block. Thus, active rotation is implemented using antenna subsets of any generic size μ instead of $t - 1$. For example, with $\mu = t$, V-STAR is identical to V-BLAST. The outage probability of this generalized V-STAR system is a function of the triplet $\{S, R, \mu\}$. For a given SNR S and data rate R , the objective of system design is to choose μ so as to minimize the outage probability:

$$L^* = \underset{L}{\operatorname{argmin}} P_{V\text{-STAR}}(S, R, L). \quad (73)$$

Given S and R , the outage probability can be evaluated numerically using Monte-Carlo simulations for all possible values of L , since closed form expressions for the exact outage probability are not mathematically tractable. The value of L that yields the minimum outage probability is chosen for the given data rate and SNR. This optimization, though exhaustive, needs to be done just once and is independent of the channel realization. When restricted to an SC decoder, the diversity order of V-STAR is a function of the transmitter rate. We now analyze V-STAR under the condition that the optimal rate is chosen by design. Let $d_{V\text{-STAR}}(L)$ denote the diversity order of V-STAR with rate L . We prove that $d_{V\text{-STAR}}(L^*) = r$.

Theorem 5. V-STAR, with optimum rate selection and SC decoding, achieves the full diversity, r , of independently coded MIMO systems.

Proof: For the given SNR S and data rate R , the multiplexing rate is chosen to minimize the outage probability. One of the possible solutions is $L = 1$. The corresponding outage probability is given by

$$P_{V\text{-STAR}}(S, R, 1) = \Pr \left\{ \log_2(1 + S \min_i(\|h_i\|^2)) < R \right\} \quad (74)$$

$$= \Pr \left\{ \min_i(\|h_i\|^2) < \frac{(2^R - 1)}{S} \right\}. \quad (75)$$

Using the above equations, the outage probability can be approximated as

$$P_{V-STAR}(S, R, 1) \cong \frac{t(2^R - 1)^r}{r! S^r}. \quad (76)$$

The diversity order of at least one of the possible choices of rate, $L = 1$, is r . The outage probability corresponding to L^* must be less than or equal to that of $L = 1$, by design:

$$P_{SM}(S, R) \leq P_{V-STAR}(S, R, L^*) \leq P_{V-STAR}(S, R, 1). \quad (77)$$

The upper bound implies that $d_{V-STAR}(L^*) \geq r$ and the lower bound requires that $d_{V-STAR}(L^*) \leq r$. Thus, $d_{V-STAR}(L^*) = r$, which is the *full* diversity of vertically layered systems.

However, our objective is to choose the rate which minimizes the outage probability, rather than just maximizing diversity. Though $L = 1$ ensures full diversity, it may not be the optimal rate in terms of minimizing the outage probability at a given SNR. Clearly, it is undesirable to have a high rate and low diversity (V-BLAST) or to have a low rate and high diversity (SIMO).

So far, the diversity order of V-STAR is accurately known for the two extreme values of rate namely, $L = 1$ and $L = t$ as $d_{V-STAR}(1) = r$ and $d_{V-STAR}(t) = 1$. Now, we obtain a lower bound on the diversity order of V-STAR for any channel dimension. In order to derive this bound, we consider a MIMO system with *antenna selection* which, for any given \mathbf{H} , is allowed to choose a subset of L antennas to be active, with the other antennas being switched off. Assume that this choice could be made with feedback from the

receiver, such that the outage probability of the resulting system with ordered SC decoding is minimized, while keeping the data rate unchanged. We will refer to this technique as L^{th} order antenna selection and the set of active antennas as U_{L^*} .

Lemma 7. The diversity order d_{AS} of an L -th order antenna selection system with linear or SC decoding is lower bounded as [43] $d_{\text{AS}}(L) \geq (t - L + 1)(r - L + 1)$.

We now use the above lemma to derive a bound on the diversity order of V-STAR.

Theorem 6. The diversity order of V-STAR with SC decoding is bounded as

$$\min\{(t - L + 1)(r - L + 1), r\} \leq d_{\text{V-STAR}}(L) \leq r. \quad (78)$$

Specifically, V-STAR with SC decoding achieves the full diversity, r , of independently coded systems for $t = 3$ and $t = 4$.

Proof: The generalized V-STAR system has $N = \binom{t}{L}$ blocks with a distinct set of L antennas being active over each. Hence, there is exactly one block over which the active antennas are identical to the set U_{L^*} . Consider an SC decoder that first decodes the layers specified by U_{L^*} . Using Lemma 7, the diversity order of outage probability of these L layers is $(t - L + 1)(r - L + 1)$ and hence the diversity order of the i^{th} layer, $d_i \geq (t - L + 1)(r - L + 1)$ for all $i \in U_{L^*}$. Given that these L layers have been decoded and canceled out, each of the remaining $t - L$ layers has exactly L unique blocks over which there is no interference from another layer. Hence, the diversity order of the last layer ($t - L$) layers is at least r . From these observations,

we have $d_i \geq r$ for all i and specifically, $d_t = r$. For the special cases of $t = 3$ and $t = 4$, $d_{\text{V-STAR}}(t - 1) = r$ for any $r \geq t$.

We use this bound on the diversity order to determine the conditions under which V-STAR can be guaranteed to achieve the full diversity, r , of spatial multiplexing systems. Clearly, V-STAR can be guaranteed to achieve a diversity r when the upper and lower bounds in (78) are equal, which requires that

$$(t - L + 1)(r - L + 1) \geq r, \quad (79)$$

$$L^2 - L(r + t + 2) + (rt + t + 1) \geq 0. \quad (80)$$

Solving for L with the constraint that L needs to be an integer, the value of L^* which guarantees that V-STAR will achieve full diversity is

$$L = \left\lfloor \frac{r + t + 2 - \sqrt{(r - t)^2 + 4r}}{2} \right\rfloor. \quad (81)$$

For square MIMO channels, i.e., $r = t$, we get

$$L = \lfloor 1 + r - \sqrt{r} \rfloor. \quad (82)$$

Fig. 25 shows the value of L^* for square MIMO channels as the MIMO channel dimension increases. We see that V-STAR enables very high rate with increasing channel dimensions while guaranteeing full diversity. The implication here is that the rate of generalized V-STAR needs to be *no less than* L^* if the goal of system design is to achieve

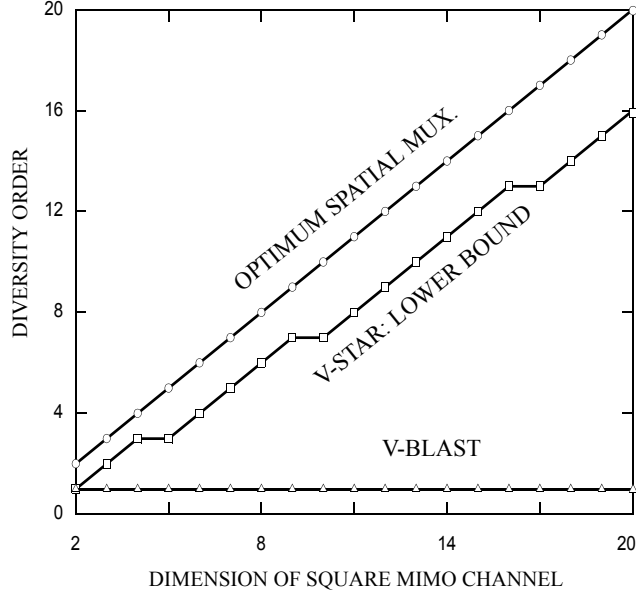


Fig. 25. Lower bound on diversity order of V-STAR over square MIMO channels.

full diversity. Note that $\min\{(t - L + 1)(r - L + 1), r\}$ is only a lower bound on the diversity order of V-STAR and hence the symbol rate for which generalized V-STAR achieves full diversity is *at least* L^* (or possibly higher).

5.3 Diversity-Multiplexing Tradeoff in V-STAR

In this section, we analyze V-STAR under the diversity-multiplexing tradeoff (DMT) framework [11]. The rate-diversity tradeoff discussed in the previous section is different from the DMT characterization in [11].

The optimal DMT for an independently coded $r \times t$ MIMO system is identical to that of a multiple access system with t independent users with one antenna each and r antennas at the receiver, since the two setups are identical. The tradeoff is given by [12]

$$d_{SM}^*(\rho) = \begin{cases} \left(1 - \frac{\rho}{t}\right)\left(r - \frac{\rho}{t}\right), & \rho \leq t \min\left(1, \frac{r}{t+1}\right) \\ (t - \rho)(r - \rho), & \rho \geq t \min\left(1, \frac{r}{t+1}\right) \end{cases}. \quad (83)$$

This tradeoff is achievable with equality using a naive spatial multiplexer with unconstrained decoding. However, it is of interest to explore how close one can get to the optimal DMT with suboptimal, low complexity decoders. We focus on decoders based on SC decoding. It was shown in [12] that the DMT for naive spatial multiplexing with SC decoding is given by

$$d_{sc}^*(\rho) = (r - t + 1)\left(1 - \frac{\rho}{t}\right). \quad (84)$$

We now characterize the DMT for the V-STAR system with SC decoding, $d_{V-STAR}^*(\rho, L)$, for different values of L . We divide the problem into three cases, namely, $L = 1$, $L = t$ and $L = \{2, 3, \dots, t - 1\}$. When $L = t$, the V-STAR system is identical to V-BLAST, hence the tradeoff is given by

$$d_{V-STAR}^*(\rho, t) = (r - t + 1)\left(1 - \frac{\rho}{t}\right). \quad (85)$$

When $L = 1$, the outage probability of V-STAR for $S \rightarrow \infty$, from (71) is given by

$$P_{V-STAR}(S, R, 1) \rightarrow \frac{t(2^R - 1)^r}{r!S^r}. \quad (86)$$

If the data rate scales as $R = \rho \log S$, then

$$P_{V-STAR}(S, R, 1) \rightarrow \frac{tS^{-r(1-\rho)}}{r!}. \quad (87)$$

Thus, the DMT of V-STAR with $L = 1$ is given by

$$d_{V-STAR}^*(\rho, 1) = r(1 - \rho). \quad (88)$$

Now, we derive an upper bound on the DMT for other values of L using a lower bound on outage probability. The outage probability of V-STAR with SC decoding is at least as much as that with unconstrained decoding, i.e., $P_{V-STAR}(S, R, L) \geq P_{V-STAR}^{ML}(S, R)$, where $P_{V-STAR}^{ML}(S, R)$ is the outage probability of STAR with joint maximum-likelihood decoding. This probability can be bounded as

$$P_{V-STAR}^{ML}(S, R) \geq \Pr\{C_q < R\} \quad (89)$$

for any layer q , where C_q is the capacity of the q^{th} layer. Using $q = \underset{i \in \{1, 2, \dots, t\}}{\operatorname{argmin}} \|\mathbf{h}_i\|^2$, and the fact that \mathbf{h}_i are independent of each other, we get

$$P_{V-STAR}(S, R, L) \geq \Pr\left\{L \log_2 \left(1 + \frac{S}{L} \min_i (\|\mathbf{h}_i\|^2)\right) < R\right\} \quad (90)$$

and

$$P_{V-STAR}(S, R, L) \geq \Pr\left\{\min_i (\|\mathbf{h}_i\|^2) < \frac{L(2^{R/L} - 1)}{S}\right\}. \quad (91)$$

As $S \rightarrow \infty$, the outage probability can be approximated as

$$P_{V-STAR}(S, R, L) \geq \frac{L^r t S^{-r(1-\rho/L)}}{r!}. \quad (92)$$

Thus, the diversity order is bounded by

$$d_{V-STAR}^*(\rho, L) \leq r \left(1 - \frac{\rho}{L}\right). \quad (93)$$

Specifically, we focus on rate $L = t - 1$, since it was observed to minimize the outage probability for all dimensions of the channel and SNRs considered.

$$d_{V-STAR}^*(\rho, t - 1) \leq r \left(1 - \frac{\rho}{t - 1}\right). \quad (94)$$

5.4 Diversity-Multiplexing tradeoff in G-STAR

In this section, we analyze G-STAR under the diversity-multiplexing framework [11]. The optimal diversity-multiplexing tradeoff curve for a group-encoded $r \times t$ MIMO system with a group size of q is identical to that of a multiple access system with t/q independent users with q antenna each and r antennas at the receiver, since the two setups are identical. The optimal diversity-multiplexing tradeoff of this system is given by

$$d_{G-SM}^*(\rho) = \begin{cases} \left(\frac{t-\rho}{q}\right)\left(r - \frac{\rho}{q}\right), & \rho \leq \frac{t}{q} \min\left(q, \frac{r}{t/q+1}\right) \\ \left(\frac{t}{q} - \rho\right)(r - \rho), & \rho \geq \frac{t}{q} \min\left(q, \frac{r}{t/q+1}\right) \end{cases}. \quad (95)$$

From (95), we see that the maximum diversity, which is achievable at any fixed data rate, $d_{G-SM}^*(0) = rt/q$. The maximum multiplexing rate is $\min(t/q, r)$. This tradeoff curve is achievable by using an unconstrained decoder with a naive group encoder. It was shown in [12] that the diversity-multiplexing tradeoff for naive group encoding with SC decoding is given by

$$d_{sc}^*(\rho) = \left(r - \frac{t}{q} + 1\right) \left(1 - \frac{\rho}{t/q}\right). \quad (96)$$

The diversity-multiplexing tradeoff of G-STAR can be upper-bounded as follows

$$d_{G-STAR}(\rho) \leq \left(q - \frac{\rho t}{t-q}\right) \left(r - \frac{\rho t}{t-q}\right), \quad (97)$$

for $q = 1, 2, \dots, t-1$, where q is a factor of t and

$$d_{G-STAR}(\rho) \leq (t - \rho)(r - \rho) \quad (98)$$

for $q = t$. This result can be proved along the same lines as V-STAR.

5.5 Summary

In this chapter, we derived the diversity-multiplexing tradeoff of V-STAR and G-STAR. We also defined the idea of rate-diversity tradeoff in V-STAR, and distinguished between this and the DMT framework. We introduced the generalized V-STAR system and showed how V-STAR trades off symbol rate in order to gain in diversity. We derived lower and upper bounds on the diversity order of this system, using which we showed that the original V-STAR system (as introduced in chapter) achieves full receive diversity for $t = 4$ and $t = 3$. We also obtained a set of conditions on the t , r and L for generalized V-STAR to achieve full diversity. We derived upper bounds on the DMT of V-STAR and G-STAR in this chapter.

CHAPTER 6

APPLICATIONS OF STAR IN MULTIPLE-ACCESS COMMUNICATIONS

In chapters 2 - 5, we have discussed several layered space-time architectures with different coding schemes. Among the coding schemes, it is easy to see that the special case of independent coding resembles a multiple-access system, where the transmit antennas are equivalent to multiple access users synchronized in time [14]. In this chapter, we explore this connection and find applications for the proposed vertically layered architectures in multiple-access communications.

The concept of space-division multiple-access (SDMA) exploits all the available degrees of freedom over a multiple-access channel, by having all the users transmit simultaneously. In theory, the best outage performance over a multiple-access channel is achieved when users transmit *simultaneously* and *continuously*, a strategy we refer to as *naive SDMA* [4][14]. In practice, however, the receiver has limited computational resources that prevent it from implementing the optimum unconstrained maximum-likelihood decoder that jointly detects and decodes. Clearly, this scenario is analogous to V-BLAST in a single user communication system.

When the receiver is constrained to use a suboptimal receiver based on successive cancellation (SC) detection, the outage performance of the system is severely degraded. Transmitter optimization algorithms such as rate allocation can be used to improve

performance with SC decoding [14], but the resulting outage performance is far from optimal. Furthermore, this approach leads to *unfair solutions* whereby some users have less data rate than others.

This chapter is divided into five sections: In Section 6.1 we describe the channel model of the multiple-access channel. In Section 6.2, we introduce the STAR transmission strategy and successive cancellation decoding at the receiver. In Section 6.3, we derive the outage probability of STAR with SC decoding, and the diversity-multiplexing tradeoff follows in Section 6.4. We present some numerical simulation results in Section 6.5, with a summary of the scheme presented in Section 6.6.

6.1 Channel Model

We consider a multiple-access system with K users, each equipped with t transmit antennas. The receiver has r antennas, with the assumption that $r \geq Kt$. We assume that the channel is flat-fading and static over a frame of T signaling intervals, but fades independently from one frame to the next. The $r \times T$ received matrix is given by

$$\mathbf{R} = \mathbf{H}\mathbf{X} + \mathbf{N}, \quad (99)$$

where the elements of the $r \times T$ noise matrix \mathbf{N} are independent, circularly symmetric Gaussian random variables with zero mean and variance N_0 . The overall channel matrix \mathbf{H} between all the users and the receiver is of dimension $r \times Kt$ and is assumed to be a random Rayleigh fading matrix, its elements being independent, circularly symmetric Gaussian random variables with zero mean and unit variance. \mathbf{X} is the $Kt \times T$ matrix containing the transmitted symbols from all users over T signaling intervals. We assume that the transmitters have no knowledge of the channel \mathbf{H} , while the receiver has perfect

knowledge of \mathbf{H} . The transmitters are assumed to be synchronized in time. We consider the *fair* scenario where each user transmits a data rate R at an average transmit energy of E per signaling interval. Under these assumptions, the average SNR per user per receive antenna is $S = E/N_0$.

6.2 The STAR Architecture

The STAR architecture has two components: a transmission strategy at the time-synchronized transmitters, and a low-complexity decoding algorithm at the receiver.

6.2.1 Transmitters

Roughly speaking, the STAR strategy is the *complement* of the TDMA strategy: the different users take turns being *inactive*, rather than being active. In particular, the STAR transmitters work as follows. Each user encodes its message into a codeword of length $T(1 - 1/K)$ signaling periods, where T is the duration over which the channel is constant and K is the number of users. The static fading frame is divided into K blocks. The first user is inactive (transmits nothing) during the first block, then transmits its codeword

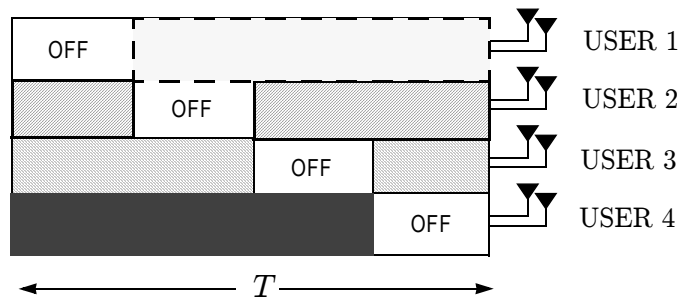


Fig. 26. The timing of transmissions in a space-time active rotation (STAR) system with $K = 4$ users equipped with $t = 2$ antennas each.

during the remaining blocks. The other users behave similarly: the j^{th} user is inactive during the j^{th} block only, while the remaining $K - 1$ users transmit simultaneously. Implicit in this arrangement is an assumption that the transmitters are synchronized.

The timing of the STAR transmissions is illustrated in Fig. 26. This transmission strategy is independent of the instantaneous channel realization.

6.2.2 Receiver

The optimum decoder for a STAR-based multiple-access system is the joint ML decoder. However, its computational complexity is high. In this section we describe a low-complexity decoder for the STAR strategy that is based on SC decoding. Surprisingly, we will see that this decoder can perform nearly as well as the joint ML decoder.

The data from the i^{th} user is a concatenation of K blocks, with the i^{th} block being inactive. Before decoding the i^{th} user, the SC decoder first *detects* all but the i^{th} block of the i^{th} user by nulling out the undetected users in that block. After detection, the symbols of the i^{th} user are decoded using optimal joint detection and decoding. Subsequently, the contribution of the decoded user is cancelled out from the received matrix before decoding the next user.

The nulling matrix $\mathbf{W}_i^{(j)}$, used to detect the j^{th} block of the i^{th} user, is the first t rows of the Moore-Penrose inverse of the matrix $[\mathbf{H}_i, \mathbf{H}_{i+1}, \dots, \mathbf{H}_{j-1}, \mathbf{H}_{j+1}, \dots, \mathbf{H}_K]$, where \mathbf{H}_i is the channel between the i^{th} user and the receiver. The estimate of the j^{th} block of the i^{th} user is obtained as $\mathbf{Y}_i^{(j)} = \mathbf{W}_i^{(j)} \mathbf{R}^{(j)}$, where $\mathbf{R}^{(j)}$ is the received matrix during the j -th block. Thus, the channel model reduces to

$$\mathbf{Y}_i^{(j)} = \mathbf{X}_i^{(j)} + \mathbf{W}_i^{(j)}\mathbf{N}^{(j)}, \quad (100)$$

where, $\mathbf{X}_i^{(j)}$ is the data transmitted from the i^{th} user during the j^{th} block and $\mathbf{N}^{(j)}$ is the noise in the j^{th} block. The equivalent channel (100) has t inputs and t outputs, with the $t \times t$ noise covariance matrix given by $N_0\mathbf{W}_i^{(j)}\mathbf{W}_i^{(j)*}$, where \mathbf{A}^* denotes the conjugate transpose of \mathbf{A} .

6.3 Outage Probability

In this section, we compute the outage probability of a STAR system with SC decoding. The event of outage is defined on the *equivalent channel* formed by the multiple-access channel in conjunction with the SC decoder. For a given \mathbf{H} , the capacity of the i^{th} user in a STAR system is

$$C_i(\mathbf{H}) = \frac{1}{K} \sum_{j \neq i} \log_2 \det \left(\mathbf{I} + \frac{S}{(t-1)} (\mathbf{W}_i^{(j)}\mathbf{W}_i^{(j)*})^{-1} \right). \quad (101)$$

Thus, the capacity of each user with SC decoding is the arithmetic average of the capacities of the K blocks. Since STAR ensures that users of various instantaneous signal strengths, including the weakest user, are turned off over one block, this averaging helps improve the performance significantly compared to naive SDMA with SC decoding.

The i^{th} user is in outage if $C_i(\mathbf{H}) < R$. The overall system is said to be in outage if *any* of the users is in outage. Hence, the outage probability is

$$P_{STAR}(S, R) = \Pr \left[\bigcup_{i=1}^K \{C_i(\mathbf{H}) < R\} \right] = \Pr[\min_i \{C_i(\mathbf{H})\} < R]. \quad (102)$$

The performance of the SC decoder depends on the order in which the users are detected. From (102), we see that the outage probability is limited by the weakest link — the minimum among the user capacities. Extending the greedy ordering algorithm of [5], we arrive at an ordering strategy that minimizes the outage probability of STAR.

Theorem 7. The outage probability of STAR with SC decoding is minimized if, for a given \mathbf{H} , the k^{th} user detected, π_k , is chosen as

$$\pi_k = \underset{i \notin \{\pi_1, \dots, \pi_{k-1}\}}{\operatorname{argmax}} \sum_{j \neq i} \log \det \left(\mathbf{I} + \frac{S}{(t-1)} (\mathbf{W}_i^{(j)} \mathbf{W}_i^{(j)*})^{-1} \right). \quad (103)$$

Proof: A straightforward application of Theorem 4.

6.4 Diversity-Multiplexing Tradeoff

In this section, we analyze STAR under the diversity-multiplexing framework [12]. We consider the symmetric scenario where all the users transmit equal data rates R , and hence have equal multiplexing gains ρ . The diversity-multiplexing tradeoff of a symmetric multiple-access system was derived in [12] as

$$d_{\text{sym}}(\rho) = \begin{cases} (t - \rho)(r - \rho), & \rho \leq \min(t, r/(K + 1)) \\ (Kt - K\rho)(r - K\rho), & \rho \geq \min(t, r/(K + 1)) \end{cases}. \quad (104)$$

The above tradeoff is achievable by naive SDMA with joint ML decoding. It was shown in [12] that the diversity-multiplexing tradeoff for naive SDMA with SC decoding is

$$d_{SC}(\rho) = (t - \rho)(t - (K - 1)t - \rho). \quad (105)$$

Obtaining the exact tradeoff for STAR with SC decoding seems mathematically intractable. We obtain a lower bound on the outage probability and hence an upper bound on the diversity-multiplexing tradeoff of a STAR system.

From the result obtained in (98), the diversity-multiplexing tradeoff of a STAR system with SC decoding is bounded as

$$d_{STAR}(\rho) \leq \left(t - \frac{\rho K}{K-1}\right) \left(r - \frac{\rho K}{K-1}\right). \quad (106)$$

We see that the upper bound achieves the full-diversity value of tr when $\rho = 0$. Also, when the number of users K is large, the upper bound in (97) approaches the optimal tradeoff in (106) whenever $\rho < \min(t, r/(K+1))$. Using the results obtained in Theorem 6 we know that for the special case of $t = 1$ and $K = 2$, $K = 3$ and $K = 4$, the bound in (106) is achieved with equality.

6.5 Simulation Results

In this section, we present simulation results for a 4-user multiple-access system 2 transmit antennas per user and 8 receiver antennas. The data rate of each user is $R = 4$ bps/Hz. Fig. 27 compares the outage probability of the STAR strategy to the naive SDMA strategy, both with unconstrained decoding and SC decoding. Note that naive SDMA is identical to the multiple-access channel itself and hence, with unconstrained decoding, naive SDMA achieves the outage probability of the underlying multiple-access channel. Thus, the left-most curve was calculated using (5) of [14].

Fig. 27 shows that the outage probability of STAR with SC decoding is only 1.6 dB short of the outage probability of the multiple-access channel. Moreover, when restricted to SC decoding, STAR outperforms naive SDMA by 8.2 dB. STAR with SC decoding is only 0.2 dB away from STAR with unconstrained decoding. However, the naive SDMA strategy with SC decoding loses 9.8 dB to the corresponding unconstrained decoder at an outage probability of 10^{-3} . Clearly, the STAR transmission strategy is much better suited to SC decoding than is the naive SDMA strategy.

6.6 Summary

We proposed the space-time active rotation (STAR) transmission strategy for multiple-access systems. STAR is an enhanced space-division multiple-access (SDMA) strategy that enables a successive-cancellation (SC) decoder to approach the outage performance of an unconstrained decoder. On the Rayleigh-fading multiple-access channel, the STAR

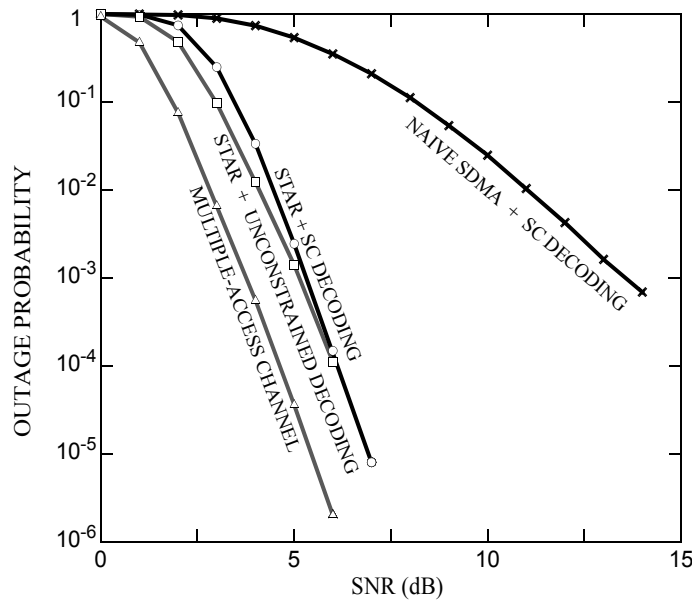


Fig. 27. Performance of the STAR strategy with SC and unconstrained decoding over a multiple-access channel with $K = 4$ users, $t = 2$, $r = 8$ and $R = 4$ bps/Hz per

strategy enables near-optimal outage performance with a low-complexity successive-cancellation decoder. We derived the outage probability and proposed an ordering algorithm for SC decoding that minimizes the outage probability of STAR. We derived an upper bound on the diversity-multiplexing tradeoff of the proposed architecture. We showed that the proposed system outperforms naive SDMA with SC decoding by 8.2 dB for a 4-user multiple-access system with 2 transmit antennas each and 8 receive antennas. We also show that STAR with SC decoding gets to within 1.6 dB of the optimum outage probability for this case. Thus, the STAR transmission strategy with SC decoding is an effective solution to achieve near-optimum outage probability of multiple-access systems at low computational complexity.

PART II

COOPERATIVE COMMUNICATIONS OVER FADING MULTIPLE- ACCESS CHANNELS

In the second part of this thesis, we explore the idea of creating and exploiting spatial diversity using a collection of distributed antennas belonging to multiple terminals in a wireless network, each with its own information to transmit. This concept is known as *cooperative communication*, where the terminals help each other during transmission by sharing their antennas and signal processing resources to create a “*virtual transmit array*” [61]-[67].

In a cooperative communication system, each user in addition to transmitting its own information to the destination listens to the transmission from other users within radio range and relays the received information to the destination. This creates multiple paths over the network between the transmitter and receiver, and hence a new form of diversity known as *cooperative diversity*. Typical examples where cooperative communication can be potentially useful include sensor networks, where the sensor nodes are often not sophisticated enough to have multiple antennas, and ad-hoc networks [61][63]. Moreover, cooperation can also be viewed as an additional source of diversity for wireless systems which already benefit from time, frequency and/or spatial diversity.

Cooperative communication systems can be of two broad categories, cooperative relay networks [67][70][73]-[75] and cooperative multiple-access networks [63]-[68]. In relay networks, there is one transmitter communicating with one receiver, with a set of relays

assisting this communication, and the relays themselves do not have any information to transmit. In cooperative multiple-access systems, a set of users want to communicate with a common destination, with each user helping the another's transmission by acting as a relay during some part of the protocol.

In this work, we address the problem of designing cooperation protocols over cooperative multiple-access systems only. We consider the design of cooperation schemes for multiple-access channels with the goal of achieving high data rates and maximum diversity gain. We aim to answer questions such as: how much cooperation is necessary? and what is the best cooperation strategy? We find some answers to these questions for the basic three-node network, with two users trying to access a common receiver. Following this, we investigate how the gains in a three-node network translate to a larger networks. We propose a new high rate cooperation scheme for an arbitrary number of users and show that our scheme achieves much higher rates than currently existing schemes, especially as the number of users increases, while still achieving full diversity.

CHAPTER 7

PROBLEM INTRODUCTION AND BACKGROUND

We consider the cooperative multiple-access channel, where two or more *users* wish to send independent messages to a common *destination*, and where these users cooperate by occasionally acting as relays for each other. By sharing their antennas and signal processing resources, the users together create a “virtual transmit array” [61]-[68] that provides each user with an additional diversity against fading, thereby increasing the reliability of communication.

A conventional non-cooperative multiple-access strategy like SDMA achieves a high rate but with low diversity. In contrast, because user cooperation necessitates that the users spend some fraction of time listening to other users and acting as relays, a cooperative strategy will have a lower rate and a higher diversity [63]. Hence, there is a fundamental tradeoff in cooperative systems between rate and diversity. Our objective of system design is to maximize the diversity gain, while keeping the rate loss to a minimum.

Cooperative multiple-access protocols can be classified as either *orthogonal* or *non-orthogonal*. Orthogonal protocols, such as the LTW protocol [63], are those in which users are constrained to transmit in non-overlapping time or frequency sub-channels, thereby avoiding interference. These protocols have the advantage of simple decoding, but suffer from low rates due to the orthogonality constraint, and consequently result in high outage probabilities. Non-orthogonal protocols, such as the CMA-NAF protocol [67], allow simultaneous transmission among users and hence enable higher rates.

The remainder of this thesis is organized as follows.

- In this chapter, we present the simple three-node multiple-access system [71], where two users communicate with a common receiver. We state the system assumptions and describe the channel model to be used in the rest of this thesis. We overview the conventional non-cooperative transmission strategies as well as some of the recently proposed cooperative multiple-access schemes.
- In chapter , we introduce *space-division relay*, a high-rate cooperation protocol with full diversity for the simple three-node network, which is shown to achieve the best outage performance among all available schemes.
- In chapter , we investigate the question of how much cooperation is necessary in multiple access channels. To answer this question, we develop the *partial cooperation framework* to measure the optimum level of cooperation needed to achieve the lowest outage probability.
- Finally in chapter , we propose a new cooperation protocol for multiple-access networks with any number of users, and show that our protocol achieves very high rates, asymptotically approaching that of SDMA, while achieving full diversity.

We begin with the basic three-node multiple-access system, with two users sending independent information to a common destination. The remainder of the chapter is organized as follows. In Section 7.1, we describe the channel model to be used and list down the system assumptions. In Section 7.2, we provide a brief overview of non-cooperative multiple-access schemes such as TDMA and SDMA. In Section 7.3, we

review some relay techniques that can be used in a cooperative communication system. In Section 7.4, we review the state-of-the-art cooperative transmission schemes namely the orthogonal LTW protocol and the non-orthogonal CMA-NAF protocol.

7.1 Channel Model

We consider a Rayleigh-fading multiple-access channel with two users communicating with a common destination. Each of the three nodes is equipped with a single antenna. We impose the constraint that a node can either transmit or receive at a given time, and cannot do both simultaneously, a restriction otherwise known as the *half-duplex* constraint [65]. We also assume that each node uses the same frequency band for both transmission and reception. In other words, we consider systems employing time-division duplexing as opposed to frequency division duplexing.

Fig. 28 outlines the possible communication links in a two-user cooperative multiple-access system, whereby each node could either be transmitting its own information or relaying the information received from the other user. The inter-user communication link is used to share and exchange information between the two users prior to the relay operation.

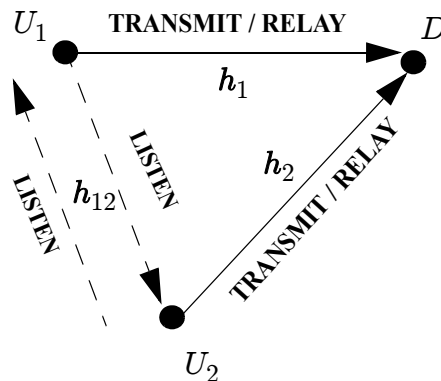


Fig. 28. A two-user cooperative multiple-access system: Possible communication links.

Let h_i denote the channel gain between the i -th user and the destination. Since the nodes transmit and receive over the same frequency band, channel gain of the communication link between the two users is identical, let h_{12} denote this gain. The channels are assumed to be linear and flat fading over the signal bandwidth. Also, the channels are assumed to be quasistatic, so that the channel response is constant over a frame consisting of T symbol periods, and it changes to an independent value from one frame to the next.

The additive noise at each receiving terminal is independent circularly symmetric Gaussian random variable with zero mean and variance N_0 . We assume that the users are frame-synchronized. We further assume that the destination knows all of the channel coefficients $\{h_1, h_2, h_{12}\}$, whereas the users know only h_{12} .

7.1.1 Cooperation and Network Topology

The wireless channel between any two terminals in a wireless network is the cumulative effect of impediments such as path loss, shadowing and fading experienced by the transmitted signal. The fading component is well approximated by Rayleigh fading model and is statistically identical for all links in the network. However, in general, users experience different path losses and shadowing owing to asymmetric distances and location with respect to the destination. For example, if U_1 is closer to the destination compared to U_2 , then the average power of the signals from U_1 as received by the destination, would likely be higher than that of U_2 , due to lower path loss experienced by the signals from U_1 . Therefore, it is clear that network topology affects the average statistical properties of communication links between terminals in a wireless network.

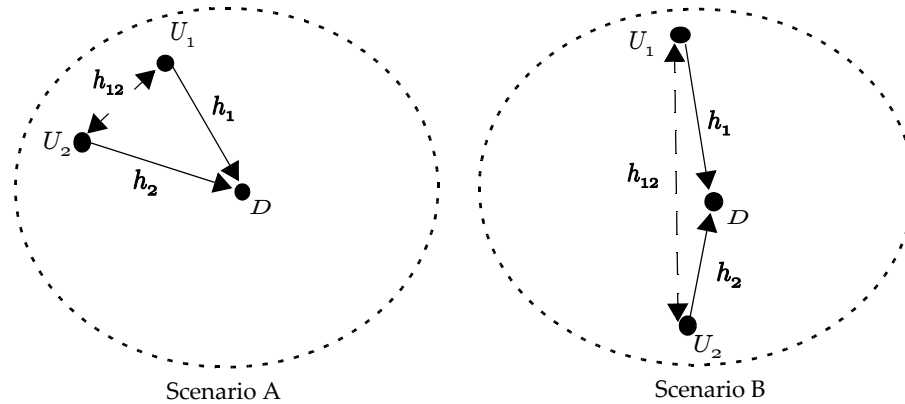


Fig. 29. Two simple network topologies with two multiple-access users communicating with a common destination.

Cooperative communication requires a user to listen to the transmission from other users and relay this information to the destination. In other words, the users are required to be within the radio range of each other, so that mutual transmissions can be received with reasonable signal strength, at least on an average. Therefore, network topology becomes a key factor in choosing when and how users must cooperate. In Fig. 29, we show two simple scenarios to explain the effect of topology on cooperation.

In scenario A, users U_1 and U_2 are within relatively close proximity and hence can listen and relay the information from each other to the destination with reasonable signal strength. However, in scenario B, although U_1 and U_2 are at similar distances to D , they are very far away from each other and hence are likely to receive the transmission from each other with feeble strength. A basic advantage of cooperation is that multiple signal paths can be created between each user and the destination by simply listening into the other's transmission and relaying this information. However, when the users are as far apart as is in scenario B, the listening and relaying operations amount to inefficient utilization of resources, since the associate signal strengths are expected to be very weak. Therefore, intuitively, cooperation seems to be counter-productive in scenario B.

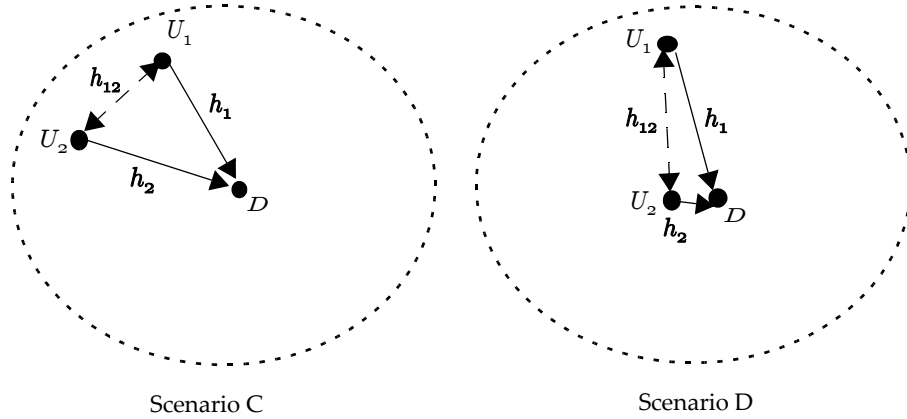


Fig. 30. Two more simple network topologies with two multiple-access users communicating with a common destination.

In Fig. 29, we studied two scenarios where the h_1 and h_2 were similar but the discrepancy in h_{12} made one scenario more conducive to cooperation than the other. Now, in Fig. 30, we consider another pair of scenarios where the h_{12} is similar but h_1 and h_2 are drastically different. In scenario C, which is similar to scenario A, the users are within the radio range of each other and also at similar distances away from the destination. Hence, it can be expected that cooperation helps both users improve their reliability.

However, in scenario D, although the inter-user channel is similar to that in scenario C, we see that U_2 is extremely close to D . Consequently, one might expect that U_2 does not need any cooperative help from U_1 to boost its signal strength and although U_1 can potentially benefit from cooperation with U_2 , mutually symmetric cooperation would mean that U_1 will have to spend some of its resources relaying U_2 's information, which is clearly unnecessary. Moreover, U_1 would be required to sacrifice some of its time on a very good channel in helping out U_2 , for which it is unlikely to gain any significant returns. Therefore, it may not be beneficial for U_1 and U_2 to cooperate, even though they have the capability to do so.

Of the numerous possible topological scenarios, the above four scenarios are just specific examples, and one could conceivably present several such examples where cooperation is a desirable idea or otherwise. But the key conclusion from this study is that it is important to choose the set of cooperating users carefully to have a topology where cooperation is mutually beneficial and the overall reliability and throughput of a group of users are improved as a consequence.

7.1.2 Symmetric Network Assumption

Although we have seen that users in a wireless network can experience drastically different average channel behavior between each other and to the destination, it can be very useful to start with a simple scenario to understand cooperation protocols in depth, before extending the breadth of their applicability. We will review some existing cooperation protocols and propose several new protocols of our own for a simple topology and analyze their properties in detail, laying the foundation for extension to specific topological scenarios.

Instead of allowing the network topology to be a '*free variable*', we make the following simplifying assumptions on the average behavior of the system: We consider a completely symmetric scenario where: (1) the channels from each user to the destination and the channel between the users are statistically identical, meaning $\{h_1, h_2, h_{12}\}$ are i.i.d. and unit variance and that the average received SNR for each user is identical; (2) both have an identical average energy of E per signalling interval; and (3) both users have an identical target data rate of R bps/Hz. Under these assumptions, the average SNR of each user at each receiving node is $S = E/N_0$.

The symmetric network assumption has been used in several previous works such as [63]-[65][69][72][81][82] and a variant of this assumption, where the inter-user channel is assumed to be 3 dB stronger on an average was used in [66]-[68][77]. The use of the symmetric network assumption has the following significant *advantages*: i) it simplifies the analysis by eliminating the topology as a free variable, and provides a common platform to evaluate all cooperation protocols and study their properties in detail, and ii) it represents a scenario where all users will likely benefit from cooperation, with no statistical compromise made on the fairness and the overall performance of the network.

However, there are also the following *disadvantages* to considering a symmetric network, namely i) it fails to capture the effect of the topological differences on the relative performance of cooperative and non-cooperative multiple-access schemes, for e.g. a specific topology could favor a specific cooperation scheme or even a non-cooperative transmission over another cooperation scheme, and ii) the symmetric network assumption is not very realistic in practice, since it is very much restrictive and requires all the inter-terminal links to be statistically symmetric. However it is possible that practical scenarios could have ‘almost’ symmetric statistical characteristics.

Moreover, cooperation protocols proposed for a symmetric network can be modified for asymmetric users by taking into account the asymmetry of the network. For example, looking back at scenario A in Fig. 29, the users could control the degree of cooperation, in terms of time and energy spent, to grow inversely in the distance between the two users. This would reduce the amount of cooperation as the inter-user distance increases. In general, the time, energy and signal processing resources spent by users acting as relay nodes can be adaptively varied based on the knowledge of instantaneous topology.

The goal of this work is to solve the following specific problem: given a set of statistically symmetric users in a multiple-access system, what is the best cooperation scheme that can be employed to minimize the outage probability of the overall network? In a network with asymmetric users, it is an interesting optimization problem to choose the set of cooperating users optimally, but it is beyond the scope of this work to consider this problem. In the following section, we will review the traditional, non-cooperative multiple-access schemes.

7.2 Non-Cooperative Multiple-Access Schemes

Conventionally, non-cooperative multiple-access strategies can be of two kinds, non-orthogonal or orthogonal, depending upon whether or not users transmit simultaneously over overlapping time / frequency channels.

Orthogonal multiple-access schemes include time division multiple-access (TDMA) and frequency division multiple-access (FDMA), where users are allocated non-overlapping channels in order to avoid interference from one another. Information

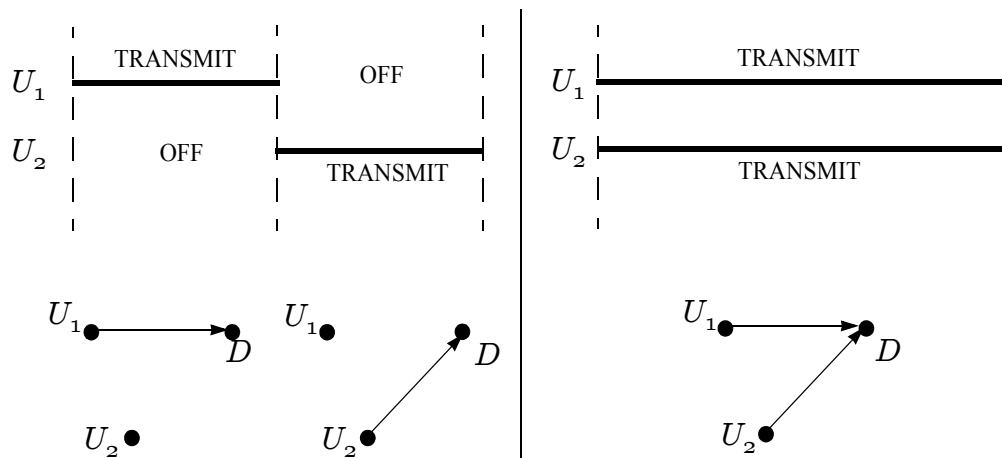


Fig. 31. i). TDMA with $N = 2$ users.

ii) SDMA with $N = 2$ users.

theoretically, TDMA and FDMA are identical given an average power constraint, except that they separate users in different domains [33]. We consider TDMA as an example of orthogonal multiple-access schemes. Orthogonal schemes, while maintaining simplicity of receiver processing, are often suboptimal in terms of achievable information rate. The optimal non-cooperative transmission scheme is space-division multiple access (SDMA) [4][27], which is a non-orthogonal scheme where all users transmit simultaneously over the same channel. Fig. 31 illustrates the TDMA and SDMA multiple-access strategies over a 2-user multiple-access channel.

A TDMA system can be summarized as follows. During each block, the received samples at D for $l \in \{1, 2, \dots, T/2\}$ are

$$\begin{aligned} y_1(l) &= h_1 x_1(l) + n_1(l), \\ y_2(l) &= h_2 x_2(l) + n_2(l), \end{aligned} \quad (107)$$

where, $y_i(l)$ is the l^{th} symbol received during the i^{th} block, $x_i(l)$ is the l^{th} symbol transmitted by U_i , $n_i(l)$ contains independent complex Gaussian noise of variance N_0 and $E[|x_i(l)|^2] = E_t$ is chosen to satisfy the average power constraint. Specifically, given that each user actively transmits for $T/2$ symbols periods, $E_t = 2E$ to maintain an average transmit energy of E and an average SNR of E/N_0 per user at the receiver. The capacity of each user is given by

$$C_i = \frac{1}{2} \log_2(1 + 2S|h_i|^2). \quad (108)$$

The outage probability of the system is defined as the probability of any of the two users being in error and is given by

$$P_{\text{TDMA}} = \Pr(\min(C_1, C_2) < R) = \Pr\left(\min(|h_1|^2, |h_2|^2) < \left(\frac{2^{2R} - 1}{2S}\right)\right). \quad (109)$$

Similarly, an SDMA system can be summarized as follows. The received samples for $l \in \{1, 2, \dots, T\}$ are

$$y(l) = h_1 x_1(l) + h_2 x_2(l) + n(l), \quad (110)$$

where $n(l)$ is independent complex Gaussian noise of variance N_0 and $E[|x_i(l)|^2] = E$ so that average SNR is E/N_0 per user. By grouping together the transmitted and received symbols for $l \in \{1, 2, \dots, T\}$, we obtain $Y = [y(1) \ y(2) \dots \ y(T)]$, and the input blocks X_1 and X_2 as $X_k = [x_k(1) \ x_k(2) \dots \ x_k(T)]$ and the block of noise elements as $N = [n(1) \ n(2) \dots \ n(T/4)]$, so that the input-output relationship is given as

$$Y = h_1 X_1 + h_2 X_2 + N. \quad (111)$$

The outage probability is specified by the union of

$$\mathcal{O}_1: C_{1|2} = \max_{p(x)} \frac{1}{T} I(X_1; Y | X_2) = \log_2(1 + S|h_1|^2) < R,$$

$$\mathcal{O}_2: C_{2|1} = \max_{p(x)} \frac{1}{T} I(X_2; Y | X_1) = \log_2(1 + S|h_2|^2) < R$$

$$\mathcal{O}_{12}: C_{12} = \max_{p(x)} \frac{1}{2T} I(X_1, X_2; Y) = \frac{1}{2} \log_2(1 + S(|h_1|^2 + |h_2|^2)) < R, \quad (112)$$

where, it can be shown that $p(x)$, the joint probability density function of X_1 and X_2 , needs to be jointly Gaussian to maximize the mutual information. The outage probability of SDMA is thus:

$$P_{\text{SDMA}} = \Pr[\mathcal{O}_1 \cup \mathcal{O}_2 \cup \mathcal{O}_{12}] = \Pr[\min\{C_{1|2}, C_{2|1}, C_{12}\} < R]. \quad (113)$$

7.3 Relay Techniques in a Cooperative Wireless Network

The previous section outlined some of the conventional non-cooperative multiple-access schemes. Now, we move on to the idea of user cooperation in wireless networks. Before describing the cooperation strategies over a network, specifically over a multiple-access system which is of interest in this work, we describe the basic relay operations considered here. These relay operations act as the building blocks in constructing cooperation protocols amongst users in a network.

Relay nodes in a cooperative wireless system could potentially use one of several strategies to forward another user's information to the destination. We consider three popular relay strategies, namely amplify-and-forward (AF), amplify/decode-and-forward (ADF) and selection-decode and-forward (SDF).

7.3.1 Amplify-and-forward (AF)

In the amplify-and-forward (AF) technique proposed in [65], the relay nodes simply scale the received samples to meet the average transmit power constraint and before forwarding to the destination. The key advantages of the AF technique is that relay nodes do not have to decode the information, reducing the burden on these nodes which would typically be low power mobile devices. However, the disadvantage is that the information symbols, corrupted by inter-user channel distortion, are forwarded along with the receiver noise at the relay node. For example, if user U_2 receives

$$y = h_{12}x + n_1, \quad (114)$$

from U_1 , then during the relay phase, U_2 forwards αy to the destination, where α is the amplification factor, given by

$$\alpha = \sqrt{\frac{E_t}{E_t|h_{12}|^2 + 1}}, \quad (115)$$

where $E[|x(l)|^2] = E_t$, and the destination receives

$$z = h_2\alpha y_2 + n_2 = \alpha h_2 h_{12} x + \alpha h_2 n_1 + n_2. \quad (116)$$

7.3.2 Amplify/decode-and-forward (ADF)

Instead of AF, the nodes could also use the amplify/decode-and-forward (ADF) relay technique [69]. An ADF relay will use its knowledge of the channel coefficients to make a decision to either act as an AF relay or a decode-and-forward relay. Specifically, if the inter-user channel is not in outage, i.e., if the data rate $R < \log_2(1 + |h_{12}|^2 E_t)$, then each user can perfectly decode the other's information assuming that the transmitted information is encoded using a capacity approaching error control code, and hence forward a clean version to the destination. The ADF relay will decode the received information and forward the decoded symbols to the destination. On the other hand, in the case of an outage, it would be counter-productive to forward erroneously decoded information, so the ADF relay simply amplifies and forwards the packet. This hybrid relay strategy was shown to be better than both AF and DF [69].

7.3.3 *Selection-decode-and-forward (SDF)*

In this technique, the relay node determines whether it should relay any information or not at all using its knowledge of the relay channel coefficients [63]. If the relay is capable of decoding the transmitted symbols, specifically, if the inter-user channel is not in outage, i.e., if $R < \log_2(1 + |h_{12}|^2 E_t)$, then each user decodes the other's information and forwards a clean version to the destination, otherwise, the relay nodes transmit nothing.

7.4 **State of the Art in Cooperation Protocols**

In this section, we discuss the popular cooperation protocols for multiple-access channels available in literature. We consider one example each for orthogonal and non-orthogonal protocols. Among orthogonal protocols, we consider the Laneman-Tse-Wornell (LTW) protocol [63], which could be viewed as an extension of TDMA to cooperative communications. The best available system among non-orthogonal protocols is the non-orthogonal amplify and forward (NAF) protocol [67], which achieves a higher rate by relaxing the orthogonality constraint, hence achieving a superior outage performance, albeit at the cost of increased complexity of receiver processing as a direct consequence of the non-orthogonal structure.

7.4.1 *Laneman-Tse-Wornell (LTW) Protocol*

The LTW protocol works as shown in Fig. 32. The static fading frame is divided into four equal-sized blocks. During the first block, the first user (U_1) transmits its information, while the second user (U_2) and the destination (D) each listen to the transmission. During the second block, U_2 relays the information it receives from U_1 to

the destination D . During the third and fourth blocks, users U_1 and U_2 reverse roles. The relay operation could be of different kinds. Some of the popular relay operations are amplify-and-forward (AF) [63], selection-decode-and-forward (SDF) [63] and amplify/decode-and-forward (ADF) [69].

The basic idea of the LTW protocol is to ensure that the information from each user is transmitted through the other's antenna, creating two independent paths from the information source to the destination, although the relayed information is affected by distortions in the inter-user fading channel. If the relay operation is chosen judiciously, it was shown in [63] that this protocol yields a diversity order of 2.

Due to the half-duplex constraint, the rate of any cooperative multiple access protocol will decrease compared to the corresponding direct transmission scheme, since each user has to spend a fraction of its time listening to another user's transmission, and also acting as a relay.

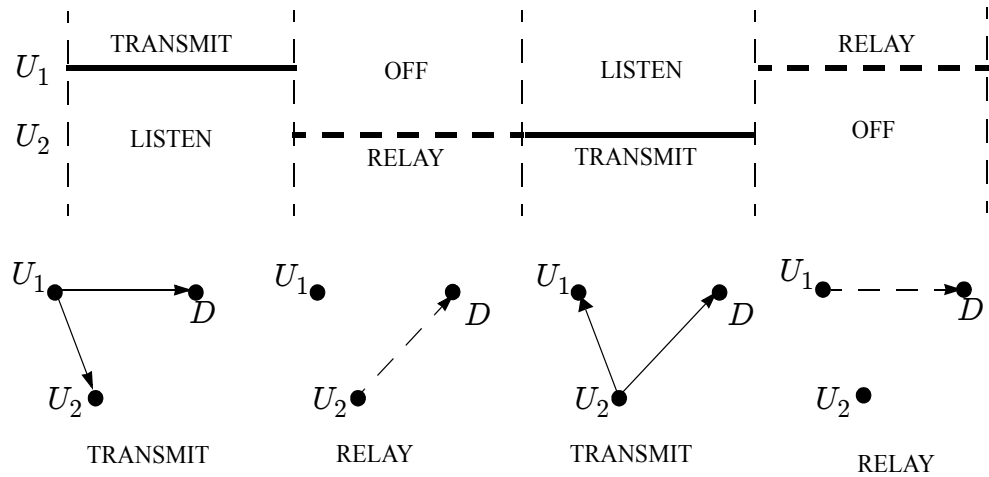


Fig. 32. Illustration of the Laneman-Tse-Wornell (LTW) cooperation protocol.

By imposing the orthogonality constraint, the LTW protocol loses even more information rate, with each user spending only 1/4 of the time transmitting its own information. The advantage of ensuring orthogonality is that the decoding complexity of the system is low. However, the outage probability of the system suffers from the rate penalty incurred. Further, in the extension of the LTW protocol for N users, each user has a rate of $1/N^2$ [64], indicating that the LTW protocol sacrifices a significant amount of rate as the number of users grows.

The LTW with AF relays can be summarized as follows. During the first block, the received samples at D and U_2 are given by

$$\begin{aligned} y_1(l) &= h_1 x_1(l) + n_1(l), \\ y_{12}(l) &= h_{12} x_1(l) + n_5(l), \end{aligned} \quad (117)$$

where $l \in \{1, 2, \dots, T/4\}$ and $x_1(l)$ is the i^{th} transmitted symbol from U_1 , with $E[|x_1(l)|^2] = E_t$ chosen to satisfy the average power constraint. Specifically, given that each user actively transmits for $T/2$ symbols periods, $E_t = 2E$ to maintain an average transmit energy of E and an average SNR of E/N_0 per user.

During the second block, the samples received by D from U_2 are given by

$$y_2(l) = \alpha h_2 y_{12}(l) + n_2(l), \quad (118)$$

where $l \in \{1, 2, \dots, T/4\}$ and α is the amplification factor, given by

$$\alpha = \sqrt{\frac{E_t}{E_t |h_{12}|^2 + 1}}. \quad (119)$$

During the third block and fourth blocks, U_1 and U_2 reverse roles. In the third block, the received samples at D and U_1 are given by

$$\begin{aligned} y_3(l) &= h_2 x_2(l) + n_3(l), \\ y_{21}(l) &= h_{12} x_2(l) + n_6(l), \end{aligned} \quad (120)$$

where, again $l \in \{1, 2, \dots, T/4\}$ and $x_2(l)$ is the l^{th} transmitted symbol from U_2 . During the fourth block, the samples received by D from U_1 are given by

$$y_4(l) = \alpha h_1 y_{21}(l) + n_4(l), \quad (121)$$

with $l \in \{1, 2, \dots, T/4\}$. By constructing the received blocks Y_1, Y_2, Y_3 and Y_4 as $Y_k = [y_k(1) \ y_k(2) \dots \ y_k(T/4)]$, the input blocks X_1 and X_2 as $X_k = [x_k(1) \ x_k(2) \dots \ x_k(T/4)]$ and the blocks of noise elements as $N_k = [n_k(1) \ n_k(2) \dots \ n_k(T/4)]$, we obtain the equivalent discrete, memoryless multiple-access channel for U_1 created by the LTW protocol as:

$$\begin{aligned} Y_1 &= h_1 X_1 + N_1, \\ Y_2 &= \alpha h_2 h_{12} X_1 + \alpha h_2 N_5 + N_2. \end{aligned} \quad (122)$$

Similarly, the equivalent channel for U_2 is

$$\begin{aligned} Y_3 &= h_2 X_2 + N_3, \\ Y_4 &= \alpha h_1 h_{12} X_2 + \alpha h_1 N_6 + N_4. \end{aligned} \quad (123)$$

In order to obtain an expression for the outage probability of each user in the LTW protocol, we need to compute the capacity of the equivalent channel created between each user and the destination. The discrete, memoryless multiple-access channel created by the LTW protocol for U_1 and U_2 with D are given by

$$\begin{bmatrix} Y_1 \\ Y_2 \end{bmatrix} = \begin{bmatrix} h_1 \\ \alpha h_2 h_{12} \end{bmatrix} X_1 + \begin{bmatrix} 1 & 0 & 0 \\ 0 & 1 & \alpha h_2 \end{bmatrix} \begin{bmatrix} N_1 \\ N_2 \\ N_5 \end{bmatrix}, \quad (124)$$

$$\begin{bmatrix} Y_3 \\ Y_4 \end{bmatrix} = \begin{bmatrix} h_2 \\ \alpha h_1 h_{12} \end{bmatrix} X_2 + \begin{bmatrix} 1 & 0 & 0 \\ 0 & 1 & \alpha h_1 \end{bmatrix} \begin{bmatrix} N_3 \\ N_4 \\ N_6 \end{bmatrix}, \quad (125)$$

respectively. Hence, the outage event for the two users in this multiple access system is:

$$\mathcal{O}_1: C_1 = \max_{p_1(x)} \frac{1}{T} I(X_1; Y_1, Y_2) < R,$$

$$\mathcal{O}_2: C_2 = \max_{p_2(x)} \frac{1}{T} I(X_2; Y_3, Y_4) < R, \quad (126)$$

where $p_i(x)$ is the probability density function of X_i . The outage probability of the multiple-access system, which we define as the probability of any of the users being in outage, is given by

$$P_o = \Pr[\mathcal{O}_1 \cup \mathcal{O}_2] = \Pr[\min\{C_1, C_2\} < R]. \quad (127)$$

For a given channel matrix, this formulation is identical to the Gaussian multiple-access channel [27]. For this case the mutual informations are maximized when the input alphabet at each source follows an independent Gaussian distribution. Upon maximization, we get

$$C_1 = \frac{1}{4} \log_2 \left(1 + 2S|h_1|^2 + \frac{2S|\alpha|^2|h_2|^2|h_{12}|^2}{(1 + |\alpha|^2|h_2|^2)} \right). \quad (128)$$

Substituting for α , we get

$$C_1 = \frac{1}{4} \log_2 \left(1 + 2S|h_1|^2 + \frac{4S^2|h_2|^2|h_{12}|^2}{1 + 2S(|h_{12}|^2 + |h_2|^2)} \right). \quad (129)$$

Similarly for U_2

$$C_2 = \frac{1}{4} \log_2 \left(1 + 2S|h_2|^2 + \frac{4S^2|h_1|^2|h_{12}|^2}{1 + 2S(|h_{12}|^2 + |h_1|^2)} \right). \quad (130)$$

In [63], the authors prove that the diversity order of this protocol is 2, which is the maximum diversity achievable over a 2-user cooperative multiple access channel with a single antenna at each terminal.

7.4.2 NAF protocol

In this section, we review the cooperative multiple-access - non-orthogonal amplify and forward (NAF) protocol proposed in [67]. As the name suggests, the NAF protocol is a non-orthogonal protocol which enables users transmit at a high rate by creating an artificial ISI channel through cooperation.

A cooperation frame in the NAF protocol consists of two consecutive symbol periods. Each user transmits once during a cooperation frame. Each user transmits a linear combination of its current symbol and the noisy signal received from its partner during the previous time slot. The NAF protocol can be summarized as follows. The transmitted signals at the start of the communication are:

$$\begin{aligned}
t_{1,0} &= ax_{1,0} \\
t_{2,0} &= ax_{2,0} + b(h_{12}t_{1,0} + n_{2,0}) \\
t_{1,1} &= ax_{1,1} + b(h_{12}t_{2,0} + n_{1,0}) \\
t_{2,1} &= ax_{2,1} + b(h_{12}t_{1,1} + n_{2,1}).
\end{aligned} \tag{131}$$

where $t_{i,j}$ is the symbol transmitted by the i^{th} user during the j^{th} cooperation frame, whereas $x_{i,j}$ is the information symbol of the i^{th} user during the j^{th} cooperation frame, and $n_{i,j}$ is the corresponding additive white Gaussian noise at the receive antenna. The coefficients a and b , called broadcast and repetition gains respectively, determine the fraction of transmitted power allocated to the relayed symbols. The corresponding received signals at the destination are

$$\begin{aligned}
y_{1,0} &= h_1 t_{1,0} + v_{1,0} \\
y_{2,0} &= h_2 t_{2,0} + v_{2,0} \\
y_{1,1} &= h_1 t_{1,1} + v_{1,1} \\
y_{2,1} &= h_2 t_{1,0} + v_{2,1}.
\end{aligned} \tag{132}$$

where $y_{i,j}$ is the received symbol corresponding to the transmission from the i^{th} user during the j^{th} cooperation frame. The NAF protocol continues transmission by linearly combining its current symbols with the received symbol during the previous instant. Thus, the NAF protocol can be viewed as an encoder with a memory that creates an artificial ISI channel. The optimum values of the cooperation and broadcast gains are determined numerically. We refer the reader to [66] for a detailed derivation of the outage probability of this scheme, where the authors show that NAF achieves the full diversity of 2.

The NAF protocol has each user transmitting new information symbols once every two slots (cooperation frame), and hence the rate of each user in this protocol is $1/2$. However, the NAF protocol suffers an SNR penalty since each user is forced to share its available transmit energy between its current symbol and past symbols of itself and the other user.

7.5 Numerical Results

In this section, we compare the outage probabilities of TDMA, SDMA, the LTW protocol with AF relays, and the NAF protocol over a 2-user cooperative multiple-access channel with a target data rate of $R = 1$ b/s/Hz for each user.

In Fig. 33, we present the numerical results on the outage probabilities of the multiple-access strategies discussed in this chapter as a function of the average SNR per user. We see that the outage probability curves for TDMA, SDMA exhibit a lower diversity gain

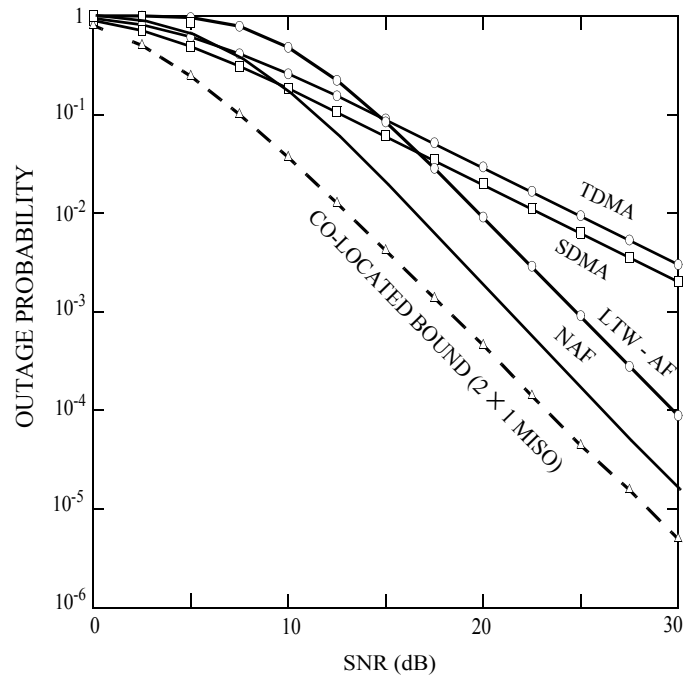


Fig. 33. Outage probabilities of various multiple access schemes for a 2-user system, with $R = 1$ bps/Hz.

compared to the cooperative transmission schemes, LTW and NAF. Also seen in Fig. 33 is the outage probability of a 2×1 MISO system, which serves as a lower bound for any CMA system.

One of the results which stand out in Fig. 33 is that TDMA and SDMA outperform LTW up to an SNR of 17 dB, in spite of the fact that LTW has a superior diversity order. This is due to the fact that LTW has a much lower symbol rate of $1/4$ compared to SDMA which has a rate 1, and at low SNR the key determinant of system performance is the symbol rate and not diversity. The converse is true at high SNR.

We also observe that the NAF protocol outperforms the LTW protocol by 3.3 dB owing to its higher rate, even though they achieve the same diversity order. The NAF protocol gets to within 3.3 dB of the MISO bound. In practice, the MISO bound itself may not be achievable since this would require the inter-user channel to be noiseless and have zero delay. A practical scheme will suffer a penalty due to the non-ideal nature of the inter-user channel, however, quantifying this penalty remains an open research problem.

7.6 Summary

In this chapter, we reviewed conventional non-cooperative multiple-access schemes TDMA and SDMA, and cooperative transmission schemes namely the LTW and NAF protocols. We reviewed the possible relay techniques that could be used over a multiple access channel – namely AF, ADF and SDF relays. We discussed the outage performance of TDMA and SDMA along with that of LTW protocol and NAF protocols with AF relays. We observe that cooperative multiple-access schemes outperform non-cooperative schemes at high SNR due to the diversity advantage. However, we also observe that

cooperation protocols typically sacrifice symbol rate in order to gain diversity, and consequently are outperformed by non-cooperative schemes in the low SNR regime. Hence, we conclude that it is crucial to design high rate cooperation protocols in order to achieve the goal of minimizing outage probability. In the next few chapters, we propose our solutions that minimize outage probability by maximizing diversity, while simultaneously achieving high rates.

CHAPTER 8

SPACE-DIVISION RELAY: A HIGH RATE NON-ORTHOGONAL COOPERATION PROTOCOL

In this chapter, we introduce an improved non-orthogonal cooperation protocol called the *space-division relay (SDR)* protocol for a simple two user cooperative multiple-access channel. Space-division relay is a non-orthogonal cooperation protocol which modifies the LTW protocol [63] by using space-division multiplexing instead of time-division multiplexing for the relays. The SDR protocol is studied in combination with three relay schemes namely AF, ADF and SDF. We show that this combination of full diversity, high rate and appropriate relaying schemes achieves the best outage performance among all previously reported orthogonal and non-orthogonal cooperation protocols.

This chapter is organized as follows. In Section 8.1, we outline the space-division relay protocol, following which in Section 8.2, we analyze the outage probability of the SDR protocol with AF relays. Subsequently, we support our analysis with numerical simulations results in Section 8.3, comparing the outage probability of other orthogonal and non-orthogonal candidate multiple-access schemes. Finally, we summarize the results in Section 8.4.

8.1 The Space-Division Relay Protocol

An illustration of the proposed SDR protocol is shown in Fig. 34. The static fading frame is divided into three equal-sized blocks. During the first block, the first user (U_1) transmits its information, while the second user (U_2) and the destination (D) each listen to

the transmission. During the second block, U_2 transmits its own independent information, while U_1 and D listen to the transmission. This completes the direct transmission part of the cooperation protocol for one frame. During the third block, both users relay the received packets from the other user *simultaneously*, in a space-division multiple access fashion, with the destination receiving a linear combination of these two transmissions. Initially, we analyze the space-division relay protocol with amplify-and-forward (AF) relays [63]. Later on, we consider two other relaying techniques, namely amplify/decode-and-forward (ADF) and selection-decode-and-forward (SDF) [63].

The basic idea of the SDR protocol is to increase the rate compared to the LTW protocol by relaxing the orthogonality constraint, while still achieving full cooperative diversity. By using spatial multiplexing during the relay phase, SDR clearly sacrifices orthogonality, in exchange for an increase in rate. Specifically, the rate of each user in the SDR protocol is $1/3$. The cooperation scheme can be summarized as follows. During the first block, the received samples at D and U_2 are given by

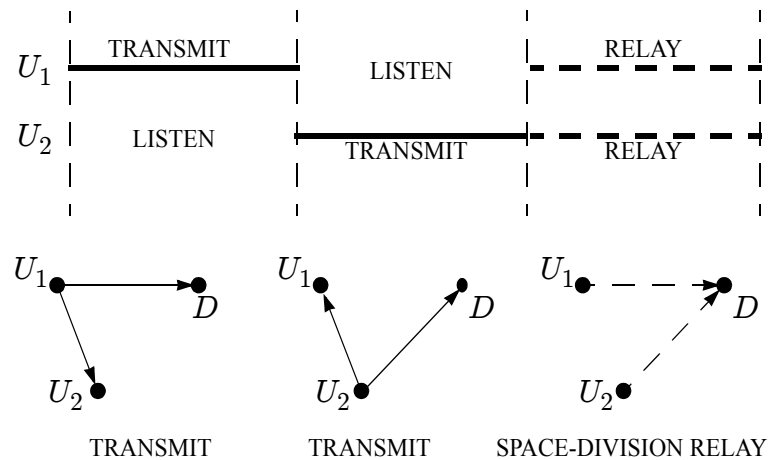


Fig. 34. Illustration of the space-division relay cooperation protocol.

$$\begin{aligned}
y_1(l) &= h_1 x_1(l) + n_1(l), \\
y_{12}(l) &= h_{12} x_1(l) + n_4(l),
\end{aligned} \tag{133}$$

where $l \in \{1, 2, \dots, T/3\}$ and $x_1(l)$ is the l -th transmitted symbol from U_1 , with $E[|x_1(l)|^2]$ is chosen to satisfy the average power constraint. During the second block, the samples received by D and U_1 are given by

$$\begin{aligned}
y_2(l) &= h_2 x_2(l) + n_2(l), \\
y_{21}(l) &= h_{12} x_2(l) + n_5(l),
\end{aligned} \tag{134}$$

where $l \in \{1, 2, \dots, T/3\}$. During the third block, also known as the relay phase, both users simultaneously relay each other's information using space-division multiplexing.

In SDR with AF, both users amplify the received symbols from the other user and relay the amplified symbols simultaneously during the relay phase, so that the destination receives

$$y_3(l) = h_1 \alpha y_2(l) + h_2 \alpha y_{12}(l) + n_3(l), \tag{135}$$

where α is the amplification factor, given by

$$\alpha = \sqrt{\frac{E_t}{\sqrt{E_t |h_{12}|^2 + 1}}}. \tag{136}$$

Since each node is silent $1/3$ of the time, the average power constraint is satisfied by choosing $E[|x_1(l)|^2] = E_t = 3E/2$.

8.2 Outage Analysis

In this section, we derive the outage probability of the SDR cooperation protocol with AF relays. In the SDR protocol, the observations at the destination consist of three received blocks Y_1 , Y_2 and Y_3 , where $Y_k = [y_k(1) y_k(2) \dots y_k(T/3)]$, corresponding to the two blocks X_1 and X_2 transmitted by the two users, where $X_k = [x_k(1) x_k(2) \dots x_k(T/3)]$. The discrete, memoryless multiple-access channel created by the SDR protocol is then

$$\mathbf{Y} = \begin{bmatrix} Y_1 \\ Y_2 \\ Y_3 \end{bmatrix} = \mathbf{H} \begin{bmatrix} X_1 \\ X_2 \end{bmatrix} + \mathbf{A}\mathbf{N}, \quad (137)$$

where the $(i, j)^{\text{th}}$ element of the noise matrix \mathbf{N} is $n_i(j)$, and where the matrices \mathbf{H} and \mathbf{A} are given by

$$\mathbf{H} = \begin{bmatrix} h_1 & 0 \\ 0 & h_2 \\ \alpha h_2 h_{12} & \alpha h_1 h_{12} \end{bmatrix}, \quad \mathbf{A} = \begin{bmatrix} 1 & 0 & 0 & 0 & 0 \\ 0 & 1 & 0 & 0 & 0 \\ 0 & 0 & 1 & \alpha h_1 & \alpha h_2 \end{bmatrix}. \quad (138)$$

Let \mathbf{H}_1 and \mathbf{H}_2 denote the first and second columns of \mathbf{H} . The outage event for this multiple access system is the union of the following three events [27]:

$$\begin{aligned} \mathcal{O}_1: C_{1|2} &= \max_{p(x)} \frac{1}{T} I(X_1; Y | X_2) < R \\ \mathcal{O}_2: C_{2|1} &= \max_{p(x)} \frac{1}{T} I(X_2; Y | X_1) < R \\ \mathcal{O}_{12}: C_{12} &= \max_{p(x)} \frac{1}{2T} I(X_1, X_2; Y) < R, \end{aligned} \quad (139)$$

where $p(x)$ is the joint probability density function of X_1 and X_2 . The outage probability is thus

$$P_o = \Pr[\mathcal{O}_1 \cup \mathcal{O}_2 \cup \mathcal{O}_{12}] = \Pr[\min\{C_{1|2}, C_{2|1}, C_{12}\} < R]. \quad (140)$$

For a given channel matrix, this formulation is identical to the Gaussian multiple-access channel [27]. For this case the mutual informations are maximized when the input alphabet at each source follows an independent Gaussian distribution. Upon maximization, we get

$$\begin{aligned} C_{1|2} &= \frac{1}{3} \log_2 \det(I + \frac{3}{2} S \mathbf{H}_1^* (\mathbf{A} \mathbf{A}^*)^{-1} \mathbf{H}_1) \\ C_{2|1} &= \frac{1}{3} \log_2 \det(I + \frac{3}{2} S \mathbf{H}_2^* (\mathbf{A} \mathbf{A}^*)^{-1} \mathbf{H}_2) \\ C_{12} &= \frac{1}{6} \log_2 \det(I + \frac{3}{2} S \mathbf{H}^* (\mathbf{A} \mathbf{A}^*)^{-1} \mathbf{H}). \end{aligned} \quad (141)$$

Intuitively, the factor $1/3$ represents the fact that the sources transmit new information only $1/3$ of the total time. Substituting for \mathbf{A} and \mathbf{H}_1 , the expression for $C_{1|2}$ further simplifies to:

$$C_{1|2} = \frac{1}{3} \log_2 \left(1 + \frac{3}{2} S |h_1|^2 + \frac{3S |\alpha|^2 |h_2|^2 |h_{12}|^2}{2(1 + |\alpha|^2 (|h_1|^2 + |h_2|^2))} \right). \quad (142)$$

Substituting for α and simplifying, we get

$$C_{1|2} = \frac{1}{3} \log_2 \left(1 + \frac{3S}{2} \left(|h_1|^2 + \frac{3S |h_2|^2 |h_{12}|^2}{(2 + 3S (|h_2|^2 + |h_1|^2 + |h_{12}|^2))} \right) \right). \quad (143)$$

The expression for $C_{2|1}$ can be obtained by exchanging h_1 and h_2 in the above expression.

We now briefly discuss the rate and diversity aspects of the SDR scheme.

Definition 6. The *rate* μ of a cooperative multiple-access protocol is the average number of information symbols transmitted by each user per signalling interval.

Contrast this with the data rate of a node, which is the number of bps/Hz. For a two-user CMA system, TDMA has rate 1/2, while SDMA has rate 1. The LTW protocol has rate 1/4, whereas the SDR protocol achieves a rate of 1/3.

Definition 7. The *diversity order* d of a cooperative system is defined as

$$d = \lim_{S \rightarrow \infty} \frac{-\log P_o(S, R)}{\log S}, \quad (144)$$

where $P_o(S, R)$ is the outage probability of the cooperation scheme. For a two-user CMA system with one antenna at each node, TDMA and SDMA achieve a diversity order of just one, whereas the LTW protocol achieves the *full* diversity ($d = 2$).

We now show that the SDR protocol with AF achieves full diversity. The diversity order of the SDR protocol can be computed as follows. Let $P_1 = \Pr[\mathcal{O}_1]$, $P_2 = \Pr[\mathcal{O}_2]$, and $P_{12} = \Pr[\mathcal{O}_{12}]$, and let the corresponding diversity orders be d_1 , d_2 and d_{12} respectively. Note that the assumption that h_1 and h_2 are statistically identical implies that $d_1 = d_2$. The outage probability can be bounded using the union bound as

$$P_\delta \leq P_o \leq P_1 + P_2 + P_{12}, \quad (145)$$

where P_δ is either of P_1 , P_2 or P_{12} . We state the following theorem on the diversity order of SDR.

Theorem 8. The SDR protocol for a two-user cooperative multiple-access channel with one antenna at each node achieves the full diversity order of $d = 2$.

Proof: Using the bound in (145), it is easy to show that $d_{\text{SDR}} = \min\{d_1, d_2, d_{12}\}$. Using the inequality $I(X_1, X_2; Y) \geq I(X_1; Y|X_2)$, we see that $2C_{1|2} \geq C_{1|2}$, implying that $d_{12} \geq d_1$. The probability P_1 can be written as

$$P_1 =$$

$$\Pr(C_{1|2} < R | |h_1|^2 < \delta) \Pr(|h_1|^2 < \delta) + \Pr(C_{1|2} < R | |h_1|^2 \geq \delta) \Pr(|h_1|^2 \geq \delta), \quad (146)$$

where, $\delta = \frac{2(2^{3R} - 1)}{3S}$. If $|h_1|^2 \geq \delta$, then $C_{1|2} \geq R$ and hence the second term in (146) is zero. Therefore

$$P_1 = \Pr(C_{1|2} < R | |h_1|^2 < \delta) \Pr(|h_1|^2 < \delta). \quad (147)$$

Using the fact that $|h_1|^2 < \delta$ in (143), we get

$$P_1 < \Pr\left(\frac{|h_2|^2 |h_{12}|^2}{|h_2|^2 + |h_{12}|^2 + \delta + \frac{2}{3S}} < \delta\right) \Pr(|h_1|^2 < \delta). \quad (148)$$

Substituting $\varepsilon = \delta + \frac{2}{3S}$,

$$P_1 < \Pr\left(\frac{\frac{|h_2|^2}{\varepsilon} \frac{|h_{12}|^2}{\varepsilon}}{\frac{|h_2|^2}{\varepsilon} + \frac{|h_{12}|^2}{\varepsilon} + 1} < \delta\right) \Pr(|h_1|^2 < \delta). \quad (149)$$

With $|h_{12}|^2$ and $|h_2|^2$ being exponential random variables, we obtain the following relationship from [63] for and $\varepsilon \rightarrow 0$ or equivalently for $S \rightarrow \infty$

$$\lim_{\varepsilon \rightarrow 0} \frac{1}{\delta} \Pr \left(\frac{\frac{\varepsilon |h_2|^2 |h_{12}|^2}{\varepsilon}}{\frac{|h_2|^2}{\varepsilon} + \frac{|h_{12}|^2}{\varepsilon} + 1} < \delta \right) = k, \quad (150)$$

for some constant k . Since $|h_1|^2$ is exponentially distributed, $\Pr(|h_1|^2 < \delta) \approx \delta$ for $\delta \rightarrow 0$. Therefore,

$$\lim_{S \rightarrow \infty} \Pr \left(\frac{\frac{\varepsilon |h_2|^2 |h_{12}|^2}{\varepsilon}}{\frac{|h_2|^2}{\varepsilon} + \frac{|h_{12}|^2}{\varepsilon} + 1} < \delta \right) \Pr(|h_1|^2 < \delta) = (k\delta)\delta, \quad (151)$$

$$\lim_{S \rightarrow \infty} P_1 < k \frac{(2^{3R} - 1)^2}{S^2}, \quad (152)$$

and hence $d_1 \geq 2$. As discussed earlier, $d_2 = d_1$ and $d_{12} \geq d_1$. The outage probability of a 2×1 MISO channel is a lower bound on P_o and has a diversity order of 2, implying that $d_1 \leq 2$. Therefore $d_1 = 2$ and we have shown that P_o decays as S^{-2} as $S \rightarrow \infty$.

It can be shown that the outage probability of SDR with ADF is strictly less than SDR with AF. Consequently, SDR with ADF also achieves full diversity.

8.3 Numerical Results

In this section, we present numerical results for a Rayleigh-fading cooperative multiple-access system with two users and a single destination, each equipped with one antenna. Each user has a target data rate of $R = 1$ b/s/Hz, and each has the same average

SNR. To achieve this target data rate, the LTW protocol needs a user to transmit information at 4 b/s/Hz during its active transmissions, while SDR and NAF require the user to transmit at 3 b/s/Hz and 2 b/s/Hz respectively when active.

In Fig. 35, we compare several candidate schemes by plotting the outage probability versus SNR. Traditional multiple access schemes such as TDMA and SDMA suffer from a lack of diversity at high SNR, while at low SNR, they perform better than the corresponding cooperation scheme. At an outage probability of 10^{-3} , SDR with AF outperforms LTW with AF by 1.9 dB. A similar trend is observed with ADF relay as well. Also shown in the figure (labeled co-located bound) is the outage probability of a 2×1 MISO channel, which serves as a lower bound on the outage probability of any CMA scheme, although it may not be achievable. We see from Fig. 35 that SDR with AF falls 4.7 dB short of the MISO bound.

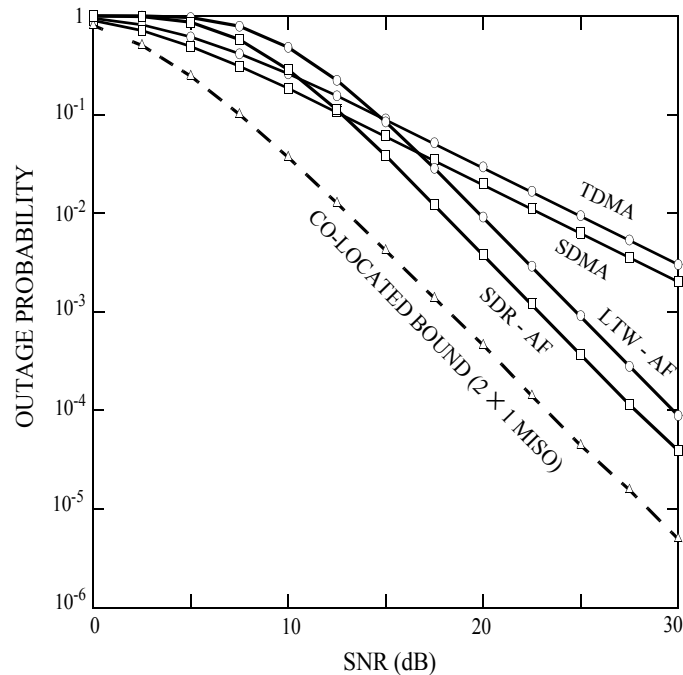


Fig. 35. Comparison of outage probabilities of various multiple access schemes for a 2-user system, with $R = 1$ bps/Hz.

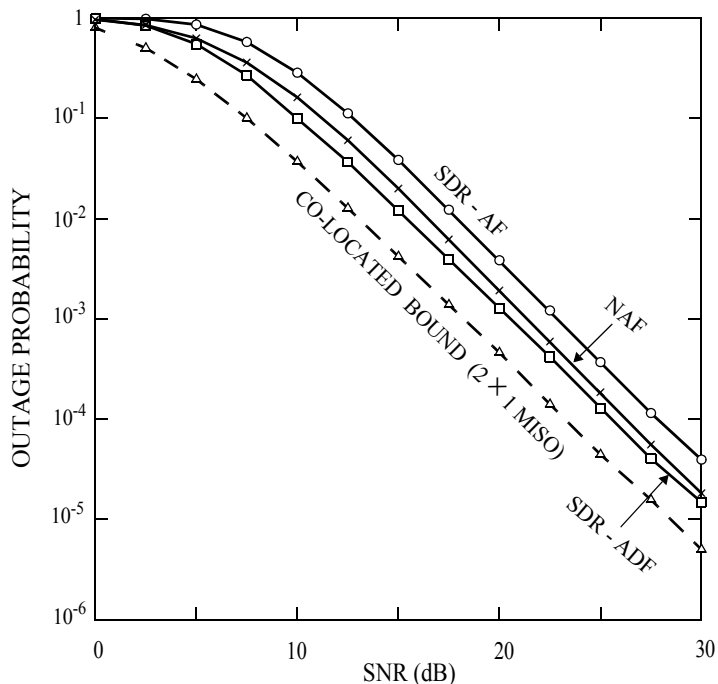


Fig. 36. Comparison of outage probabilities of non-orthogonal cooperation schemes for a 2-user system, with $R = 1$ bps/Hz.

In Fig. 36, we compare the performance of some non-orthogonal cooperation protocols, namely SDR with AF, SDR with ADF and the NAF protocol. We see that SDR with AF is 1.4 dB worse than NAF. However, SDR with ADF outperforms NAF by 1 dB. SDR with ADF achieves the best outage performance among all previously reported cooperation protocols, falling only 2.3 dB short of the MISO bound. For $R = 2$ b/s/Hz, SDR with ADF outperforms NAF by 1.2 dB and LTW with ADF by 4.5 dB at an outage probability of 10^{-3} .

Both SDR and NAF achieve full diversity and the rate of NAF ($1/2$) is higher than that of SDR ($1/3$). However, the NAF protocol suffers an SNR penalty since each user is forced to share its available transmit energy between current and past symbols of itself and the other user. Moreover, the NAF protocol has not been considered with ADF strategy in

literature so far, since the sequential nature of NAF mandates the use of AF. Error-free decoding requires a sufficiently long block length, whereas in NAF, symbols are relayed at every instant. Due to these reasons SDR-ADF outperforms NAF.

The relative performance of multiple access schemes depends on the target data rate and SNR. We study this problem by comparing the SNR required by different multiple-access schemes to achieve an outage probability of 10^{-3} as a function of the target data rate. In Fig. 37, we present numerical results for this comparison for data rates ranging from $R = 0.5$ to 6 b/s/Hz in steps of 0.5 . From Fig. 37, we see that the SNR improvement of SDR over LTW increases as the target data rate increases, since SDR has a higher rate compared to LTW. Based on the same reasoning, one would expect NAF to outperform SDR at higher data rates, which it does for $R > 3.5$ b/s/Hz. However, for $R > 3.5$ b/s/

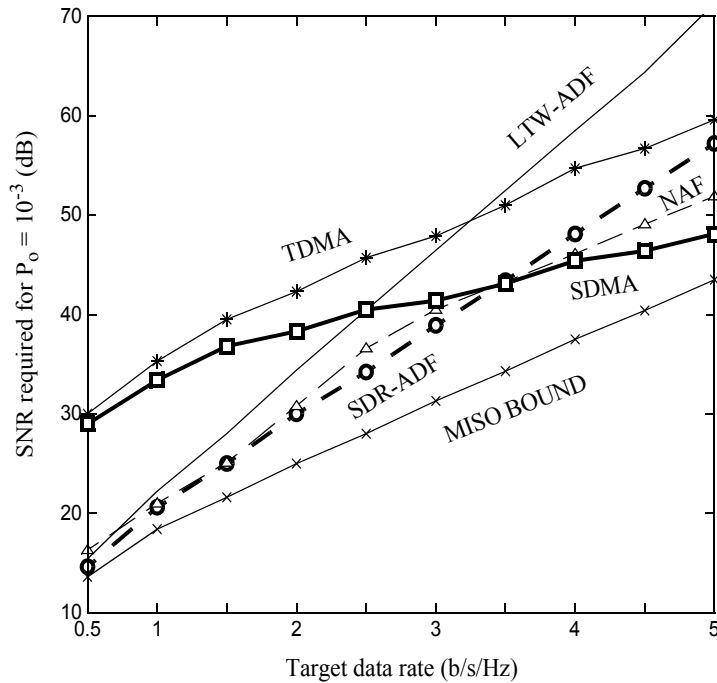


Fig. 37. Comparison of the SNR required for multiple-access schemes to achieve an outage probability of 10^{-3} as a function of the target data rate.

Hz, it turns out that SDMA requires the lowest SNR to achieve the target outage probability amongst all multiple access schemes. Overall, the best outage performance could be achieved by switching between SDR and SDMA as the data rate and SNR vary.

8.4 Summary

We proposed a new cooperative multiple-access strategy called *space-division relay* (SDR). Space-division relay is a simple non-orthogonal cooperation protocol that achieves the full cooperative diversity. SDR employs the space-division multiplexing concept for its relay phase to achieve a higher transmission rate. We investigated SDR with both amplify-and-forward and amplify/decode-and-forward relays. We show that the high rate of SDR-AF enables it to outperform the LTW-AF protocol by 1.9 dB at an outage probability of 10^{-3} at a target data rate of 1 bps/Hz. We also show that SDR-ADF outperforms NAF by 1 dB. We also observed that SDR-ADF achieves the best outage performance among all previously reported protocols, falling only 2.3 dB short of the ideal cooperation bound.

CHAPTER 9

HOW MUCH COOPERATION IS NECESSARY IN COOPERATIVE MULTIPLE ACCESS CHANNELS?

In chapter and chapter , we studied the diversity benefits of cooperation in multiple-access systems. Although we see that well designed cooperation protocols effectively tap the diversity gain offered by the channel, the common theme among these protocols is the nonzero rate penalty incurred in this process [63][66][81][82][89]. The fundamental problem of computing capacity of a cooperative multiple-access channel still remains an open research problem, though some results are known for cooperative relay channels [73][83]-[87]. Currently, the approach to this problem has been to propose new and better cooperation schemes, so that the outage probability of the best scheme serves as a lower bound on the achievable outage probability over the cooperative multiple-access channel, with the MISO bound serving as the upper bound [65][66][71][72][76][89].

It is well documented that diversity order is primarily a high SNR phenomenon and does not necessarily guarantee superior error performance at all SNRs [15][40]. A closer look at Fig. 35 tells us that conventional non-cooperative multiple-access techniques such as TDMA and SDMA actually outperform the cooperation protocols at low SNR due to their high rate. Of course, the opposite is true at high SNR, when diversity order is the key determinant of system performance, as opposed to the symbol rate.

This observation suggests that one could conceivably design flexible, adaptive cooperation schemes which give priority to rate or diversity depending on the operating conditions [88]. In order to design such schemes, we start with a basic question: how

much cooperation is necessary in cooperative multiple access channels? A more specific question would be: In the process of enhancing diversity, how much rate loss should be tolerated to achieve the goal of minimizing outage probability? We propose the framework of partial cooperation to answer these questions. We propose the partial cooperation framework for the two user cooperative multiple-access channel and analyze the level of cooperation necessary as the operating SNR and target data rate vary. We propose this framework as a tool to measure the degree of importance of cooperation, which could possibly be a generic extension for any given cooperation protocol, orthogonal or non-orthogonal.

In this chapter, we organize our discussion of partial cooperation as follows. In Section 9.1, we present the generic framework of partial cooperation, which could be applied to any cooperation protocol to optimize it further. In Section 9.2, we consider the specific example of the LTW protocol to show the benefits of partial cooperation with orthogonal protocols along with analysis and numerical results. In Section 9.3, we provide a similar illustration for partial cooperation with the SDR protocol. We summarize the observation in Section 9.4.

9.1 Partial Cooperation Framework

As in our previous discussions, we consider a Rayleigh-fading multiple-access channel with two users communicating with a common destination over a quasistatic fading channel. We assume that the users are frame-synchronized and that the destination knows all of channel coefficients $\{h_1, h_2, h_{12}\}$, whereas the users know only h_{12} . The partial cooperation framework works as follows.

The static fading frame is divided into two windows, the *direct transmission window* and the *cooperation window*. During the direct transmission window of length βT symbols, where $0 \leq \beta < 1$, users employ full rate non-cooperative schemes such as TDMA or SDMA for orthogonal and non-orthogonal systems respectively, and during the cooperation window of length $(1 - \beta)T$ symbol periods, the users employ a cooperation scheme of choice. Based on the target data rate, average SNR and the instantaneous channel information, (if available), the relative proportion of the window lengths is varied by tuning the parameter β . As the parameter β increases from 0 towards 1, the degree of cooperation increases.

9.2 Example of an Orthogonal Protocol with Partial Cooperation

In this section, we propose the partial cooperation framework for orthogonal cooperation protocols, using the example of the LTW protocol with amplify-and forward relays to illustrate this. In Section 7.2, we observed that TDMA suffers from poor diversity gain and hence high outage probabilities at high SNR. In Section 7.4, we observed that the LTW protocol, an orthogonal cooperative multiple-access scheme, achieves higher diversity by cooperation, but sacrifices 1/2 the transmission rate in this process. In this section, we propose the partial cooperation framework which combines TDMA with LTW in order to achieve a flexible tradeoff between rate and diversity.

Let β be the fraction of the time over which TDMA is used, with each user transmitting information over half of the direct transmission window. During the cooperation window, each user transmits over a duration of $(1 - \beta)T/2$ symbol periods, out of which only $(1 -$

$\beta)T/4$ are used to transmit its own information symbols, with the remaining being used for forwarding the other user's information. Hence, each user has $\beta T/2 + (1 - \beta)T/4$ symbol periods to transmit its own information in one frame.

To start with, the information to be transmitted is encoded into $\beta T/2 + (1 - \beta)T/4$ symbols by each user. The first $\beta T/2$ symbols constitute $X_i^{(D)}$ and are sent using the direct transmission scheme, which is TDMA for the orthogonal case. The remaining symbols form $X_i^{(C)}$ and are sent using the LTW cooperation protocol, as shown in Fig. 38. At the destination, the symbols received during each block can be grouped together as in Section 7.4.1. For example, the direct transmission window which uses TDMA has two blocks, during which users U_1 and U_2 transmit respectively, whereas the cooperation frame consists of four blocks of equal length. Symbols corresponding to U_1 's transmission are received during the first, third and the fourth blocks, and can be grouped into blocks as

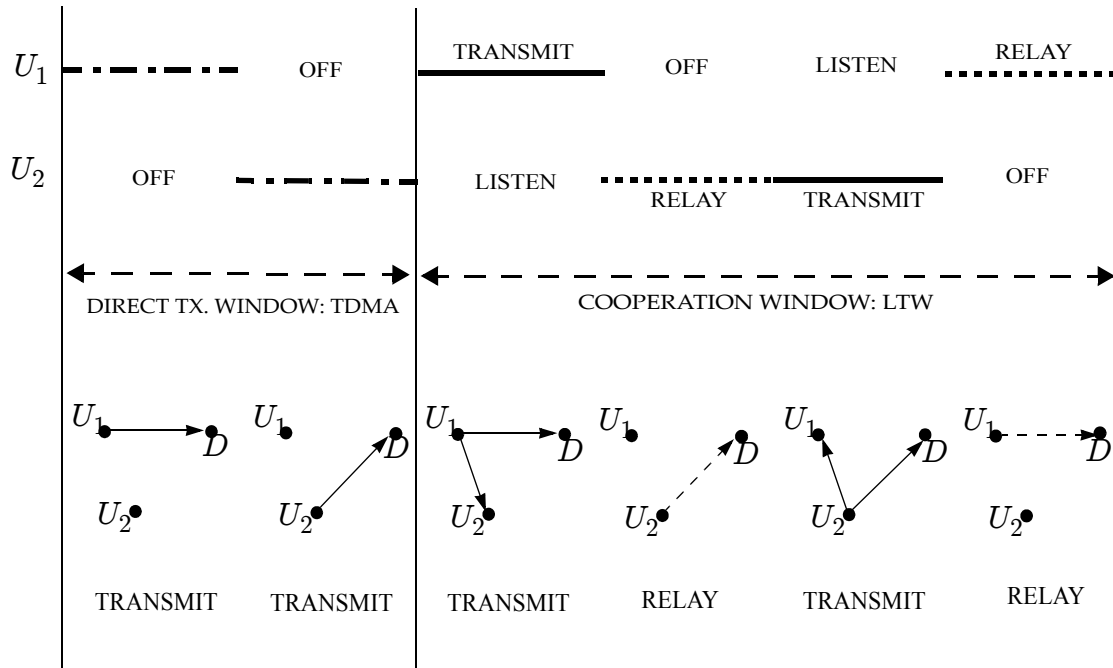


Fig. 38. Partial cooperation with the LTW protocol for $N = 2$.

$$\begin{aligned}
Y_1 &= h_1 X_1^{(D)} + N_1 \\
Y_3 &= h_1 X_1^{(C)} + N_2 \\
Y_4 &= \alpha h_2 h_{12} X_1^{(C)} + \alpha h_2 N_7 + N_4,
\end{aligned} \tag{153}$$

where, N_i 's consist of independent, circularly symmetric complex Gaussian noise elements, whereas Y_i is the block of received symbols during the i^{th} block. Similarly, for U_2 the received blocks can be written as

$$\begin{aligned}
Y_2 &= h_2 X_2^{(D)} + N_3 \\
Y_5 &= h_2 X_2^{(C)} + N_5. \\
Y_6 &= \alpha h_1 h_{12} X_2^{(C)} + \alpha h_1 N_8 + N_6.
\end{aligned} \tag{154}$$

In order to ensure that the power constraint is satisfied regardless of β , the average energy per symbol over each window is forced to be E . Specifically, $E[\|X_i^{(D)}\|^2]/\beta T = E_t^{(D)} = 2E$ and $E[\|X_i^{(C)}\|^2]/(1-\beta)T = E_t^{(C)} = 2E$. In this case, we see that $E_t^{(D)} = E_t^{(C)}$ since the users transmit over equal fractions in both windows. However, this is not always true.

9.2.1 Outage Analysis:

We now analyze the outage event for this transmission scheme. The outage event for the two users in this multiple access system is given by:

$$\begin{aligned}
\mathcal{O}_1: C_1 &= \max_{p_1(x)} \frac{1}{T} I(X_1^{(C)}, X_1^{(D)}; Y_1, Y_3, Y_4) < R \\
\mathcal{O}_2: C_2 &= \max_{p_2(x)} \frac{1}{T} I(X_2^{(C)}, X_2^{(D)}; Y_2, Y_5, Y_6) < R,
\end{aligned} \tag{155}$$

where $p_i(x)$ is the probability density function of X_i . Using the fact that noise is independent across time, (155) can be simplified as

$$C_1 = \max_{p_1(x)} \frac{1}{T} (I(X_1^{(C)}; Y_1) + I(X_1^{(D)}; Y_3, Y_4))$$

$$C_2 = \max_{p_2(x)} \frac{1}{T} (I(X_2^{(C)}; Y_2) + I(X_2^{(D)}; Y_5, Y_6)) < R. \quad (156)$$

The outage probability of the multiple-access system, which is the probability of any of the users being in outage, is given by:

$$P_o = \Pr[\mathcal{O}_1 \cup \mathcal{O}_2] = \Pr[\min \{C_1, C_2\} < R]. \quad (157)$$

The mutual informations in are maximized when the input alphabet at each source follows an independent Gaussian distribution [27]. Maximizing and substituting for α , we get

$$C_1 = \frac{\beta}{2} \log_2(1 + 2S|h_1|^2) + \frac{1-\beta}{4} \log_2 \left(1 + 2S|h_1|^2 + \frac{4S^2|h_2|^2|h_{12}|^2}{1 + 2S(|h_{12}|^2 + |h_2|^2)} \right). \quad (158)$$

Similarly for U_2

$$C_2 = \frac{\beta}{2} \log_2(1 + 2S|h_2|^2) + \frac{1-\beta}{4} \log_2 \left(1 + 2S|h_2|^2 + \frac{4S^2|h_1|^2|h_{12}|^2}{1 + 2S(|h_{12}|^2 + |h_1|^2)} \right). \quad (159)$$

We now discuss the diversity order of partial cooperation using the LTW protocol. Let $P_1 = \Pr[\mathcal{O}_1]$, $P_2 = \Pr[\mathcal{O}_2]$ and let the corresponding diversity orders be d_1 and d_2 . The outage probability in (157) can be bounded as

$$P_\delta \leq P_o \leq P_1 + P_2, \quad (160)$$

where P_δ is either of P_1 or P_2 . Since h_1 and h_2 are i.i.d, $d_1 = d_2$.

Theorem 9. The LTW protocol with partial cooperation achieves the full diversity order of $d = 2$ over a two-user cooperative multiple-access channel with one antenna at each node, for any β in the range $0 \leq \beta < 1$.

Proof: The capacity of user 1, C_1 , can be bounded as

$$\frac{1-\beta}{4} \log_2 \left(1 + 2S|h_1|^2 + \frac{4S^2|h_2|^2|h_{12}|^2}{1 + 2S(|h_{12}|^2 + |h_2|^2)} \right) \leq C_1 \leq \log_2(1 + S(|h_1|^2 + |h_2|^2)). \quad (161)$$

The lower bound is obtained by dropping a term in (158) and the upper bound is true since C_1 cannot exceed the capacity of a 2×1 MISO channel. Using (158), we get

$$\Pr\left(\frac{1}{4} \log_2 \left(1 + 2S|h_1|^2 + \frac{4S^2|h_2|^2|h_{12}|^2}{1 + 2S(|h_{12}|^2 + |h_2|^2)} \right) < R\right) < k \frac{(2^{4R} - 1)^2}{S^2}, \quad (162)$$

as $S \rightarrow \infty$ for some constant k . Combining (161) and (162),

$$\lim_{S \rightarrow \infty} \Pr\left(\frac{1-\beta}{4} \log_2 \left(1 + 2S \left(|h_1|^2 + \frac{2S|h_2|^2|h_{12}|^2}{1 + 2S(|h_{12}|^2 + |h_2|^2)} \right) \right) < R\right) < k \frac{\left(2^{\frac{4R}{1-\beta}} - 1 \right)^2}{S^2}, \quad (163)$$

for $\beta \neq 1$. Of course, the upper bound evaluates to 1 for $\beta = 1$. For $0 \leq \beta < 1$, the probability of error decays at least as $1/S^2$ for large S , hence $d_1 \geq 2$. The capacity of

a 2×1 MISO channel is an upper bound on C_1 and has a diversity order of 2, implying that $d_1 \leq 2$, which can be true only iff $d_1 = 2$. Since $d_2 = d_1$, we have shown that P_o decays as S^{-2} as $S \rightarrow \infty$.

The above result states that *as long as the cooperation window occupies a nonzero fraction of every frame*, the system achieves full diversity.

Corollary 2. The LTW protocol with partial cooperation achieves the full diversity order of $d = 2$ and a rate $R = 1/2 - (1 - \beta)/4$ per user for $0 \leq \beta < 1$.

The implication of this result is that, in theory, the LTW protocol with partial cooperation simultaneously achieves a diversity gain of 2, and a rate arbitrarily close but not equal to $1/2$. However, in practice, if we choose a value of β arbitrarily close but not equal to 1, the capacity of each user will be numerically very close to that over a TDMA system. Of course, the theoretical assertion of full diversity from Theorem 9 still holds, only that the effect of full diversity on the outage probability curve is seen at extremely high SNRs beyond the realm of practical interest.

As stated earlier, our goal is not to maximize the diversity gain or the rate but to use these as design tools to minimize outage probability. In the following section, we show how the partial cooperation framework can be used to optimize the outage probability. Specifically, for a given data rate R and SNR S , we determine the optimal value of β using an exhaustive numerical search. Simulation results are presented in the next section to illustrate how this optimization improves the outage performance.

9.2.2 Numerical Results

In this section, numerical results are presented for partial cooperation using the LTW protocol over a 2-user cooperative multiple-access channel with a target data rate of $R = 1$ b/s/Hz per user.

In Fig. 39, we compare the outage probabilities of TDMA, SDMA and LTW-AF against LTW-AF with partial cooperation. For the latter scheme, we compute the outage probability curve as follows: For each value of S from 0, 2.5, ..., 30 dB, we compute the outage probability as a function of β , and choose the value of β which yields the minimum outage probability for the given S to be the optimum one. The effective outage curve is obtained by connecting together the optimized points. Also shown in Fig. 39 is the outage probability for the MISO bound. From Fig. 39, we see that LTW-AF with partial cooperation combines the merits of TDMA and SDR-AF. At low SNR, the performance is

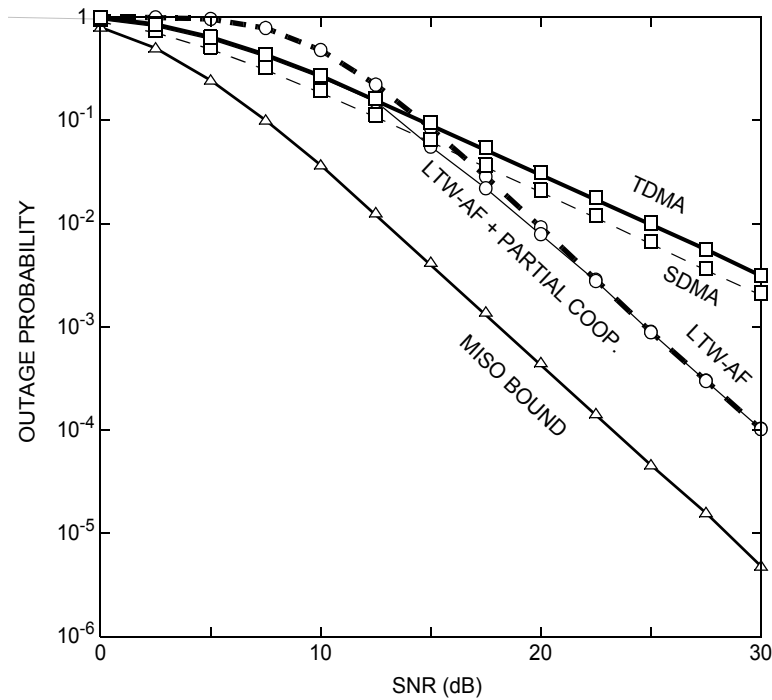


Fig. 39. Outage performance of LTW with partial cooperation over a 2-user cooperative multiple access system, $R = 1$ b/s/Hz.

at least as good as TDMA and at high SNR, the partial cooperation framework performs at least as well as SDR-AF. The optimum values of β are [1 1 0.9996 0.2191 0.1216 0.0523 0.0132] for $S = [0 \ 5 \ 10 \ 15 \ 20 \ 25 \ 30]$ dB. As expected, the optimal fraction of direct transmission decreases as the SNR increases, since cooperation is more important in the high SNR regime, whereas a high symbol rate is crucial at low SNR. For SNR < 12.5 dB, it is optimal to use TDMA for the entire frame, whereas for SNR > 40 dB, using cooperation for the entire frame minimizes outage probability.

Fig. 40 shows the comparison of outage probabilities for $R = 2$ b/s/Hz per user. The optimal widths of direct transmission window for this case are [1.00 1.00 1.00 1.00 1.00 0.9427 0.3502 0.1660 0.0376] T for $S = [0 \ 5 \ 10 \ 15 \ 20 \ 25 \ 30 \ 35 \ 40]$ dB. We observe that *higher the data rate and / or lower the SNR of operation, greater the importance of symbol rate over diversity, and hence larger must be the window of direct transmission.*

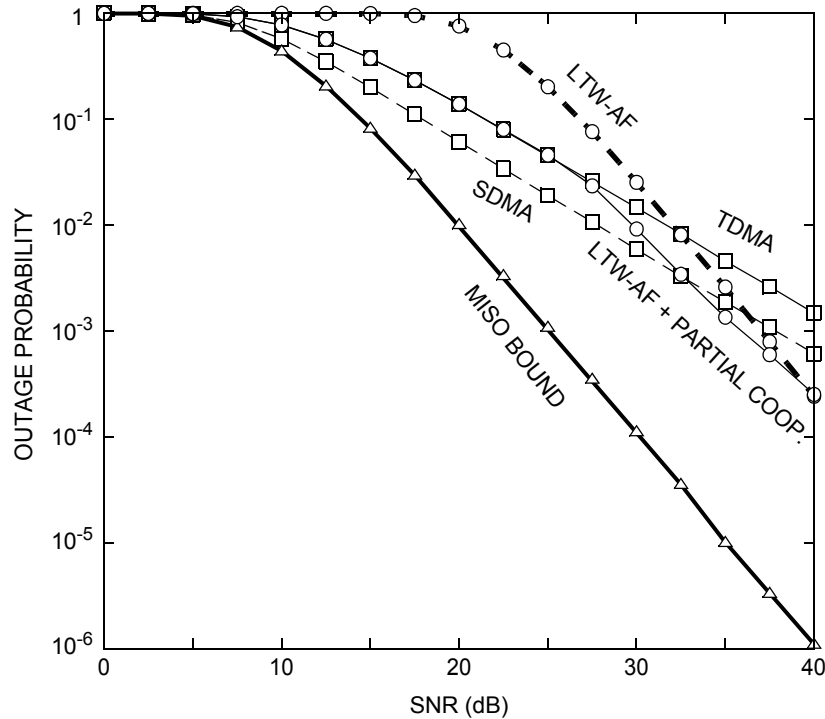


Fig. 40. Outage performance of LTW with partial cooperation over a 2-user cooperative multiple access system, $R = 2$ b/s/Hz.

9.3 Example of a Non-Orthogonal System with Partial Cooperation

This section presents the partial cooperation framework for non-orthogonal cooperation protocols with amplify-and-forward relays. In the absence of the orthogonality constraint, it is well known that SDMA helps each user achieve the maximum possible rate over a multiple-access channel by allowing simultaneous transmissions.

The partial cooperation framework combines SDMA, where each user has a rate 1 and diversity 1, with the SDR protocol, where each user achieves the full diversity of 2, but only a rate of $1/3$. The basic idea, as discussed before, is to determine the relative importance of rate and diversity for the given operating conditions, in order to achieve the ultimate goal of achieving the lowest possible outage probability. Each user encodes the information to be transmitted into $\beta T + (1 - \beta)T/3$ symbols. The first βT symbols constitute $X_i^{(D)}$ and are sent SDMA in the direct transmission window. The remaining

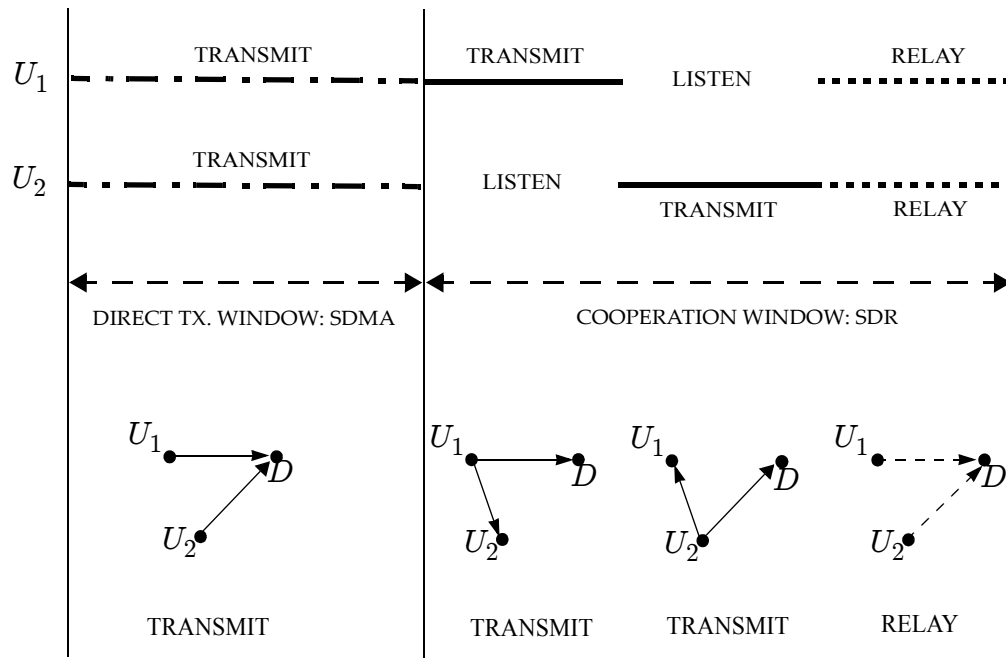


Fig. 41. Partial cooperation with the SDR protocol for $N = 2$.

symbols form $X_i^{(C)}$ and are sent using the SDR cooperation protocol, as shown in Fig. 41.

Overall, the received symbols at the destination can be grouped into 4 blocks, one in the direct transmission window and 3 during the cooperation window.

$$\begin{aligned}
Y_1 &= h_1 X_1^{(D)} + h_2 X_2^{(D)} + N_1 \\
Y_2 &= h_1 X_1^{(C)} + N_2 \\
Y_3 &= h_2 X_2^{(C)} + N_3 \\
Y_4 &= \alpha h_2 h_{12} X_1^{(C)} + \alpha h_1 h_{12} X_2^{(C)} + \alpha h_1 N_5 + \alpha h_2 N_6 + N_4,
\end{aligned} \tag{164}$$

where, N_i 's consist of independent, circularly symmetric complex Gaussian noise elements, whereas Y_i is the block of received symbols during the i^{th} block. The received blocks during the cooperation window can be written in matrix form as

$$Y = \begin{bmatrix} Y_1 \\ Y_2 \\ Y_3 \end{bmatrix} = \mathbf{H} \begin{bmatrix} X_1^{(C)} \\ X_2^{(C)} \end{bmatrix} + \mathbf{A} \begin{bmatrix} N_2 \\ N_3 \\ N_4 \\ N_5 \\ N_6 \end{bmatrix}, \tag{165}$$

where the $(i, j)^{\text{th}}$ element of the noise matrix \mathbf{N} is $n_i(j)$, the matrices \mathbf{H} and \mathbf{A} given by

$$\mathbf{H} = \begin{bmatrix} h_1 & 0 \\ 0 & h_2 \\ \alpha h_2 h_{12} & \alpha h_1 h_{12} \end{bmatrix}, \quad \mathbf{A} = \begin{bmatrix} 1 & 0 & 0 & 0 & 0 \\ 0 & 1 & 0 & 0 & 0 \\ 0 & 0 & 1 & \alpha h_1 & \alpha h_2 \end{bmatrix}, \tag{166}$$

where, α , the amplification factor is as defined in (136).

To ensure that the power constraint is satisfied regardless of the value of β , the average energy per symbol over each window is forced to be E . Specifically, $E[\|X_i^{(D)}\|^2]/\beta T = E_t^{(D)} = E$ and $E[\|X_i^{(C)}\|^2]/(1-\beta)T = E_t^{(C)} = 3E/2$.

9.3.1 Outage Analysis

The outage event for this multiple access system is the union of the following three events [27]:

$$\begin{aligned} \mathcal{O}_1: C_{1|2} &= \max_{p(x)} \frac{1}{T} I(X_1^{(D)}, X_1^{(C)}; Y_1, Y_2, Y_4 | X_2^{(C)}) < R \\ \mathcal{O}_2: C_{2|1} &= \max_{p(x)} \frac{1}{T} I(X_2^{(C)}, X_2^{(D)}; Y_1, Y_3, Y_4 | X_1^{(C)}) < R \\ \mathcal{O}_{12}: C_{12} &= \max_{p(x)} \frac{1}{2T} I(X_1^{(C)}, X_1^{(D)}, X_2^{(C)}, X_2^{(D)}; Y_1, Y_2, Y_3, Y_4) < R, \end{aligned} \quad (167)$$

where $p(x)$ is the joint probability density function of X_1 and X_2 . The outage probability is thus:

$$P_o = \Pr[\mathcal{O}_1 \cup \mathcal{O}_2 \cup \mathcal{O}_{12}] = \Pr[\min\{C_{1|2}, C_{2|1}, C_{12}\} < R]. \quad (168)$$

The mutual informations are maximized when the input alphabet at each source follows an independent Gaussian distribution [27]. Maximizing and substituting for α , we get

$$C_{1|2} = \beta \log_2(1 + S|h_1|^2) + \frac{1-\beta}{3} \log_2 \left(1 + \frac{3S}{2} \left(|h_1|^2 + \frac{3S|h_2|^2|h_{12}|^2}{2 + 3S(|h_{12}|^2 + |h_2|^2 + |h_1|^2)} \right) \right),$$

$$C_{2|1} = \beta \log_2(1 + S|h_2|^2) + \frac{1-\beta}{3} \log_2 \left(1 + \frac{3S}{2} \left(|h_2|^2 + \frac{3S|h_1|^2|h_{12}|^2}{2 + 3S(|h_{12}|^2 + |h_2|^2 + |h_1|^2)} \right) \right),$$

$$C_{12} = \frac{\beta}{2} \log_2(1 + S|h_2|^2 + S|h_2|^2) + \frac{1-\beta}{6} \log_2 \det(\mathbf{I} + \frac{3}{2} S \mathbf{H}^* (\mathbf{A} \mathbf{A}^*)^{-1} \mathbf{H}), \quad (169)$$

where, \mathbf{H} and \mathbf{A} are as defined in (166).

We now discuss the diversity order of partial cooperation using the SDR cooperation protocol. Similar to the definitions in Section 8.2, let $P_1 = \Pr[\mathcal{O}_1]$, $P_2 = \Pr[\mathcal{O}_2]$, and $P_{12} = \Pr[\mathcal{O}_{12}]$ and let the corresponding diversity orders be d_1 , d_2 and d_{12} respectively. the outage probability in (168) can be bounded using the union bound as

$$P_{\delta} \leq P_o \leq P_1 + P_2 + P_{12}, \quad (170)$$

where P_{δ} is either of P_1 , P_2 or P_{12} . Since h_1 and h_2 are statistically identical, $d_1 = d_2$. We state the following theorem on the diversity order of SDR.

Theorem 10. The SDR protocol with partial cooperation and AF relays achieves the full diversity order of $d = 2$ over a two-user cooperative multiple-access channel with one antenna at each node, for any value of β in the range $0 \leq \beta < 1$. In other words, full diversity of SDR is preserved by partial cooperation provided $\beta \neq 1$.

Proof: Using the bound in (170), it is easy to show that $d_{\text{SDR}} = \min\{d_1, d_2, d_{12}\}$.

Further, using the inequality $I(X_1, X_2; Y) \geq I(X_1; Y|X_2)$, we get $2C_{12} \geq C_{1|2}$,

implying that $d_{12} \geq d_1$. Thus, it suffices to prove that $d_1 = 2$. Using (152) we get

$$\lim_{S \rightarrow \infty} \Pr\left(\frac{1}{3} \log_2 \left(1 + \frac{3S}{2} \left(|h_1|^2 + \frac{3S|h_2|^2|h_{12}|^2}{2 + 3S(|h_{12}|^2 + |h_2|^2 + |h_1|^2)} \right) \right) < R\right) < k \frac{(2^{3R} - 1)^2}{S^2}. \quad (171)$$

Further, $C_{1|2}$ can be bounded as

$$\frac{1-\beta}{3} \log_2 \left(1 + \frac{3S}{2} \left(|h_1|^2 + \frac{3S|h_2|^2|h_{12}|^2}{2 + 3S(|h_{12}|^2 + |h_2|^2 + |h_1|^2)} \right) \right) \leq C_{1|2} \leq \log_2(1 + S(|h_1|^2 + |h_2|^2)). \quad (172)$$

The lower bound is obtained by simply dropping a term in (169) and the upper bound is true since $C_{1|2}$ clearly cannot exceed the capacity of a fictitious MISO channel created jointly by U_1, U_2 with D . Combining (171) and (172),

$$\lim_{S \rightarrow \infty} \Pr\left(\frac{1-\beta}{3} \log_2 \left(1 + \frac{3S}{2} \left(|h_1|^2 + \frac{3S|h_2|^2|h_{12}|^2}{2 + 3S(|h_{12}|^2 + |h_2|^2 + |h_1|^2)} \right) \right) < R\right) < k \frac{\left(2^{\frac{3R}{1-\beta}} - 1 \right)^2}{S^2}, \quad (173)$$

for $\beta \neq 1$. Of course, for $\beta = 1$ the above probability is 1. For any other value of β , the outage probability decays at least as fast as $1 / S^2$ for large S , hence $d_1 \geq 2$. The capacity of a 2×1 MISO channel is an upper bound on $C_{1|2}$ and has a diversity order of 2, implying that $d_1 \leq 2$, thus making $d_1 = 2$. As discussed earlier, $d_2 = d_1$ and $d_{12} \geq d_1$. Hence, we have shown that P_o decays as S^{-2} as $S \rightarrow \infty$.

Corollary 3. The SDR protocol with partial cooperation achieves the full diversity order of $d = 2$ and a rate $R = 1 - 2(1 - \beta)/3$ for $0 \leq \beta < 1$, i.e., *full diversity and any constant rate < 1 is achievable over a two-user cooperative multiple access channel* with a single antenna at each node.

In theory, the implication of the above result is that partial cooperation with SDMA and SDR guarantees full diversity *as long as the cooperation window occupies a nonzero fraction of every frame*. This might seem surprising to the reader, especially in a scenario where β is arbitrarily close but not equal to 1, say 0.999, since the numerical values of the mutual information for this case will be very close to that of SDMA. Here, we recall the definition of diversity order as an asymptotic quantity. Larger the value of β , smaller the effect of cooperation on the capacity and larger the SNR at which the it is *high enough* for the diversity phenomenon to manifest itself as the slope of the outage curve. Of course, the theoretical assertion of full diversity from Theorem 10 still holds, only that the effect of full diversity on the outage probability curve is seen at extremely high SNRs.

Although partial cooperation guarantees full diversity for a wide range of values of β , achieving the lowest possible outage probability is another matter. In the following section, we show how the partial cooperation framework can be used to optimize the outage probability of the SDR protocol. For a given data rate R and SNR S , we determine

the optimal value of β using an exhaustive numerical search experiment. We present simulation results in the next section to illustrate how this optimization improves the outage performance.

9.3.2 Numerical Results

We now present numerical results for partial cooperation SDR over a Rayleigh-fading cooperative multiple-access channel with $N = 2$ users and a single destination. Each user has a target data rate of $R = 1$ b/s/Hz, and each has the same average SNR S .

In Fig. 42, we compare the outage probabilities of SDR-AF with and without partial cooperation against the outage probability of TDMA and SDMA. Also shown in Fig. 42 is the outage probability of a 2×1 MISO channel, labelled as the ‘MISO bound’. Previously, we observed that cooperative schemes outperform non-cooperative schemes at high SNR,

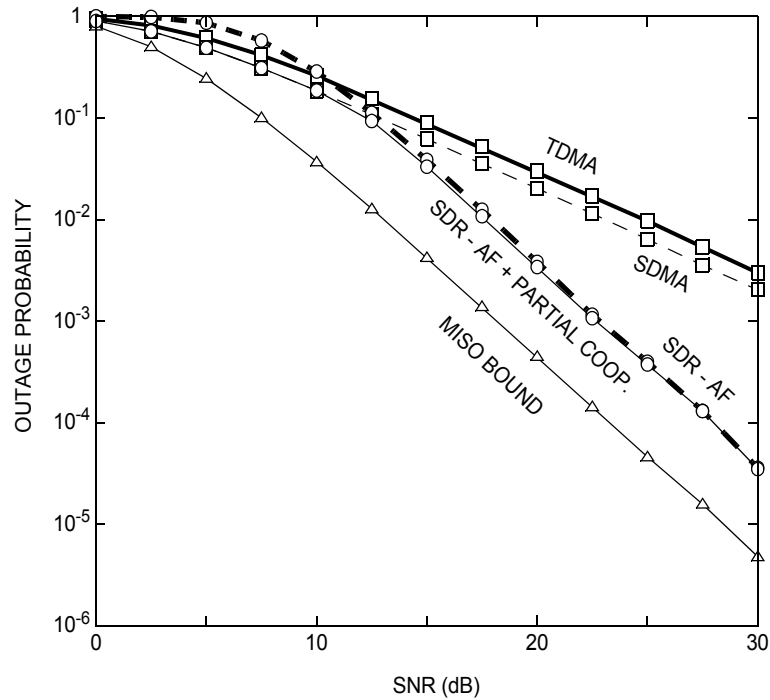


Fig. 42. Outage performance of SDR with partial cooperation over a 2-user cooperative multiple access system, $R = 1$ b/s/Hz.

but that the converse is true at low SNR. From Fig. 42, we see that partial cooperation fixes this problem. SDR-AF with partial cooperation performs at least as well as SDMA at low SNR and at least as well as the original SDR-AF at high SNR. SDR-AF with partial cooperation is strictly better than SDR-AF and SDMA and falls within 4.5 dB of the MISO bound at an outage probability of 10^{-3} .

The optimum value of β was determined to be [1.00 1.00 0.9726 0.1706 0.1012 0.0317 0.0061] for $S = [0 \ 5 \ 10 \ 15 \ 20 \ 25 \ 30]$ dB. The optimal width of direct transmission decreases as the SNR increases, which is in agreement with the intuition that diversity gain, and hence cooperation is more important at high SNR, whereas symbol rate is more important at low SNR. For SNR < 10 dB, it is optimal to use SDMA for the entire frame, whereas for SNR > 25 dB, using SDR-AF for the entire frame minimizes outage probability.

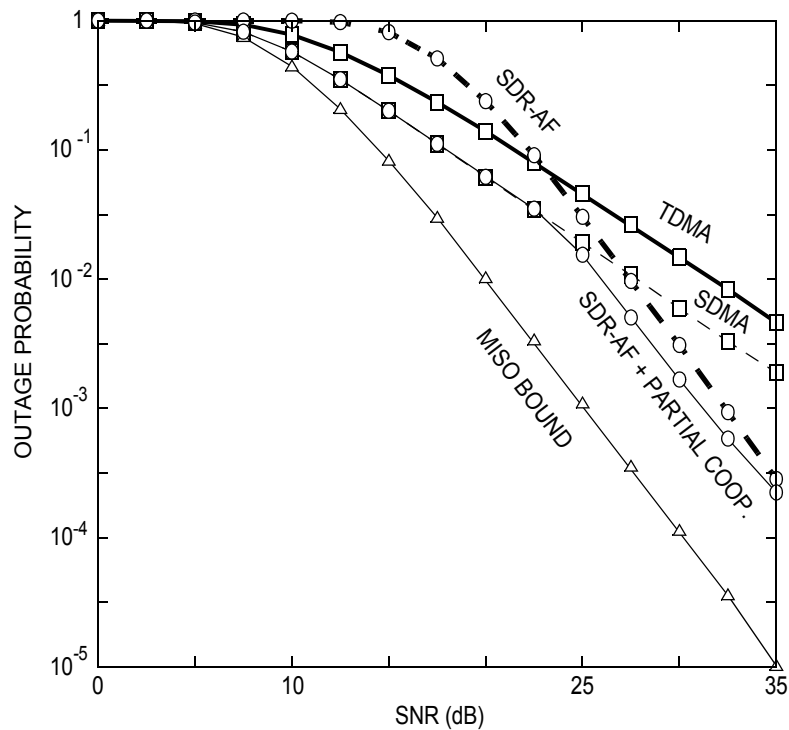


Fig. 43. Outage performance of SDR with partial cooperation over a 2-user cooperative multiple access system, $R = 2$ b/s/Hz.

To study the effect of a higher target data rates, we present numerical results for SDR-AF with partial cooperation at a data rate of $R = 2$ b/s/Hz for $N = 2$ users in Fig. 43. The optimal fractions of direct transmission are $[1.00 \ 1.00 \ 1.00 \ 1.00 \ 0.9793 \ 0.3311 \ 0.1660 \ 0.0346]T$ for $S = [0 \ 5 \ 10 \ 15 \ 20 \ 25 \ 30 \ 35]$ dB. As expected, it is observed that for a given SNR, the optimal width of direct transmission window with SDR-AF is larger for $R = 2$ b/s/Hz as opposed to $R = 1$ b/s/Hz. Partial cooperation significantly improves outage performance in the $R = 2$ b/s/Hz case, for example, at an outage probability 10^{-3} , partial cooperation improves the performance by 1.1 dB over SDR-AF with $R = 2$ b/s/Hz as opposed to an improvement of just 0.2 dB at $R = 1$ b/s/Hz.

9.4 Summary

In this chapter, we studied the partial cooperation framework along with known orthogonal and non-orthogonal cooperation protocols. This study shows the importance of using the optimal amount of cooperation in a multiple-access network depending on the target data rate and SNR of operation.

At the extremities of very high and very low SNR, partial cooperation essentially takes the form of pure cooperation and pure non-cooperative transmission respectively. But in the intermediate range of SNR, numerical results show that partial cooperation provides new operating points with SNR improvements in the order of 1 – 2 dB by gaining an optimal amounts of cooperation gain while not losing out on the transmission rate, to achieve the goal of minimizing the outage probability.

CHAPTER 10

SCALABLE HIGH RATE COOPERATION PROTOCOLS FOR MULTIPLE-ACCESS CHANNELS

In the previous chapters, we considered protocol design for user cooperation over a simple two-user multiple-access channel. Although this problem gave us good insight into designing cooperation protocols, it is important to design cooperation protocols which will extend these performance benefits to a larger wireless network, in terms of maximizing diversity and transmission rate.

Currently, there are few solutions to this problem: the cooperation protocols that have been proposed are very low rate. For example, over a N user multiple-access system the multiuser extension of the LTW protocol has a rate of $1 / N^2$ per user [64], with the rate loss incurred mainly due to the orthogonality constraint which affects the transmission as well as the relay phases. The best available non-orthogonal protocols is the NAF protocol, which improves the rate to $1 / N$ [66] by the use of an artificial ISI channel-like structure. However, the rate per user still decreases as the number of users increase. In fact, over large multiple-access systems, it might be more important to maintain a high rate than to achieve full diversity!

In this chapter, we propose an extension of the space-division relay (SDR) protocol for a cooperative multiple-access channel with an arbitrary number of users N . We show that the SDR protocol achieves a rate of $(N - 1)/(N + 1)$. We discuss the SDR protocol with amplify-and-forward as well as selection decode-and-forward relays. We show that SDR with selection decode-and-forward achieves the full diversity of N over the CMA channel.

We start, in Section 10.1, with a description of the channel model of the N -user CMA system. In Section 10.2, we propose an extension of the SDR protocol for N users. We discuss SDR with AF relays and derive the outage probability of this combination in Section 10.3. Following this, we discuss SDR with SDF relays and present a detailed analysis of this combination in Section 10.4. In Section 10.5, we present simulation results for the above cases and compare the outage performance with other candidate schemes. We summarize the results in Section 10.6.

10.1 Channel Model

We consider a Rayleigh-fading multiple-access channel with N users communicating with a common destination. Each node is equipped with a single antenna and can either transmit or receive over the same time and frequency band, i.e., a node cannot transmit and receive simultaneously over the same channel. In Fig. 44, we illustrate the possible communication links in a N -user cooperative multiple-access system, where each node could either be transmitting its own information or relaying the information received from the other user to the destination.

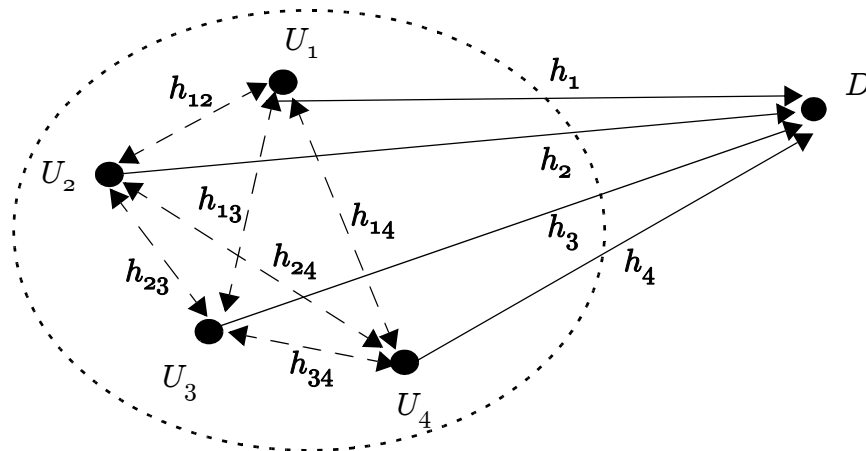


Fig. 44. Example of an N -user cooperative multiple-access system with $N = 4$

To simplify our presentation we consider a completely symmetric scenario: (1) All users have an identical target data rate of R bps/Hz; (2) All users have an identical average energy of E per signalling interval; and (3) the average received SNR for each user is identical. Asymmetry in any of these variables is easily incorporated into the system design without affecting the design principle.

Let h_i denote the channel gain between the i^{th} user and the destination, and let h_{ij} denote the channel gain between the i^{th} user and the j^{th} user, with $i \neq j$. The channels are assumed to be linear and flat fading over the signal bandwidth. Also, the channels are assumed to be quasistatic, so that the channel response is constant over a frame consisting of T symbol periods, and it changes to an independent value from one frame to the next. During a given static fading frame the communication between any two users is over the same frequency band, and channel gain is symmetric between any two users, in other words, $h_{ij} = h_{ji}$. Therefore, we simplify the notation by referring to h_{ij} as h_{ji} , if $i > j$.

The channel coefficients $\{h_i, h_{ij}\}$ with $i, j = 1, 2, \dots, N$ and $i \neq j$ are i.i.d. circularly symmetric complex Gaussian random variables with zero mean and unit variance. The additive noise at each receiving terminal is independent circularly symmetric Gaussian random variable with zero mean and variance N_0 . Under these assumptions, the average SNR of each user at the receiving node is $S = E/N_0$. We assume that the users are frame-synchronized. We further assume that the destination knows all of channel coefficients $\{h_i, h_{ij}\}$ whereas the i^{th} user knows only $\{h_{ij}\}$ for $j = 1, 2, \dots, N$.

As discussed earlier, the LTW and NAF protocols have been extended to the N user case [64][68]. However, they achieve very low rates in an attempt to maximize diversity gain. We extend the SDR protocol and show that significantly higher rate could be achieved without compromising on full diversity.

10.2 Space-Division Relay (SDR) for N -users

SDR can be extended to a multiple-access system with N users by employing space-division multiplexing over the transmission phase as well as the relay phase. In Fig. 45 we illustrate how the SDR protocol applies to the case of $N = 3$ users.

In general, the static fading frame is divided into $N + 1$ blocks. For $i = 1, 2, \dots, N$, during the i^{th} block all but the i^{th} user transmit, while the i^{th} user receives a linear combination of the transmissions of users $1, 2, \dots, i - 1, i + 1, \dots, N$, as does the destination. After N blocks, each of the N users would have each received one block of linearly combined information from all the other users. During the relay phase, these packets are forwarded using some relay operation to the destination in a spatially multiplexed fashion, i.e., the relay packets are transmitted simultaneously by all N users during the $(N + 1)^{\text{th}}$ block. The exact relay operations will be specified in the next section.

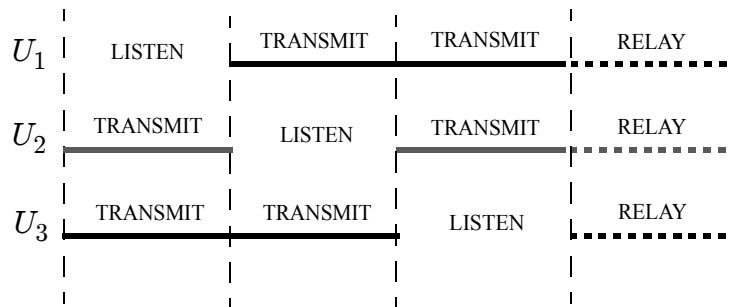


Fig. 45. Extension of the SDR protocol to $N = 3$ users.

With this set-up, we see that each user transmits new information during $(N - 1)$ blocks, listens during one block and relays the information from other users during one block. In the $N = 3$ case, we see that the rate of each user is $1/2$, since each user transmits new information for 2 out of the 4 blocks. In general, the rate of the SDR protocol for an N -user system is $(N - 1)/(N + 1)$. Interestingly, the rate of the SDR protocol per user grows with N . In stark contrast, the rate for LTW is $1/N^2$, while the rate for NAF is $1/N$. Despite the high rate, we will show that the SDR protocol is sufficient to ensure good diversity performance, and specifically that SDR protocol achieves full diversity over a N -user system with selection-decode-and-forward relays.

During the i^{th} block, the i^{th} user and the destination act as receivers while all the other users transmit information. The received symbols at the i^{th} user and the destination are given by

$$y_i(l) = \sum_{\substack{j=1 \\ j \neq i}}^N h_{ij}x_j(l) + n_{ii}(l),$$

$$y(l) = \sum_{\substack{j=1 \\ j \neq i}}^N h_jx_j(l) + n_i(l), \quad (174)$$

respectively for $l = (i - 1)T/(N + 1) + 1, \dots, iT/(N + 1)$ and $i = 1, 2, \dots, N$. The transmission during the $(i + 1)$ -th block by each user is determined by the specific relay method chosen. In general, the received symbol at the destination can be written as

$$y(l) = \sum_{j=1}^N h_jf(y_j(l)) + n_{N+1}(l), \quad (175)$$

for $l = NT/(N + 1) + 1, \dots, T$ and $i = 1, 2, \dots, N$. As in the previous examples, the received symbols can be grouped together, with the received block at the i -th user during the i -th block is obtained as $Y_{ii} = [y_i(1) y_i(2) \dots y_i(T/(N + 1))]$ for $i = 1, 2, \dots, N$. The received blocks at destination are defined as $Y_i = [y((i - 1)T/(N + 1) + 1), \dots, y(iT/(N + 1))]$ for $i = 1, 2, \dots, N + 1$. The block of information transmitted by the j -th user in the i -th block is given by $X_j^{(i)}$ for $i, j = 1, 2, \dots, N$ and with $X_i^{(i)} = \mathbf{0}$, since the user is assigned the task of listening to other users during that block. Finally, the transmitted word corresponding to the j -th user is $X_j = [X_j^{(1)}, X_j^{(2)}, \dots, X_j^{(N)}]$, the set of blocks transmitted by active users in the i -th block is $X^{(i)} = [X_1^{(i)}, X_2^{(i)}, \dots, X_N^{(i)}]$ and the received information at the destination is $Y = [Y_1, Y_2, \dots, Y_{N+1}]$.

In the previous chapters, we considered popular relay strategies such as AF, ADF and SDF. Now, we describe how AF and SDF work with SDR, while ADF can be obtained as a simple combination of these ideas.

10.3 Amplify-and-forward (AF)

In SDR with AF relays, the nodes simply scale the received samples to meet the average transmit power constraint and forward them to the destination. The difference in this technique for N users, as opposed to two, is that the received sample in itself is a linear combination of symbols from several users.

As before, the key advantage of the AF relaying is that users do not have to decode the information, thus keeping the burden on relay nodes to a minimum. However, in the case of multiple users, the disadvantage is that information symbols from several interfering

users, each corrupted by channel distortion, are forwarded along with additive noise. In addition, the transmit power of each relay is split amongst symbols of several users as well. For example, if user U_i receives

$$y_i(l) = \sum_{\substack{j=1 \\ j \neq i}}^N h_{ij}x_j(l) + n_{ii}(l), \quad (176)$$

then during the relay phase, U_i forwards αy to the destination, where α is the amplification factor chosen to meet the power constraint, given by

$$\alpha_i = \frac{\sqrt{\frac{E_t}{N}}}{\sqrt{1 + \sum_{\substack{j=1 \\ j \neq i}} E_t |h_{ij}|^2}}, \quad (177)$$

where $E[|x_j(l)|^2] = E_t$, and the destination receives

$$y(l) = \sum_{i=1}^N \alpha_i h_i y_i(l) + n_{N+1}(l). \quad (178)$$

The equivalent matrix channel created by the cooperation protocol using AF relays is

$$\begin{bmatrix} Y_1 & Y_2 & \dots & Y_N \end{bmatrix} = \begin{bmatrix} h_1 & h_2 & \dots & h_N \end{bmatrix} \begin{bmatrix} 0 & X_1^{(2)} & \dots & X_1^{(N-1)} & X_1^{(N)} \\ X_2^{(1)} & 0 & \dots & X_2^{(N-1)} & X_2^{(N)} \\ \cdot & & \dots & & \cdot \\ X_{N-1}^{(1)} & & \dots & 0 & X_{N-1}^{(N)} \\ X_N^{(1)} & X_N^{(2)} & \dots & X_N^{(N-1)} & 0 \end{bmatrix} + \begin{bmatrix} N_1 & N_2 & \dots & N_N \end{bmatrix}, \quad (179)$$

$$Y_{ii} = \begin{bmatrix} h_{1i} & \dots & h_{(i-1)i} & h_{(i+1)i} & \dots & h_{Ni} \end{bmatrix} \begin{bmatrix} X_1^{(i)} \\ \cdot \\ X_{i-1}^{(i)} \\ X_{i+1}^{(i)} \\ \cdot \\ X_N^{(i)} \end{bmatrix} + N_{ii}, \quad (180)$$

and

$$Y_{N+1} = \begin{bmatrix} \alpha_1 h_1 & \alpha_2 h_2 & \dots & \alpha_N h_N \end{bmatrix} \begin{bmatrix} Y_{11} \\ Y_{22} \\ \cdot \\ \cdot \\ Y_{NN} \end{bmatrix} + N_{N+1}. \quad (181)$$

10.3.1 Outage Analysis

We now analyze the outage probability of SDR with AF relays. The Gaussian discrete memoryless multiple access channel created by the cooperation protocol has $N + 1$ output blocks, with each of the N users transmitting $N - 1$ blocks of information, each of length $T/(N + 1)$ symbol periods. The probability of error is defined as the probability that

$$\Pr(\mathcal{E}) = \Pr\left(\bigcup_{\gamma \in \Gamma} \mathcal{E}_\gamma\right), \quad (182)$$

where, Γ is the set of all $2^N - 1$ nonempty subsets of $\{1, 2, \dots, N\}$, with γ denoting each element of Γ i.e., $\Gamma = [\{1\}, \{2\}, \dots, \{N\}, \{1, 2\}, \{1, 3\}, \{2, 3\}, \dots, \{N-1, N\}, \dots, \{1, 2, \dots, N\}]$ and \mathcal{E}_γ is the event corresponding to the elements in γ being in error jointly,

regardless of the other sets being in error. Let $X(\gamma) = \{X_k: k \in \gamma\}$, then, for a codeword of length n and any given set γ , the error probability can be upper-bounded as

$$\Pr(\mathcal{E}_\gamma) \leq 2^{\{-n [I(X(\gamma); Y | X(\gamma^X)) - R_\gamma - \epsilon_\gamma]\}}, \quad (183)$$

for some $\epsilon_\gamma > 0$, where R_γ is the sum of data rates transmitted by the users in γ . Since we assume a symmetric scenario with all users transmitting equal data rates, $R_\gamma = R|\gamma|$. The probability of any of the users being in error can be upper bounded as

$$\Pr(\mathcal{E}) \leq \sum_{\gamma \in \Gamma} \Pr(\mathcal{E}_\gamma). \quad (184)$$

Each term in the above expression will be arbitrarily close to zero iff $I(X(\gamma); Y | X(\gamma^C)) > R|\gamma|$, i. e., if the joint channel created by the users in γ with the destination is outage-free.

The outage event for the set of users γ is

$$\mathcal{O}_\gamma: = \max_{p(x)} \frac{1}{T} I(X(\gamma); Y | X(\gamma^X)) < R|\gamma|, \quad (185)$$

where $p(x)$ is the probability density function of X . Hence, the outage probability of the system is:

$$P_{\text{SDR-AF}} = \Pr\left[\bigcup_{\gamma \in \Gamma_j} \mathcal{O}_\gamma \right], \quad (186)$$

where, $\Gamma_j = \{\gamma: j \in \gamma\}$. For a given channel realization, the above probability of error is arbitrarily close to zero if each of the conditional mutual informations is greater than the corresponding data rate. However, if any of the following outage events is true,

$$\begin{aligned}
\mathcal{O}_j &\equiv \max_{p(x)} \frac{1}{T} I(X_j; Y | X_1, \dots, X_N \setminus X_j) < R \\
\mathcal{O}_{ij} &\equiv \max_{p(x)} \frac{1}{T} I(X_i, X_j; Y | X_1, \dots, X_N \setminus X_i, X_j) < 2R \\
&\vdots \\
\mathcal{O}_{12\dots j\dots N} &\equiv \max_{p(x)} \frac{1}{T} I(X_1, X_2, \dots, X_N; Y) < NR, \tag{187}
\end{aligned}$$

then, the probability of error is bounded away from zero. Since the multiple access channel is Gaussian, the mutual informations are maximized by choosing a independent Gaussian input distributions at each user. For a generic set of users γ , the outage event is defined as

$$C_\gamma := \max_{p(x)} \frac{1}{T} I(X(\gamma); Y | X(\gamma^X)) < R_\gamma. \tag{188}$$

Given $X(\gamma^C)$, we define $Y(\gamma)$ as the reduced received block, after cancelling out the contributions of $X(\gamma^C)$. Since the encoding function at the relays is linear, $Y(\gamma)$ can be written as $Y(\gamma) = A_\gamma X(\gamma) + B_\gamma N_\gamma$ for some A_γ and B_γ , for which the mutual information can be computed easily. As an example, we evaluate

$$C_j := \max_{p(x)} \frac{1}{T} I(X_j; Y | X_1, \dots, X_N \setminus X_j) < R. \tag{189}$$

The first step is to establish the relationship between the reduced received block is $Y(\{j\})$ and the input $N - 1$ information blocks $X_j^{(1)}, \dots, X_j^{(j-1)}, X_j^{(j+1)}, \dots, X_j^{(N)}$ that constitute U_j 's transmitted word, after cancelling out the contributions of $X_1, \dots, X_{j-1}, X_{j+1}, \dots, X_N$ from Y . This relationship is given by

$$\begin{bmatrix} Y(\{j\})^{(1)} \\ \vdots \\ Y(\{j\})^{(j-1)} \\ Y(\{j\})^{(j+1)} \\ \vdots \\ Y(\{j\})^{(N)} \\ Y(\{j\})^{(N+1)} \end{bmatrix} = A_\gamma \begin{bmatrix} X_j^{(1)} \\ \vdots \\ X_j^{(j-1)} \\ X_j^{(j+1)} \\ \vdots \\ X_j^{(N)} \end{bmatrix} + B_\gamma \begin{bmatrix} N_1 \\ \vdots \\ N_{j-1} \\ N_{j+1} \\ \vdots \\ N_N \end{bmatrix}, \quad (190)$$

where, $A_\gamma = \begin{bmatrix} h_j \mathbf{I} \\ \mathbf{v} \end{bmatrix}$, $\mathbf{v} = [\alpha_1 h_{1j} h_1, \dots, \alpha_{j-1} h_{(j-1)j} h_{j-1}, \alpha_{j+1} h_{(j+1)j} h_{j+1}, \dots, \alpha_N h_{jN} h_N]$, and $B_\gamma = \begin{bmatrix} h_j \mathbf{I} \\ \mathbf{w} \end{bmatrix}$, with $\mathbf{w} = [\alpha_1 h_1, \dots, \alpha_{j-1} h_{j-1}, \alpha_{j+1} h_{j+1}, \dots, \alpha_N h_N]$, where \mathbf{I} is an identity matrix of size $(N-1) \times (N-1)$.

The above equation represents an $(N-1)$ -input, N -output Gaussian channel with a channel transfer function of A_γ and a noise covariance matrix B_γ . The mutual information between the input and output for this channel is maximized when the input distribution is Gaussian. The corresponding maximum value of C_j can be computed as

$$C_j = \frac{1}{N+1} \log_2 \det(\mathbf{I} + (B_\gamma^* B_\gamma)^{-1} A_\gamma^* A_\gamma). \quad (191)$$

For the given matrices A_γ and B_γ , the argument of the determinant can be computed as

$$I + (B_\gamma^* B_\gamma)^{-1} A_\gamma^* A_\gamma = \left[\begin{array}{c|c} (1 + E_t |h_j|^2) \mathbf{I} & \frac{\mathbf{v}^\dagger h_j \sqrt{E_t}}{N_0 |\mathbf{w}|^2} \\ \hline \mathbf{v} h_j^* \sqrt{E_t} & \left(1 + \frac{|\mathbf{v}|^2}{|\mathbf{w}|^2}\right) \frac{1}{N_0} \end{array} \right]. \quad (192)$$

Substituting in (191), C_j can be evaluated as follows

$$C_j = \frac{1}{N+1} \log_2 \left(\left(1 + \frac{E_t}{N_0} |h_j|^2 \right)^{N-1} + \frac{\left(1 + \frac{E_t}{N_0} |h_j|^2 \right)^{N-2} |v|^2}{(1 + |w|^2)} \right). \quad (193)$$

Similarly, each of the $2^N - 1$ outage events can be evaluated and the outage probability can be computed accurately for the cooperative multiple-access system.

10.4 Selection-Decode-and-Forward (SDF)

In the previous chapter, SDR with SDF relaying for a two user cooperative multiple-access channel was defined based on the inter-user channel strength. However, when the protocol is extended to multiple users, each relay receives a linear combination of information packets from multiple users as given by (176), thus creating a multiple-access channel during each block with the i -th user acting as the receiver in the i -th block. The SDF algorithm is explained in two parts: A) Selection and B) Forwarding.

10.4.1 Selection

In this part, we explain how each relay node selects which users to decode and forward to the destination during the relay phase. We now analyze this multiple-access channel with $N - 1$ transmitters and 1 receiver. Specifically we look into the event where the relay is capable of decoding the information from a set of users, but not others, depending on the instantaneous channel strengths. The multiple-access channel created with the i -th user as the receiver is given by

$$Y_{ii} = \begin{bmatrix} h_{1i} & h_{2i} & \cdots & h_{(i-1)i} & h_{(i+1)i} & \cdots & h_{Ni} \end{bmatrix} \begin{bmatrix} X_1^{(i)} \\ \cdot \\ X_{i-1}^{(i)} \\ X_{i+1}^{(i)} \\ \cdot \\ X_N^{(i)} \end{bmatrix} + N_{ii}. \quad (194)$$

For a Gaussian multiple-access channel with $N - 1$ transmitters and 1 receiver, the probability of any user being in error can be written as [27]

$$\Pr(\mathcal{E}) = \Pr\left(\bigcup_{\gamma \in \Gamma} \mathcal{E}_\gamma\right), \quad (195)$$

where, Γ is the set of all $2^{N-1}-1$ nonempty subsets of $\{1, 2, \dots, i-1, i+1, \dots, N\}$, γ denotes each element of Γ and \mathcal{E}_γ is the event where the elements in γ are in error. Therefore, the events which correspond to user j being in error are $\{\mathcal{E}_j, \mathcal{E}_{j1}, \dots, \mathcal{E}_{jN}, \dots, \mathcal{E}_{12\dots j\dots N}\}$. Let $X^{(i)}(\gamma) = \{X_k^{(i)}: k \in \gamma\}$, then, for a codeword of length n and a set γ , the error probability can be upper-bounded as

$$\Pr(\mathcal{E}_\gamma) \leq 2^{\{-n [I(X^{(i)}(\gamma); Y | X^{(i)}(\gamma^c)) - R_\gamma - \epsilon_\gamma]\}}, \quad (196)$$

for some $\epsilon_\gamma > 0$, where R_γ is the sum of data rates transmitted by the users in γ [27]. Since the rate of the cooperation protocol is $(N-1)/(N+1)$, each user when active transmits at a rate $R' = (N+1)R/(N-1)$. Since we assume a symmetric scenario with all users transmitting equal data rates, $R_\gamma = R'|\gamma|$. Clearly, this probability of error will be arbitrarily close to zero iff $I(X^{(i)}(\gamma); Y | X^{(i)}(\gamma^c)) > R'|\gamma|$, i. e., if the joint channel created

by the users in γ with the receiver is outage-free. Hence, the outage event for the set of users γ is

$$\mathcal{O}_\gamma \equiv \max_{p(x)} \frac{1}{T} I(X^{(i)}(\gamma); Y | X^{(i)}(\gamma^X)) < R' |\gamma|. \quad (197)$$

where $p(x)$ is the probability density function of X . The probability of user j being in error is the probability of the union of events $\{\mathcal{E}_j, \mathcal{E}_{j1}, \dots, \mathcal{E}_{jN}, \dots, \mathcal{E}_{12\dots j\dots N}\}$. The outage probability is:

$$\Pr(U_j \text{ is decoded erroneously by } U_i) = P_{ij} = \Pr\left[\bigcup_{\gamma \in \Gamma_j} \mathcal{E}_\gamma \right], \quad (198)$$

where, $\Gamma_j = \{\gamma: j \in \gamma\}$. Further, the probability of user j being decoded erroneously can be upper bounded using the union bound as

$$P_{ij} \leq \Pr(\mathcal{E}_j) + \Pr(\mathcal{E}_{j1}) + \dots + \Pr(\mathcal{E}_{jN}) + \dots + \Pr(\mathcal{E}_{12\dots j\dots N}). \quad (199)$$

For a given channel realization, the above probability of error is arbitrarily close to zero if each of the conditional mutual informations is greater than the corresponding data rate. We now compute the outage probability for this system.

Since the multiple access channel is Gaussian, the mutual informations are maximized by choosing a independent Gaussian input distributions at each user. This choice is compatible with the choice of input distribution of the entire transmitted word in order to maximize the capacity of the cooperative multiple-access channel as a whole.

This is ensured if all of the following outage events are false, in other words, if any of the following events is true, the error probability is bounded away from zero. By choosing independent Gaussian distributions for the input symbols, we get

$$\begin{aligned}
\mathcal{O}_j^{(i)} &: \log_2(1 + |h_{ji}|^2 E_t/N_0) < R' \\
\mathcal{O}_{j1}^{(i)} &: \log_2(1 + (|h_{1i}|^2 + |h_{ji}|^2) E_t/N_0) < 2R' \\
&\vdots \\
\mathcal{O}_{jN}^{(i)} &: \log_2(1 + (|h_{ji}|^2 + |h_{Ni}|^2) E_t/N_0) < 2R' \\
&\vdots \\
\mathcal{O}_{12\dots j\dots N}^{(i)} &: \log_2(1 + \sum_{\substack{k=1 \\ k \neq i}}^N |h_{ki}|^2 E_t/N_0) < (N-1)R'. \tag{200}
\end{aligned}$$

Let us define $\mathcal{O}_j^{(i)*}$ as the union of all the above events. In order to implement SDF relays, the receiver (user i in the i^{th} block) computes the conditional mutual information $I(X(\gamma); Y|X(\gamma^C))$ for every set γ in (200) using its knowledge of the channel information. If the node determines that *any* of the above outage events is true, then the probability of error cannot be guaranteed to be arbitrarily small and hence the relay node does not decode user j . However, if all of the above outage events are false for the given channel realization, then the relay node can decode U_j 's information with arbitrarily small error probability.

10.4.2 Forwarding

Each relay node creates a set of *decodable users* for every channel realization based on the instantaneous channel state information and subsequently forwards the information from the decoded users during the user $(N+1)^{\text{th}}$ block, as will be explained in this section.

We define the decode indicator matrix, \mathcal{D} , which is computed for every channel realization, in other words, every static fading frame. The element, \mathcal{D}_{ij} , of the matrix is 1 if the i^{th} user is able to decode the j^{th} user's transmissions. The SDF algorithm determines this using the outage criterion determined in the previous section. Each user computes \mathcal{D}_i , the i^{th} row of the matrix \mathcal{D} , which indicates the set of users that user i can decode with a 1, and others with a 0. We call this the *relay set* of user i . The *decoding set* $\mathcal{D}(i)$ of user i is defined as the set of users which can decode user i , and are indicated by a 1 in the i^{th} column of the matrix \mathcal{D} .

Each user would potentially have to relay information from multiple users jointly to the destination during the relay phase. Hence, the relays must re-encode the information from various sources before forwarding it to the destination. We impose the following constraints on the encoding function:

- 1) The relay node should only use *linear functions* to encode the information from various sources jointly.
- 2) Further, the encoding function should be *symmetric*, ensuring that the *available transmit power is split equally* among all users in the decoded set.

Let us define this encoding function as $g_i(\mathbf{X}^{(i)}) = \sum_r \alpha_r X_r^{(i)}$ for $\{r: \mathcal{D}_i(r) = 1\}$. In order to ensure equal power split among the relayed information packets, it is easy to show that $|\alpha_r|^2 = 1$. However in this case, letting $\alpha_r = 1$ does not change the system from an information theoretic perspective, hence we assume the same in the remainder of this discussion. Therefore, the encoding function can be simplified as $g_i(\mathbf{X}^{(i)}) = \sum_r X_r^{(i)}$ for $\{r: \mathcal{D}_i(r) = 1\}$. Note that α_r being an arbitrary complex rotation might be of great interest

in a practical implementation of this system, enabling the designer to choose appropriate lattices to transmit symbols from. Before transmission, the jointly encoded stream is scaled by a constant λ_i to enforce the average power constraint. For an average transmit energy per symbol of E_t , it is easy to show that $\lambda_i = \sqrt{\frac{E_t}{\sum \mathcal{D}_i}}$, and hence the i^{th} user transmits $\sqrt{\frac{E_t}{\sum \mathcal{D}_i}} \sum X_r^{(i)}$ during the relay phase.

The observations at the destination and relay nodes during the first N blocks are identical in this case to that in SDR with AF relays. During the relay phase, the nodes use the linear mapping function as discussed above, the information transmitted from the i^{th} user during the relay phase is given by

$$\begin{aligned} X_i^{(N+1)} &= \sqrt{\frac{E_t}{\sum \mathcal{D}_i}} \sum X_r^{(i)} \text{ for } \{r: \mathcal{D}_i(r) = 1\}, \\ &= 0, \quad \text{if } \sum \mathcal{D}_i = 0, \end{aligned} \quad (201)$$

and the block received at the destination during the relay phase is

$$Y_{N+1} = \begin{bmatrix} h_1 & h_2 & \dots & h_N \end{bmatrix} \begin{bmatrix} X_1^{(N+1)} \\ X_2^{(N+1)} \\ \vdots \\ X_N^{(N+1)} \end{bmatrix} + N_{N+1}. \quad (202)$$

10.4.3 Outage Analysis

We now analyze the outage probability of the SDR protocol with SDF relays. The cooperation protocol creates an equivalent discrete memoryless Gaussian multiple access channel between the N users and the destination. As discussed in the previous section, the outage probability of the cooperative multiple-access system is defined as [12][68]

$$P_{\text{SDR-SDF}} = \Pr(\mathcal{O}) = \Pr\left(\bigcup_{\gamma \in \Gamma} \mathcal{O}_\gamma\right), \quad (203)$$

where, Γ is the set of all $2^N - 1$ nonempty subsets of $\{1, 2, \dots, N\}$, with γ denoting each element of Γ . \mathcal{O}_γ is the event corresponding to the elements in γ being in outage jointly, given by

$$\mathcal{O}_\gamma := \max_{p(x)} \frac{1}{T} I(X(\gamma); Y | X(\gamma^C)) < R|\gamma|, \quad (204)$$

where $p(x)$ is the probability density function of X . Since the multiple access channel is Gaussian, the mutual informations are maximized by choosing an independent Gaussian input distributions for each user. For a set of users γ , the outage event is defined as follows

$$C_\gamma := \frac{1}{|\gamma|} \max_{p(x)} \frac{1}{T} I(X(\gamma); Y | X(\gamma^C)) < R. \quad (205)$$

Similar to the case of SDR with AF relays, we define $Y(\gamma)$ as the reduced received block as a function of $X(\gamma)$, after cancelling out the contributions of $X(\gamma^C)$. Since the equivalent multiple-access channel created by the cooperation protocol is linear, $Y(\gamma) = A_\gamma X(\gamma) + B_\gamma N_\gamma$ for some A_γ and B_γ .

For example, we now evaluate C_j i. e., C_γ with $\gamma = \{j\}$ as follows

$$C_j := \max_{p(x)} \frac{1}{T} I(X_j; Y | X_1, \dots, X_{j-1}, X_{j+1}, \dots, X_N) < R. \quad (206)$$

The relationship between the reduced received block is $Y(\{j\})$ and the input $N - 1$ information blocks $X_j^{(1)}, \dots, X_j^{(j-1)}, X_j^{(j+1)}, \dots, X_j^{(N)}$ after cancelling out the contributions of $X_1, \dots, X_{j-1}, X_{j+1}, \dots, X_N$ from Y is

$$\begin{bmatrix} Y(\{j\})^{(1)} \\ \cdot \\ Y(\{j\})^{(j-1)} \\ Y(\{j\})^{(j+1)} \\ \cdot \\ Y(\{j\})^{(N)} \\ Y(\{j\})^{(N+1)} \end{bmatrix} = A_\gamma \begin{bmatrix} X_j^{(1)} \\ \cdot \\ X_j^{(j-1)} \\ X_j^{(j+1)} \\ \cdot \\ X_j^{(N)} \end{bmatrix} + \begin{bmatrix} N_1 \\ \cdot \\ N_{j-1} \\ N_{j+1} \\ \cdot \\ N_N \end{bmatrix}, \quad (207)$$

where, $A_\gamma = \begin{bmatrix} h_j \mathbf{I} \\ \tilde{\mathbf{v}} \end{bmatrix}$, and

$$\tilde{\mathbf{v}} = \left[\sqrt{\frac{E_t}{\sum \mathcal{D}_1}} \mathcal{D}_{1j} h_1, \dots, \sqrt{\frac{E_t}{\sum \mathcal{D}_{j-1}}} \mathcal{D}_{j-1j} h_{j-1}, \sqrt{\frac{E_t}{\sum \mathcal{D}_{j+1}}} \mathcal{D}_{j+1j} h_{j+1}, \dots, \sqrt{\frac{E_t}{\sum \mathcal{D}_N}} \mathcal{D}_{Nj} h_N \right]. \quad (208)$$

Similar to the case of SDR with AF relays, this equation represents an $(N - 1)$ -input, N -output Gaussian channel with a channel transfer function of A_γ and a noise covariance matrix B_γ . The mutual information between the input and output for this channel is maximized when the input distribution is Gaussian, with the corresponding value of C_j given as

$$C_j = \frac{1}{(N+1)} \log_2 \det(\mathbf{I} + (B_\gamma^* B_\gamma)^{-1} A_\gamma^* A_\gamma). \quad (209)$$

For the given matrices A_γ and B_γ , the argument of the determinant can be computed as

$$I + (B_\gamma^* B_\gamma)^{-1} A_\gamma^* A_\gamma = \begin{bmatrix} (1 + E_t |h_j|^2) \mathbf{I} & \frac{\tilde{\mathbf{v}}^\dagger h_j \sqrt{E_t}}{N_0} \\ \hline \tilde{\mathbf{v}} h_j^* \sqrt{E_t} & \frac{1 + |\tilde{\mathbf{v}}|^2}{N_0} \end{bmatrix}. \quad (210)$$

Substituting (210) in (209), and using $S = E_t N / (N_0 (N+1))$ we get

$$C_j = \frac{1}{(N+1)} \log_2 \left(\left(1 + \frac{S(N+1)}{N} |h_j|^2 \right)^{N-2} \left(1 + \frac{S(N+1)}{N} |h_j|^2 + |\tilde{\mathbf{v}}|^2 \right) \right). \quad (211)$$

Each of the $2^N - 1$ outage events can be evaluated in a similar fashion to compute the outage probability of the cooperative multiple-access system accurately. We now state the following theorem about the diversity order of the SDR protocol with SDF relays.

Theorem 11. The space-division relay cooperation protocol with selection-decode and forward relays achieves the full diversity, N , over a multiple-access channel with N users with one antenna at each user and the destination.

$$d_{\text{SDR-SDF}} = \lim_{S \rightarrow \infty} \frac{-\log P_{\text{SDR-SDF}}(S, R)}{\log S} = N. \quad (212)$$

Proof: From (203), $P_{\text{SDR-SDF}} = \Pr(\cup_{\gamma \in \Gamma} \mathcal{O}_\gamma)$, where each outage event is defined as $\mathcal{O}_\gamma = \max_{p(x)} \frac{1}{T} I(X(\gamma); Y | X(\gamma^c)) < R|\gamma|$ for the set γ , of users. For any two sets of users γ_1 and γ_2 , such $\gamma_2 \subseteq \gamma_1$ the inequality $I(X(\gamma_1); Y | X(\gamma_1^c)) \geq I(X(\gamma_2); Y |$

$X(\gamma_2^C)$ is true. Therefore, it follows that $C_{\gamma_1} \geq \frac{|\gamma_2|}{|\gamma_1|} C_{\gamma_2}$. Let us define d_γ as the diversity order corresponding to $\Pr(\mathcal{O}_\gamma)$. Using the above inequality, it is clear that $d_{\gamma_1} \geq d_{\gamma_2}$ if $\gamma_2 \subseteq \gamma_1$. We also know that $d_i = d_j$ for all $i, j = 1, 2, \dots, N$. Combining these two observations, we get $\min_\gamma d_\gamma = d_i$ for any $i = 1, 2, \dots, N$. Using the union bound, we get the following equations:

$$P_{\text{SDR-SDF}} \leq \sum_{\gamma \in \Gamma} \Pr(\mathcal{O}_\gamma), \quad (213)$$

$$d_{\text{SDR-SDF}} = \min_\gamma d_\gamma = d_j \text{ for any } j = 1, 2, \dots, N. \quad (214)$$

Using (211), $\Pr(\mathcal{O}_j)$ is computed as

$$\Pr(\mathcal{O}_j) = \Pr \left\{ \left(1 + \frac{S(N+1)}{N} |h_j|^2 \right)^{N-2} \left(1 + \frac{S(N+1)}{N} |h_j|^2 + |\tilde{\mathbf{v}}|^2 \right) < 2^{R(N+1)} \right\}. \quad (215)$$

$\Pr(\mathcal{O}_j)$ can be written as

$$\begin{aligned} \Pr(\mathcal{O}_j) &= \Pr[\mathcal{O}_j | (|h_j|^2 < \theta_1)] \Pr[|h_j|^2 < \theta_1] + \\ &\Pr[\mathcal{O}_j | (|h_j|^2 \geq \theta_1)] \Pr[|h_j|^2 \geq \theta_1], \end{aligned} \quad (216)$$

$$\text{where, } \theta_1 = \frac{2^{\frac{R(N+1)}{N-1}} - 1}{S((N+1)/N)}.$$

If $\Pr[|h_j|^2 \geq \theta_1]$, it is clear that $C_j \geq R$, and hence $\Pr[\mathcal{O}_j | (|h_j|^2 < \theta_1)] = 0$ and

$$\Pr(\mathcal{O}_j) = \Pr[\mathcal{O}_j | (|h_j|^2 < \theta_1)] \Pr[|h_j|^2 < \theta_1]. \quad (217)$$

Clearly, $\Pr[\mathcal{O}_j(|h_j|^2 < \theta_1)]$ depends on the *decoding set* $\mathcal{D}(j)$ of user j , defined as the set of users which can decode user j . Therefore,

$$\Pr(\mathcal{O}_j) = \Pr[\mathcal{O}_j(|h_j|^2 < \theta_1, \mathcal{D}(j))] \Pr[|h_j|^2 < \theta_1] \Pr[\mathcal{D}(j)]. \quad (218)$$

Now, $\Pr[\mathcal{O}_j(|h_j|^2 < \theta_1)]$ can be upper bounded as

$$\Pr[\mathcal{O}_j(|h_j|^2 < \theta_1)] \leq \Pr[|\tilde{\mathbf{v}}|^2 < 2^{R(N+1)}]. \quad (219)$$

where,

$$\begin{aligned} \tilde{\mathbf{v}} = [& \sqrt{\frac{E_t}{\sum \mathcal{D}_1}} \mathcal{D}_{1j} h_1, \dots, \sqrt{\frac{E_t}{\sum \mathcal{D}_{j-1}}} \mathcal{D}_{(j-1)j} h_{j-1}, \sqrt{\frac{E_t}{\sum \mathcal{D}_{j+1}}} \mathcal{D}_{(j+1)j} h_{j+1}, \dots, \\ & \sqrt{\frac{E_t}{\sum \mathcal{D}_N}} \mathcal{D}_{Nj} h_N], \end{aligned} \quad (220)$$

with $\mathcal{D}_{ij} = 1$ in iff $i \in \mathcal{D}(j)$. Consider $\Pr[\mathcal{O}_j(|h_j|^2 < \theta_1, \mathcal{D}(j))]$:

$$\Pr[\mathcal{O}_j(|h_j|^2 < \theta_1, \mathcal{D}(j))] \leq \Pr[|\tilde{\mathbf{v}}|^2 < 2^{R(N+1)} | \mathcal{D}(j)]. \quad (221)$$

Given the decoding set $\mathcal{D}(j)$, $|\tilde{\mathbf{v}}|^2 = \sum_{m \in \mathcal{D}(j)} \frac{E_t}{\sum \mathcal{D}_m} |h_m|^2$, where $0 < \sum \mathcal{D}_m \leq N-1$ when $m \in \mathcal{D}(j)$. The probability in (221) can be bounded as

$$\Pr[\mathcal{O}_j(|h_j|^2 < \theta_1, \mathcal{D}(j))] \leq \Pr \left[\sum_{m \in \mathcal{D}(j)} |h_m|^2 < \frac{(N-1/N)}{S} 2^{R(N+1)} \right], \quad (222)$$

$$\Pr[\mathcal{O}_j(|h_j|^2 < \theta_1, \mathcal{D}(j))] \leq \Pr \left[\sum_{m \in \mathcal{D}(j)} |h_m|^2 < \theta_2 \right]. \quad (223)$$

where, $\theta_2 = \frac{2^{R(N+1)}}{S} \left(N - \frac{1}{N}\right)$. The next component in (218) is $\Pr[\mathcal{D}(j)]$. $\Pr[\mathcal{D}(j)]$ is the probability that users in the set $\mathcal{D}(j)$ can decode user j and others cannot, and it is given by

$$\Pr[\mathcal{D}(j)] \leq \left(\bigcap_{k \in \mathcal{D}(j)} \Pr\left(\left(\mathcal{O}_{jk}^*\right)^C\right) \right) \cap \left(\bigcap_{l \notin \mathcal{D}(j)} \Pr\left(\mathcal{O}_{jl}^*\right) \right). \quad (224)$$

To evaluate this, we define the event $\mathcal{R}_{ji}: \log_2(1 + |h_{ji}|^2 E_t / N_0) > (N - 1)R$ ($= (N + 1)R$). A careful examination of (200) tells us that if \mathcal{R}_{ji} is true then all the events in (200) are false and user j is *decodable* by user i . Thus, it is clear that $\mathcal{O}_j^{(i)*} \subseteq \mathcal{R}_{ji}^C$ and also from (200) that $\left(\left(\mathcal{O}_j^{(i)*}\right)^C\right) \subseteq \left(\mathcal{O}_j^{(i)}\right)^C$. Hence,

$$\Pr[\mathcal{D}(j)] \leq \left(\bigcap_{k \in \mathcal{D}(j)} \Pr\left(\left(\mathcal{O}_j^{(k)}\right)^C\right) \right) \cap \left(\bigcap_{k \notin \mathcal{D}(j)} \Pr\left(\mathcal{R}_{jk}^C\right) \right), \quad (225)$$

where,

$$\Pr\left(\left(\mathcal{O}_j^{(k)}\right)^C\right) = \Pr\left(|h_{jk}|^2 > \frac{2^R - 1(1 + (1/N))}{S}\right),$$

$$\Pr\left(\mathcal{R}_{jk}^C\right) = \Pr\left(|h_{jk}|^2 < \frac{(2^{R(N+1)} - 1)(1 + (1/N))}{S}\right). \quad (226)$$

Since $|h_j|^2$ is an exponential random variable, $\Pr([|h_j|^2 \geq \theta_1] \approx \theta_1)$ for small θ_1 [11] and equivalently large S . Similarly, since all $|h_j|^2$ and $|h_{ij}|^2$ are exponential random variables, it is easy to show that $\Pr\left(\left(\mathcal{O}_j^{(k)}\right)^C\right) \approx 1 - \theta_3$ and $\Pr\left(\mathcal{R}_{jk}^C\right) \approx \theta_4$ for small θ_3 and θ_4 or equivalently large S as evident from the fact that

$$\theta_3 = \frac{(2^R - 1)(1 + (1/N))}{S} \text{ and } \theta_4 = \frac{(2^{R(N+1)} - 1)(1 + (1/N))}{S}. \quad (227)$$

In (225), there are $|\mathcal{D}(j)|$ terms such that $k \in \mathcal{D}(j)$ and $N - |\mathcal{D}(j)| - 1$ terms such that $l \notin \mathcal{D}(j)$, with all events being independent of each other. Therefore,

$$\Pr[\mathcal{D}(j)] \leq (1 - \theta_3)^{|\mathcal{D}(j)|} \theta_4^{N - |\mathcal{D}(j)| - 1} \approx \theta_4^{N - |\mathcal{D}(j)| - 1}, \quad (228)$$

for small values of θ_3 and θ_4 . Now, from (223), we get

$$\Pr[\mathcal{O}_j | (|h_j|^2 < \theta_1, \mathcal{D}(j))] \leq \Pr \left[\sum_{m \in \mathcal{D}(j)} |h_m|^2 < \theta_2 \right]. \quad (229)$$

Here, $\sum_{m \in \mathcal{D}(j)} |h_m|^2$ follows a $\chi^2(2|\mathcal{D}(j)|)$ distribution. For a random variable Z with $\chi^2(2n)$ distribution, it is well known that $\Pr[Z < \varepsilon] \approx \varepsilon^n$ for small values of ε .

Therefore,

$$\Pr[\mathcal{O}_j | (|h_j|^2 < \theta_1, \mathcal{D}(j))] \leq \Pr \left[\sum_{m \in \mathcal{D}(j)} |h_m|^2 < \theta_2 \right] \approx (\theta_2)^{|\mathcal{D}(j)|}. \quad (230)$$

Combining (218), (223), (228) and (230),

$$\Pr(\mathcal{O}_j) \leq \frac{\lambda}{(S)(S^{|\mathcal{D}(j)|})(S^{N - |\mathcal{D}(j)| - 1})} = \frac{\lambda}{S^N} \text{ as } S \rightarrow \infty, \quad (231)$$

for some constant λ . Hence, we have shown that $d_{\text{SDR-SDF}} \geq N$. The upper bound on the diversity order is easy to show, since $P_{\text{SDR-SDF}}(S, R) \geq P_{\text{MISO}}(NS, R, N)$ where, $P_{\text{MISO}}(S, R, N)$ is the outage probability of a MISO channel with N transmit antennas and one receive antenna, with a total power constraint of E at the

transmitter. It is well known that $d_{\text{MISO}} = \lim_{S \rightarrow \infty} \frac{-\log P_{\text{MISO}}(NS, R, N)}{\log S} = N$.

Therefore, $d_{\text{SDR-SDF}} \leq N$ as well. The only way both inequalities on $d_{\text{SDR-SDF}}$ can be true is $d_{\text{SDR-SDF}} = N$. Hence, it is proved that SDR with SDF achieves full diversity N over the cooperative multiple-access channel considered.

Hence, the conclusion is that the SDR protocol with SDF relays achieves the full diversity of the cooperation multiple-access channel considered. In the next section, simulation results are presented to study the actual performance improvement of the cooperation schemes proposed over non-cooperative schemes as well as the proximity to the ideal genie-aided cooperative system.

10.5 Numerical results

In this section, we discuss numerical results for several transmission schemes over a Rayleigh-fading cooperative multiple-access channel with N ($= 3$ and 4) cooperating users and a single destination, each equipped with one antenna. Each user has a target data rate of $R = 1$ bps/Hz, and each has the same average SNR S . To achieve a data rate of $R = 1$ bps/Hz, the LTW protocol needs a user to transmit information at N^2 bps/Hz during its active transmissions, while SDR requires the user to transmit at $(N + 1)/(N - 1)$ b/s/Hz when active. The outage probability is compared against that of conventional non-cooperative multiple-access schemes such as TDMA and SDMA.

In Fig. 46, the outage probability of several candidate multiple access schemes for a 3-user CMA system are compared. Non-cooperative schemes such as TDMA and SDMA outperform LTW at low SNRs, due to their higher rate, suffer from a lack of diversity at

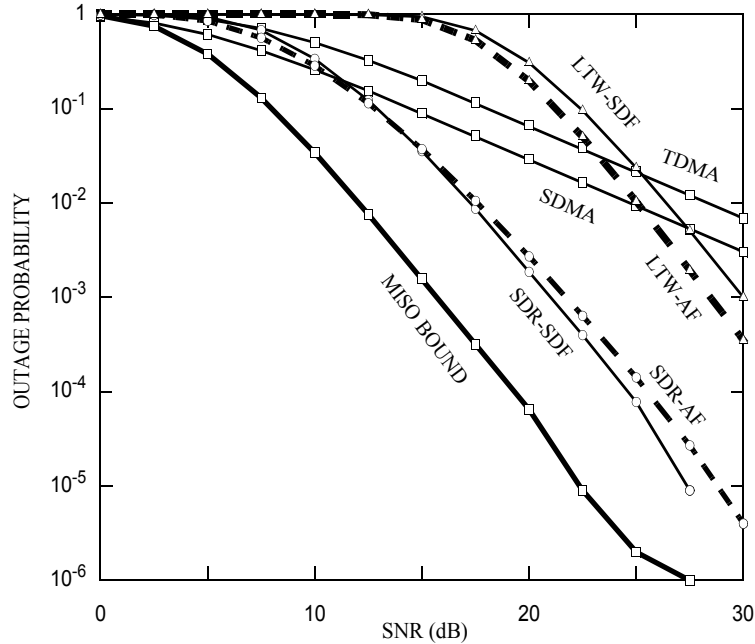


Fig. 46. Comparison of outage probabilities of SDR and LTW protocols with AF and SDF relays for $N = 3$ with $R = 1$ b/s/Hz per user.

high SNR. However, SDR significantly minimizes this drawback due to its high transmission rate. For outage probabilities less than 10^{-1} , SDR comfortably outperforms non-cooperative schemes due to its full diversity and minimal rate loss.

Among the available schemes, SDR-SDF achieves the lowest outage probability at high SNR. At an outage probability of 10^{-3} , SDR-SDF outperforms SDR-AF by 0.7 dB, LTW-AF by 7.5 dB and LTW-SDF by 9 dB. Fig. 46 also shows the MISO bound which is the outage probability of a 3×1 MISO channel and serves as a lower bound on the outage probability of any 3-user CMA scheme, and it may or may not be achievable. The SDR-SDF protocol falls 5.3 dB short of the MISO bound.

A similar comparison is made in Fig. 47 for a 4-user CMA system, with the same set of assumptions. It is again seen that SDR-SDF emerges as the protocol with the best performance for outage probabilities lower than 10^{-3} . This scheme outperforms SDR-AF

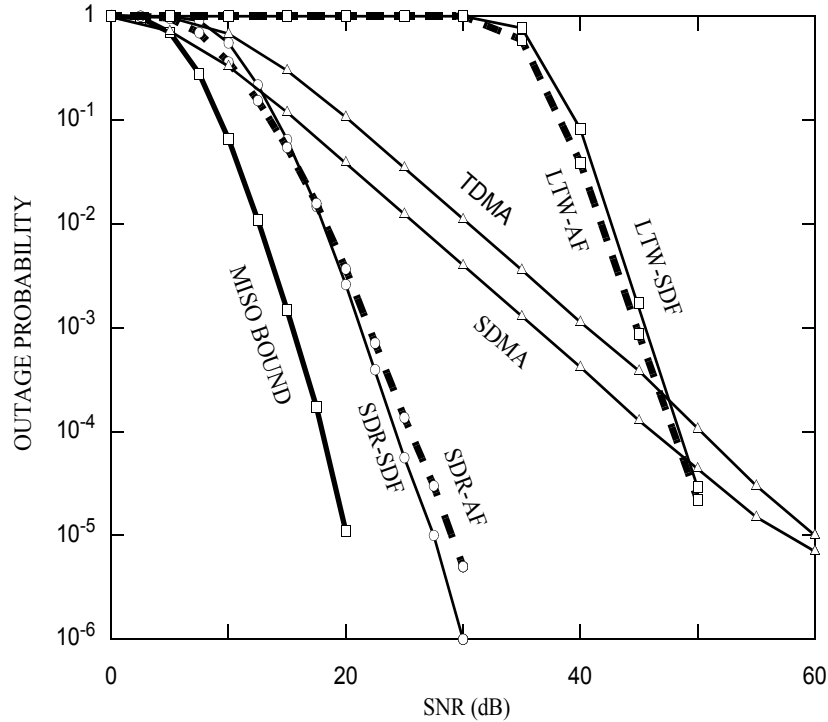


Fig. 47. Comparison of outage probabilities of SDR and LTW protocols with AF and SDF relays for $N = 4$ with $R = 1$ b/s/Hz per user.

by 0.7 dB, LTW-AF by 23.5 dB and LTW-SDF by 24.4 dB, while getting to within 5.8 dB of the MISO bound. Numerical results for the other non-orthogonal transmission scheme, the NAF protocol, are not available for $N > 2$ cooperating users in the original work, but given that SDR has a rate of $(N - 1)/(N + 1)$ compared to a rate of NAF with $1/N$ per user, SDR-SDF is clearly expected to outperform NAF, given that both protocols achieve full diversity.

10.6 Summary

In this chapter, we presented an extension of the space-division relay (SDR) protocol for a cooperative multiple-access channel with an arbitrary number of users N . Our goal was to design cooperation protocols with full diversity and high rate, especially as the

number of users increase. We showed that the SDR protocol achieves this goal with a rate of $(N - 1)/(N + 1)$. We showed that SDR with SDF relays achieves the full diversity of N over the cooperative multiple-access channel.

Though it remains an open problem to prove the diversity order for SDR with AF relays, numerical results indicate that AF relays perform almost as well as SDF relays falling short only by 0.7 dB. From numerical results, we concluded that SDR-SDF achieves the lowest outage probability among all known multiple access schemes at high SNR for 3 and 4 user systems. For $N = 3$ and $N = 4$, SDR-SDF is seen to outperform LTW-AF by 7.5 dB and 23.5 dB respectively at an outage probability of 10^{-3} . Also, we see that SDR-SDF decays at a similar rate as the MISO bound, an observation which is consistent with the theoretical proof that SDR-SDF achieves full diversity.

These results show the importance of designing high rate cooperation protocols, rather than just focussing on full diversity. With a rate of $(N - 1)/(N + 1)$ which approaches the full rate 1 as N grows, and full diversity N , SDR-SDF seems to be a very promising candidate for cooperative multiple-access systems of any dimension.

CHAPTER 11

11 CONCLUSION

In this thesis, we addressed the problem of designing spatial diversity techniques for single-user and multiuser wireless communications systems over slow fading channels. This thesis contains two parts: In the first part, we dealt with the design layered space-time architectures for single user wireless communication systems. The second part of this thesis dealt with the design of cooperation schemes for multiple-access channels.

11.1 Main Contributions

PART I: Layered Space-Time Architectures

- We proposed rate-normalized BLAST architecture [28]: An enhanced version of the conventional V-BLAST architecture obtained by joint transmit-receive optimization. We proposed a) the rate-normalized ordering algorithm which minimizes outage probability and b) the partially uniform rate and energy allocation, which in combination with RN ordering improves the performance of V-BLAST at no extra cost.
- We introduced the STAR family of layered space-time architectures [56][58]. STAR is a new family of architectures designed specifically to suit linear and successive cancellation decoders. We proposed three versions of STAR, namely V-STAR, G-STAR and D-STAR with vertical, group and diagonal coding respectively.

- We showed that V-STAR achieves near-optimal outage performance while requiring just a low complexity SC decoder, while performing better than every other vertically layered space-time architecture. We proved that V-STAR achieves full diversity for a range of MIMO channel dimensions.
- We showed that G-STAR significantly outperforms other group coded architectures. Finally, we showed that D-STAR while achieving comparable outage performance as D-BLAST, comfortably overcomes practical issues faced by the latter such as short code lengths and error propagation.
- We showed an application of the STAR transmission strategy to multiple-access communications, based on its similarity to vertically layered ST architectures [57].

PART II: Cooperative Multiple-Access Systems

- We developed *space-division relay*, a high-rate cooperation protocol for a simple 2-user multiple access channel. Space-division relay was shown to achieve full diversity and the best outage performance among all available schemes [89].
- We developed the *partial cooperation framework* to measure the optimum level of cooperation needed to achieve the lowest outage probability. The results from this framework answers questions such as how much cooperation is necessary in multiple access channels, and how much rate loss can be tolerated to gain diversity.
- Finally, we proposed an extension of the space division relay protocol to arbitrarily large multiple-access networks. We showed that this extension preserves high rate and full diversity as the number of users increase. In fact, space-division relay achieves a rate of $o(1)$ while still achieving full diversity.

11.2 Future Work

PART I: Layered Space-Time Architectures

- The problem of building practical codes which approach the outage probability of the schemes discussed here is of great importance. It would be interesting to study the ability of finite length codes to approach layer capacities, and the gap of the FER of a practical system to the outage probability.
- In the special case of D-BLAST, characterization of the codelength vs rate tradeoff needs further study. This analysis requires characterization of the performance of error control codes as a function of codelength. Application of tools such as the error exponent and the sphere-packing bound to an analogous problem can be found in [27][60].

PART II: Cooperative Multiple-Access Systems

- There are several unanswered problems in this fairly recent research topic. Fundamentally, the achievable performance limits of cooperation protocols over fading multiple-access channels are still unknown.
- Allowing limited feedback from the destination to the users would open the doors to several new ideas and better cooperation protocols. Though this topic is being actively researched, it still warrants further work [61][62][70][71][76][83].
- Thus far, the decoding complexity of CMA schemes has not been discussed at length. In the future, designing cooperation protocols with affordable computational complexity at the relay nodes as well as the destination is a desirable goal.

REFERENCES

- [1] E. Biglieri, Proakis and S. Shamai, "Fading Channels: Information-Theoretic and Communications Aspects," *IEEE Trans. on Information Theory*, vol. 44, 1998.
- [2] D. Gesbert, M. Shafi, Da-shan Shiu, P. J. Smith and A. Naguib, "From Theory to Practice: an Overview of MIMO Space-Time Coded Wireless Systems," *IEEE Journal on Selected Areas in Comm.*, Vol. 21, No. 3, pp. 281-302, 2003.
- [3] G. J. Foschini and M. J. Gans, "On the limits of wireless communications in a fading environment when using multiple antennas," *Wireless Personal Comm.*, vol. 6, no. 3, pp. 311-355, Mar 1998.
- [4] I. E. Telatar, "Capacity of multiantenna Gaussian channels," *European Trans. on Telecomm.*, vol. 10, pp. 585-95, November/December 1999.
- [5] P. W. Wolniansky, G. J. Foschini, G. D. Golden and R. A. Valenzuela, "V-BLAST: An Architecture for Realizing Very High Data Rates Over the Rich-Scattering Wireless Channel," *Proc. ISSSE-98*, Pisa, Italy, Sept. 29, 1998.
- [6] G. D. Golden, G. J. Foschini, R. A. Valenzuela and P. W. Wolniansky, "Detection Algorithm and Initial Laboratory Results using the V-BLAST Space-Time Communication Architecture," *Electronics Letters*, Vol. 35, No. 1, Jan. 7, 1999, pp. 14-15.
- [7] S. M. Alamouti, "A simple transmitter diversity scheme for wireless communications," *IEEE Journal on Selected Areas in Comm.*, vol. 16, no.8, pp. 1451-1458, 1998.
- [8] V. Tarokh, N. Seshadri and A. R. Calderbank, "Space-time codes for high data rate wireless communication: performance criterion and code construction," *IEEE Trans. on Information Theory*, vol. 44, pp. 744-765, Mar. 1998.
- [9] Da-Shan Shiu and M. Kahn, "Layered space-time codes for wireless communications using multiple transmit antennas," *IEEE International Conference on Communications*, 1999.
- [10] X. Ma and G. B. Giannakis, "Layered Space-Time Complex Field Coding: Full-Diversity with full rate, and trade-offs," *Proc. of the 2nd Sensor Array and Multichannel SP Workshop*, Rosslyn, VA, pp. 442-446, August 2002.
- [11] L. Zheng and D. Tse, "Diversity and Multiplexing: A Fundamental trade-off in Multiple Antenna Channels," *IEEE Trans. on Information Theory*, 2002.

- [12] David N. C. Tse, Pramod Viswanath and Lizabeth Zheng, "Diversity-multiplexing tradeoff in multiple access channels", *IEEE Trans. on Information Theory*, Vol. 50, No. 9, pp. 1859-1874, Sept. 2004.
- [13] Robert W. Heath Jr. and David J. Love, "Multi-mode antenna selection for spatial multiplexing systems with linear receivers", *Proc. Allerton Conf. on Signals and Systems*, Monticello, IL, Oct. 2003.
- [14] N. Prasad and M. K. Varanasi, "Outage Analysis and Optimization for Multiaccess V-BLAST Architecture over MIMO Rayleigh Fading Channels", *41st Annual Allerton Conf. on Comm. Control, and Comput.*, Monticello, IL, Oct., 2003.
- [15] B. Hassibi and B. M. Hochwald, "High-rate codes that are linear in space and time," *IEEE Trans. on Information Theory*, vol. 48, no. 7, July 2002.
- [16] T. Guess, H. Zhang, and T. V. Kotschiv, "The outage capacity of BLAST for MIMO channels," in *Proc. IEEE Intl. Conf. on Communications*, Anchorage, Alaska, May 2003.
- [17] Ravi Narasimhan, "Spatial Multiplexing with transmit antenna and constellation selection for correlated MIMO fading channels", *IEEE Trans. on Signal Processing, Special Issue on MIMO Wireless Communications*, vol. 51, no. 11, pp 2829-2838, Nov. 2003.
- [18] D. A. Gore, R. W. Heath Jr. and A. J. Paulraj, "Statistical antenna selection for spatial multiplexing systems", *IEEE Int. Conf. On Communications*, vol 1. pp 450-454, 2002.
- [19] S. T. Chung, A. Lozano and H. C. Huang, "Approaching eigenmode BLAST channel capacity using V-BLAST with rate and power feedback", in *Proc. VTC 2001*, Atlantic City, Oct. 2001.
- [20] S. H. Nam and K. B. Lee, "Transmit power allocation for an extended V-BLAST system", *Proc. IEEE PIMRC 2002*, Sept. 2002, pp. 843-848.
- [21] R. W. Heath Jr., S. Sandhu, and A. J. Paulraj, "Antenna Selection for spatial multiplexing systems with linear receivers", *IEEE Communication Letters*, vol. 5, no. 4, pp 142-144, April 2001.
- [22] N. Prasad and M. K. Varanasi, "Analysis of Decision Feedback Detection for MIMO Rayleigh-Fading Channels and the Optimization of Power and Rate Allocations," *IEEE Trans. on Information Theory*, vol. 50, No. 6, pp. 1009-1025, June 2004.

- [23] N. Prasad and M. K. Varanasi, "Outage Capacities of Space-Time Architectures," *Proc. IEEE Information Theory Workshop*, San Antonio, Texas, Oct. 24-29, 2004.
- [24] G. D. Forney Jr. and M. V. Eyuboglu, "Combined Equalization and Coding using Precoding", *IEEE Communications Magazine*, Dec. 1991.
- [25] C. E. Shannon, "A mathematical theory of communications: Parts I and II," *Bell Systems Tech. Journal.*, vol. 27, pp. 379-423, 623-656, 1948.
- [26] R. J. Muirhead, *Aspects of Multivariate Statistical Theory*, John Wiley & Sons, 1982.
- [27] T. M. Cover and J. A. Thomas, *Elements of Information Theory*, John Wiley and Sons, 1991.
- [28] A. Kannan, B. Varadarajan and J. R. Barry, "Joint optimization of transmitter rate and BLAST ordering to minimize outage probability", in *Proc. IEEE Wireless Communications and Networking Conf.*, New Orleans, vol 1, pp. 550-555, May 2005.
- [29] M. Godavarti and A. O. Hero, "Diversity and degrees of freedom in wireless communications," *2002 IEEE Int. Conf. on Acoustics, Speech and Sig. Proc.*, vol. 3, pp. 2861-2864, 2002.
- [30] M. O. Damen and H. El Gamal, "On the Diversity-vs.-Rate Trade-off in MIMO systems," *Proc. IEEE Info. Theory Workshop*, pp. 357-360, March 31-April 4, 2003.
- [31] V. Tarokh, A. Naguib, N. Seshadri and A. Calderbank, "Combined array processing and space-time coding," *IEEE Trans. Info. Theory.*, vol. 44, no. 2, pp. 14-16, Jan. 1999.
- [32] W. J. Choi, R. Negi, and J. Cioffi, "Combined ML and DFE decoding for the V-BLAST system," *IEEE Conf. on Communications*, pp. 1243-1248, 2000.
- [33] D. Tse and P. Viswanath, "Fundamentals of Wireless Communication", *Cambridge University Press*, 2005.
- [34] J. R. Barry, E. A. Lee and D. G. Messerschmitt, "Digital Communication," *Kluwer Academic Publishers*, 2003.
- [35] B. Sklar, "Rayleigh Fading Channels in mobile digital communication systems Part I: Characterization," *IEEE Communications Magazine*, pp. 90-100, July 1997.

- [36] B. Sklar, "Rayleigh fading channels in mobile digital communication systems Part II: Mitigation," *IEEE Communications Magazine*, pp. 148-155, Sept. 1997.
- [37] S. Verdú, *Multiuser Detection*, Cambridge University Press, 1998.
- [38] N. Prasad and M. K. Varanasi, "Optimum Efficiently Decodable Layered Space-Time Block Codes," *Proc. Asilomar Conf. on Signals, Systems and Computers*, Monterey, CA, Nov. 2001.
- [39] N. Prasad and M. K. Varanasi, "D-BLAST Lattice Codes for MIMO Block Rayleigh Fading Channels," *40th Annual Allerton Conf. on Comm. Control and Comput.*, Monticello, IL, Oct., 2002.
- [40] K. Azarian and H. El Gamal, "The Throughput-Reliability Tradeoff in MIMO Channels," submitted to *IEEE Trans. on Information Theory*, Aug. 2005.
- [41] H. El Gamal, G. Caire, and M. O. Damen, "Lattice coding and decoding achieve the optimal diversity-vs-multiplexing tradeoff of MIMO channels," *IEEE Trans. on Information Theory*, June 2004.
- [42] M. O. Damen, H. El Gamal, and N. C. Beaulieu, "Linear Threaded Algebraic Space-Time Constellations," *IEEE Trans. on Information Theory*, Oct. 2003.
- [43] H. Zhang, H. Dai, Q. Zhou and B. L. Hughes, "On the Diversity Order of Transmit Antenna Selection for Spatial Multiplexing Systems," in *Proc. IEEE Globecom*, St. Louis, MO, Dec 2005.
- [44] D. MacKay and R. M. Neal, "Near Shannon Limit Performance of Low Density Parity Check Codes", *Electronics Letters*, July 1996.
- [45] T. J. Richardson and M. Amin Shokrollahi and R. Urbanke, "Design of Capacity-Approaching Irregular Low-Density Parity-Check Codes," *IEEE Transactions in Information Theory*, 47(2), February 2001.
- [46] C. Berrou, A. Glavieux, and P. Thitimajshima, "Near shannon limit error correcting coding and decoding: Turbo-codes (1)," in *Proc. of IEEE International Conference on Communications*, pp. 1064-1070, May 1993, Geneva, Switzerland.
- [47] C. Guey, M.P. Fitz, M.R. Bell and W.-Y. Kuo, "Signal Design for transmitter Diversity Wireless Communication Systems over Rayleigh Flat Fading," *IEEE Trans. on Communications*, vol. 47, no.4, pp.527-537, April 1999.
- [48] M. Damen, A. Tewfik and J. Belfiore, "A construction of a space-time code based on number theory," *IEEE Trans. on Information Theory*, March 2002.

- [49] M. K. Varanasi and T. Guess, "Optimum decision feedback multiuser equalization with successive decoding achieves the total capacity of the Gaussian multiple-access channel," *Thirty-First Asilomar Conference on Signals, Systems & Computers*, Vol. 2, pp: 1405-1409, Nov. 1997.
- [50] E. Viterbo and J. Boutros, "A universal lattice code decoder for fading channels," *IEEE Trans. Inf. Theory*, vol.45, no.5, pp.1639–1642, July 1999.
- [51] B. M. Hochwald and S. ten Brink, "Achieving near-capacity on a multiple-antenna channel," *IEEE Trans. Commun.*, vol. 51, no. 3, pp. 389–399, March 2003.
- [52] C. Windpassinger, and R. F. H. Fischer, "Low-complexity near-maximum-likelihood detection and precoding for MIMO systems using lattice reduction," *Proc. IEEE Inf. Th. Workshop (ITW)*, pp. 345-348, April 2003.
- [53] D. Wübben, R. Böhnke, V. Kühn, and K. Kammeyer, "Near-maximum-likelihood detection of MIMO systems using MMSE-based lattice-reduction," *IEEE Conf. on Commun.*, vol. 2, pp. 798-802, June. 2004.
- [54] M. Sellathurai and S. Haykin, "Further results on diagonal-layered space-time architectures," *Proc. IEEE Vehicular Technology Conference*, Spring 2001.
- [55] M. Sellathurai and G. J. Foschini, "Stratified diagonal layered space-time architectures: signal processing and information theoretic aspects," *IEEE Transactions on Acoustics, Speech, and Signal Processing*, vol. 51, no. 11, pp: 2943 - 2954, Nov. 2003.
- [56] A. Kannan and J. R. Barry, "Space-Time Active Rotation (STAR): A New Layered Space-Time Architecture", in *Proc. IEEE Globecom*, St. Louis, MO, Dec 2005.
- [57] A. Kannan and J. R. Barry, "An Improved Space-Division Strategy for Rayleigh Fading Multiple Access Channels," in *Proc. International Zurich Seminar on Communications*, Feb 2006.
- [58] A. Kannan and J. R. Barry, "Space-Time Active Rotation (STAR): A New Class of Layered Space-Time Architectures," in preparation.
- [59] G. J. Foschini, "Layered Space-Time Architecture for Wireless Communications in a Fading Environment When Using Multi-Element Antennas," *Bell Labs Technical Journal*, Aug 1996.
- [60] S. Dolinar, D. Divsalar, and F. Pollara, "Code Performance as a Function of Block Size," *The Telecommunications and Mission Operations Progress Report*, TMO PR 42-133, January-March 1998, pp.1-23.

- [61] A. Sendonaris, E. Erkip and B.Aazhang, "User Cooperation Diversity. Part I. System Description," *IEEE Transactions on Communications*, pp. 1927 - 1938, Volume: 51, Issue: 11, Nov. 2003.
- [62] A. Sendonaris, E. Erkip and B.Aazhang, "User Cooperation Diversity. Part II. Implementation Aspects and Performance Analysis," *IEEE Transactions on Communications*, pp. 1939 - 1948, Volume: 51, Issue: 11, Nov. 2003.
- [63] J. N. Laneman, D. N. C. Tse and G. W. Wornell, "Cooperative Diversity in Wireless Networks: Efficient Protocols and Outage Behavior," *IEEE Transactions on Information Theory*, Vol. 50, No. 12, pp 3062 - 3080, Dec. 2004.
- [64] J. N. Laneman and G. W. Wornell, "Distributed Space-Time Coded Protocols for Exploiting Cooperative Diversity in Wireless Networks," *IEEE Transactions on Information Theory*, Volume 49, Issue: 10, Oct. 2003, Pages: 2415-2425.
- [65] J. N. Laneman, "Cooperative Diversity in Wireless Networks: Algorithms and Architectures," Ph.D. Dissertation, MIT, MA, 2002.
- [66] K. Azarian, H. El Gamal and P. Schniter, "Achievable Diversity-vs-Multiplexing Tradeoffs in Half-Duplex Cooperative Channels," *Proc. IEEE Information Theory Workshop*, San Antonio, TX, Oct 2004.
- [67] K. Azarian, H. El Gamal and P. Schniter, "On the achievable diversity-multiplexing tradeoff in half-duplex cooperative channels," *IEEE Trans. on Info. Theory*, Vol. 51, No. 12, pp 4152 - 4172, Dec. 2005.
- [68] K. Azarian, H. El Gamal and P. Schniter, "On the Design of Cooperative Transmission Schemes Conference," *Allerton Conf. on Commun, Control and Computing*, Monticello, IL, 2003.
- [69] X. Bao and J. Li, "Decode-Amplify-Forward – A New Class of Forwarding Strategy for Wireless Relay Channels," *Proc. IEEE SPAWC*, New York, pp. 816 - 820, June 2005.
- [70] D. Gesbert, A. Hjørungnes and H. Skjjevling, "Cooperative Spatial Multiplexing with Hybrid Channel Knowledge," *Proc. International Zurich Seminar on Communications*, Feb. 2006.
- [71] L. Lai, K. Liu and H. El Gamal, "The Three Node Wireless Network: Achievable Rates and Cooperation Strategies," *IEEE Transactions on Information Theory*, Vol. 52, No. 3, pp. 805 - 828, March 2006.
- [72] N. Prasad and M. K. Varanasi, "Diversity and Multiplexing Tradeoff Bounds for Cooperative Diversity Protocols," *Proc. IEEE Intl. Symposium on Information Theory*, Chicago, IL, p. 268, June 2004.

- [73] T. M. Cover and A. A. El Gamal, "Capacity theorems for the relay channel," *IEEE Transactions on Information Theory*, vol. 25, no. 5, pp. 572–584, Sep. 1979.
- [74] R. U. Nabar, H. Bölcskei, and F.W. Kneubühler, "Fading relay channels: Performance limits and space-time signal design," *IEEE Journal on Selected Areas in Comm.*, vol. 22, no. 6, pp. 1099-1109, Aug. 2004.
- [75] G. Kramer, M. Gastpar and P. Gupta, "Cooperative Strategies and Capacity Theorems for Relay Networks," submitted to *IEEE Transactions on Information Theory*, Feb. 2004.
- [76] A. Stefanov and E. Erkip, "Cooperative Coding for Wireless Networks," *IEEE Transactions on Communications*, accepted for publication.
- [77] A. Murugan, K. Azarian, and H. El Gamal, "Cooperative Lattice Coding and Decoding," to appear in *IEEE Journal on Selected Areas in Comm.*, 2007.
- [78] M. Janani, A. Hedayat, T. Hunter and A. Nosratinia, "Coded Cooperation in Wireless Communications: Space-time transmission and iterative decoding," *IEEE Transactions on Signal Processing*, Vol. 52, Issue: 2, pp:362-371, Feb. 2004.
- [79] G. Wang, Y. Zhang and M. G. Amin, "Space-time cooperation diversity using high-rate codes," *Int. Symposium on Antennas and Propagation*, Sendai, Japan, Aug. 2004.
- [80] S.W. Kim and R. Cherukuri, "Cooperative spatial multiplexing for high-rate wireless communications," *IEEE Workshop in Signal Processing Advances in Wireless Communications*, New York, pp. 181–185, June 2005.
- [81] P. Dayal and M. K. Varanasi, "Diversity-multiplexing tradeoff for QAM based Multiuser Cooperation Strategies," *Conf. on Information Sciences and Systems*, The Johns Hopkins University, Baltimore, MD, Mar. 2005.
- [82] P. Dayal and M. K. Varanasi, "Efficient Multiuser Cooperation Strategies Using QAM Space-Time Block Codes," *Proc. IEEE Inform. Theory Workshop*, San Antonio, Texas, Oct. 24-29, 2004.
- [83] R. U. Nabar, F. W. Kneubühler, and H. Bölcskei, "Performance limits of amplify-and-forward based fading relay channels," in *Proc. IEEE Int. Conf. Acoustics, Speech and Signal Processing*, vol. 4, Montreal, QC, Canada, May 2004, pp. 565–568.

- [84] R. U. Nabar, H. Bölcskei, and F.W. Kneubuhler, “Fading relay channels: Performance limits and space-time signal design,” *IEEE Journal on Selected Areas in Comm.*, vol. 22, no. 6, pp. 1099–1109, Aug. 2004.
- [85] G. Kramer, M. Gastpar, and P. Gupta, “Cooperative strategies and capacity theorems for relay networks,” *IEEE Transactions on Information Theory*, vol. 51, no. 9, pp. 3037–3063, Sep. 2005.
- [86] A. Host-Madsen, “On the capacity of cooperative diversity in slow fading channels,” in *Proc. 40th Allerton Conf. Communications, Control and Computing*, Monticello, IL, Oct. 2002.
- [87] H. El Gamal, “The diversity-multiplexing tradeoff in half-duplex cooperative channels: Achievable curves and optimal strategies,” in *LIDS Colloquia*. Cambridge, MA: MIT Electrical Engg. Comp. Sci. Dept., May 2004.
- [88] C. T. K. Ng, J. N. Laneman and A. J. Goldsmith, “The role of SNR in achieving MIMO rates in cooperative systems,” in *Proc. Information Theory Workshop*, Punta del Este, Uruguay, March 13-17, 2006.
- [89] A. Kannan and J. R. Barry, “Space-Division Relay: A High-Rate Cooperation Scheme for Fading Multiple-Access Channels,” submitted to *IEEE Global Communications Conference (Globecom 2007)*, Washington, D.C., November 26-30, 2007.